

Developmental Changes in Synaptic Function in a Giant Auditory Synapse

Developmental Changes in Synaptic Function in a Giant Auditory Synapse  Tom Crins

Tom Crins



UITNODIGING

Voor het bijwonen van de
openbare verdediging van het
proefschrift

“Developmental
Changes in
Synaptic Function
in a Giant Auditory
Synapse”

Op woensdag 15 juni 2016 om
11.30 uur

Querido zaal Erasmus MC –
Faculteit
dr. Molenwaterplein 50
Rotterdam

Aansluitend receptie



Tom Crins
Smaragdstraat 39
4817 JL, Breda
06-12959567
t.crins@erasmusmc.nl

Paranimfen:

Paul Nagtegaal
06-14524585
a.nagtegaal@erasmusmc.nl

John Soria van Hoeve
06-41794582
j.soriavanhoeve@erasmusmc.nl

Developmental Changes in Synaptic Function in a Giant Auditory Synapse

Tom Crins

ISBN: 978-94-6182-673-2

Cover design: Tom Crins

Layout and printing: Off Page, Amsterdam

Copyright © 2016 by Tom Crins

Acknowledgments: printing made possible by DOS
Medical B.V. and Daleco Pharma B.V.

**Developmental Changes in Synaptic Function
in a Giant Auditory Synapse**

Veranderingen van synaptische functie gedurende de
ontwikkeling van een auditieve reuzensynaps

Proefschrift

**ter verkrijging van de graad van doctor aan de Erasmus Universiteit Rotterdam
op gezag van de rector magnificus**

Prof.dr. H.A.P. Pols

en volgens besluit van het College voor Promoties.

De openbare verdediging zal plaats vinden op

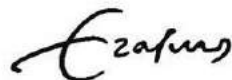
woensdag 15 juni 2016 om 11.30 uur

door

Tom Theodorus Hubertus Crins

geboren te Tegelen

Erasmus University Rotterdam

The logo of Erasmus University Rotterdam, featuring a stylized, handwritten-style script of the word "Erasmus" in a dark, possibly black, ink.

Promotiecommissie

Promotoren:

Prof.dr. J.G.G. Borst

Prof.dr. R.J. Baatenburg de Jong

Overige leden:

Prof.dr. J. van der Steen

Prof.dr. C.N. Levelt

Dr. A. Goedegebure

TABLE OF CONTENTS

| | | |
|------------------|---|-----|
| Chapter 1 | General introduction | 7 |
| Chapter 2 | Calcium action potentials in hair cells pattern auditory neuron activity before hearing onset | 27 |
| | Supplementary Information | 35 |
| Chapter 3 | Developmental changes in short-term plasticity at the rat calyx of Held synapse | 51 |
| Chapter 4 | Developmental changes in parvalbumin in the rodent calyx of Held synapse and its role in controlling short-term synaptic plasticity | 83 |
| Chapter 5 | General discussion | 103 |
| Chapter 6 | Summary / Samenvatting | 117 |
| Addendum | Curriculum vitae | 127 |
| | PhD portfolio | 129 |
| | Dankwoord | 133 |



chapter **ONE**

General introduction

The auditory system is a fascinating and highly complex system which can detect and decode sound. Sound is a pressure wave, which can put the tympanic membrane and the three ossicles of the middle ear into motion. The ossicles transmit this kinetic energy to the inner ear where motion of the perilymph will bend a hair bundle at the surface of a hair cell, which generates an electrical signal in the hair cell. This signal excites fibers in the eighth cranial nerve, which in turn can relay these signals to central nuclei in the brainstem, and further to the thalamus and cerebral cortex.

This thesis has as its main topic the developmental changes in the electrophysiological properties of the calyx of Held synapse, a giant synapse in the medial nucleus of the trapezoid body (MNTB) of the auditory brainstem. Since development is the main topic in this thesis, we start this general introduction with a description of the normal development of the human auditory system. Since all experiments in this thesis were done on rodents this introduction will next address what is known about the development of the calyx of Held synapse in rodents. The role of electrical activity during development and in certain critical periods in the development of neural circuitry in the auditory system will be further explored. Short term plasticity (STP), a phenomenon seen in the developing auditory system, and parvalbumin, a protein that has a function in calcium buffering during synaptic transmission, are introduced. Two of the main methods to measure STP and parvalbumin will be clarified in the Methods section. The closing section of this general introduction contains a description of the scope of this thesis.

DEVELOPMENT OF THE HUMAN AUDITORY SYSTEM

During the 1st to 13th week of the embryonic period the otic placode is formed out of a thickening of the epidermis on the lateral side of the head. Next, the otic vesicle or otocyst is formed (Streeter 1906; O’Rahilly 1963). The otic vesicle divides into vestibular and cochlear segments, and the cochlear portion elongates to become a tubular structure: the cochlear duct. By the 8th fetal week, the duct has its full two and a half turns. In the following weeks the duct becomes surrounded by cartilage and a fluid-filled space is formed between this shell and the coiled cochlear duct. The organ of Corti appears at the 9th week (Bredberg 1968; Lavigne-Rebillard and Pujol 1987). The characteristic three rows of outer hair cells and a single row of inner hair cells are formed next and a beginning of a tectorial membrane can be seen. In parallel, the development of the cochlear nerve starts from the 4th week with the formation of the statoacoustic ganglion that becomes the spiral ganglion. These immature neurons will contact the developing hair cells by the 10th to 12th week (Pujol and Lavigne-Rebillard 1985). All of the auditory nuclei in the brainstem and the cortical plate are identifiable by the 7th to 8th fetal weeks (Cooper 1948). The cochlea matures rapidly, and by the end of the second trimester (14th to 26th fetal weeks), its anatomy is adult-like. By week 22, the process of myelination within the cochlea begins and from the 24th week, thin myelin sheaths and Schwann cells become visible (Lavigne-Rebillard and Pujol 1988). The nuclei of

the brainstem auditory pathway are well delineated early in the second trimester, and they rapidly increase in size as the second trimester progresses.

At the beginning of the third trimester (27th to 29th fetal weeks), myelin is first seen in the cochlear nerve (Moore and Linthicum 2001). Not until a few weeks before full term birth, generally, functional cochlear maturity is achieved (Moore and Linthicum 2007).

DEVELOPMENT OF THE RODENT MNTB AND THE CALYX OF HELD SYNAPSE

The auditory brainstem contains one of the largest synapses of the brain, which is formed between the globular bushy cells of the cochlear nucleus and the principal neurons of the MNTB (Figure 1). This synapse has a calyx-like shape that was described for the first time by Hans Held (Held 1893), hence the name “calyx of Held synapse”. Similar to other giant synapses such as the squid giant synapse or the neuromuscular junction, the calyx of Held synapse has been a very popular synapse amongst physiologists for studying synaptic transmission, and especially presynaptic transmitter release mechanisms. Commonly, brain

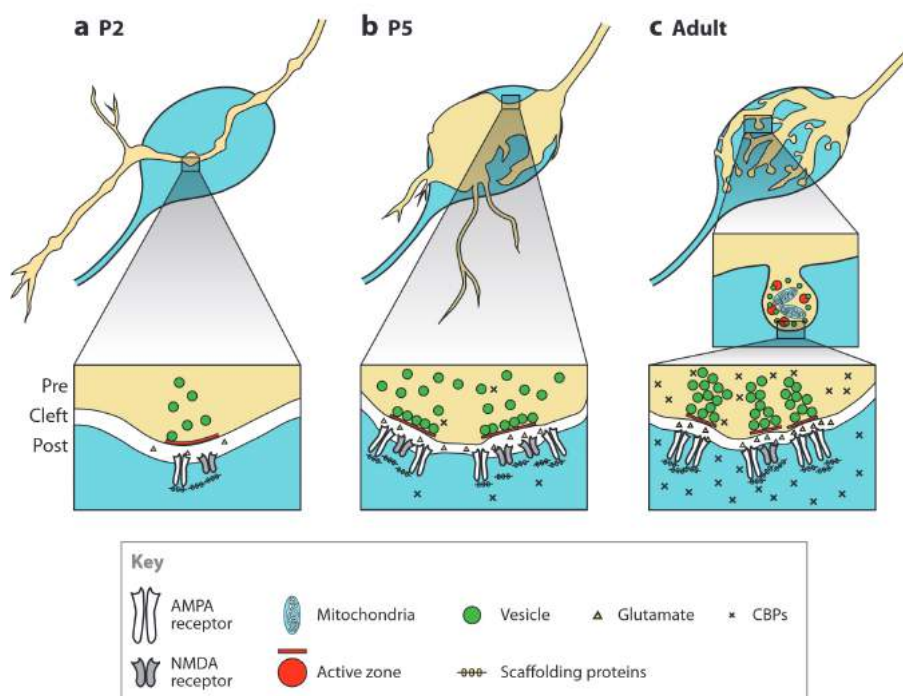


Figure 1. Developmental stages of a rodent calyx synapse. A. P2: the first contact with the postsynaptic principal cell (blue) is made. Protocalyx. B. P5: cup-shaped immature calyx. C. Adult: mature calyx (from: (Borst and Soria van Hoeve 2012))

slices of rodents are used for this purpose (*ex vivo recordings*), since the calyx synapse can be visualized under a microscope, making it possible to make direct electrical recordings from both the presynaptic and the postsynaptic side (Forsythe 1994; Borst et al. 1995; Borst and Sakmann 1996). Alternatively, *in vivo* recordings can be used to study synaptic transmission along this synapse in alive animals (Guinan and Li 1990; Mc Laughlin et al. 2008; Rodriguez-Contreras et al. 2008; Englitz et al. 2009; Lorteije et al. 2009). The fact that much of the development of the auditory brainstem takes places after birth in rodents makes them an ideal choice for developmental studies. The availability of transgenic mice is also an important argument for choosing rodents. Rodents and humans have in many respects a comparable physiology and anatomy of the auditory brainstem, and rodent studies are therefore likely to be informative about the human auditory system.

After 19-20 days of pregnancy, a mouse will deliver on average 6 pups. In contrast to humans, mice cannot yet hear when they are born. During the first 9-10 days after birth, they cannot yet hear air-borne sounds, because, among others, of the presence of mesenchymal embryonic tissue in the middle ear, and the external ear canal is still closed. After this period the ear canal opens, the middle ear becomes air-filled, and the pup will gradually become sensitive to airborne sound from postnatal day (P) 12-13 (Blatchley et al. 1987; Geal-Dor et al. 1993). Hearing is not yet fully mature during the next weeks, as the neuronal circuitry is still developing.

The development of the calyx of Held synapse has been relatively well studied, among others because of its well-defined function, and because of the fact that the postsynaptic principal neurons can be readily identified by their eccentric nucleus, which is already present prenatally, well before the calyx of Held synapse forms. The earliest synaptic contacts between cells of the cochlear nucleus and the principal neurons of the MNTB are formed in the mouse at embryonic day 17 (E17) (Hoffpauir et al. 2010). The initial innervation is divergent, and many of these contacts are dendritic (Hoffpauir et al. 2006b; Rodriguez-Contreras et al. 2008; Hoffpauir et al. 2010). The calyx of Held synapse is formed at about postnatal day 2-3 (P2-3) in rodents (Kandler and Friauf 1993; Kil et al. 1995; Rodrigues and Oertel 2006), when a presumably pre-existing somatic contact expands to form a protocalyx (Figure 2). The early calyx has many collaterals, which can contact nearby principal neurons (Rodriguez-Contreras et al. 2008). Afterwards, the calyx undergoes major morphological changes and develops from a cup-shaped form into the characteristic calyx-like structure (Morest 1968; Kandler and Friauf 1993; Kil et al. 1995). In the adult situation, a postsynaptic principal cell is typically contacted by a single calyx of Held, although during early development principal neurons can receive multiple large inputs (Bergsman et al. 2004; Hoffpauir et al. 2006a)(Figure 1). The mechanisms that ensure that a principal neuron receives only a single calyx of Held are still unclear. In the adult brain the calyx of Held covers more than half of the surface of the principal neuron (Figure 1, panel C). The presence of the (adult) calyx (Jean-Baptiste and Morest 1975; Pasic et al. 1994) is of great importance for the proper development and survival of the principal neuron (Maricich et al. 2009; Toyoshima et al. 2009).

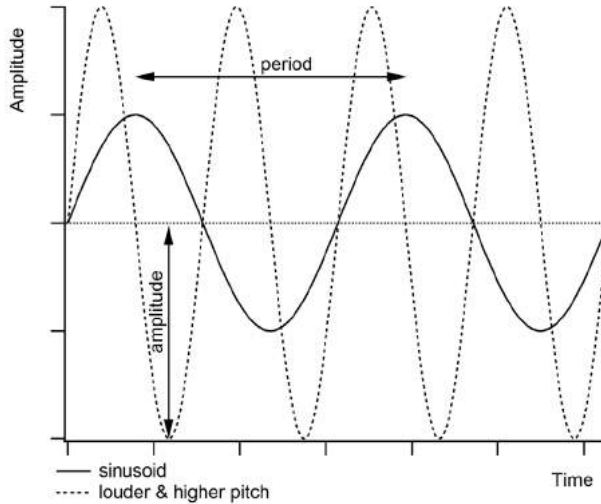


Figure 2. Sound pressure wave.

The presynaptic terminal contains a large vesicle pool, many release sites, and many proteins that transport vesicles to the release sites, buffer calcium and manage the reuptake of neurotransmitter (von Gersdorff and Borst 2002). These features ensure that the calyx synapse exhibits fast and reliable transmission.

PHYSIOLOGY OF SOUND DETECTION

Sounds can vary in amplitude, which we perceive as variations in loudness, and in frequency (longer or shorter period), which gives variations in pitch (Figure 2). Sounds can be as loud as 130 decibel sound pressure level (dB SPL), at which point they become painful, but humans with good hearing can detect sounds as low as 0 dB, and have a hearing range from about 20 Hz to 20 kHz.

The cochlea has an essential role in sound detection. It is filled with fluid: perilymph in the scala vestibuli and the scala tympani and endolymph in the scala media. The scala vestibuli and the scala tympani spiral towards the tip of the cochlea where they meet in the helicotrema. Pressure changes resulting from sounds set up a traveling wave along the basilar membrane, on which the organ of Corti, which includes hair cells and their support structures, rest (Figure 3). The hair cells have hair bundles that are embedded in the tectorial membrane. The traveling wave causes the hair bundles to bend, resulting in a membrane conductance change in the hair cells. Each inner hair cell is innervated by multiple spiral ganglion cells (type-I). Inner hair cells are the principal sensory receptors of hearing, whereas outer hair cells affect the sensitivity of the cochlea owing to their ability to vary in length. Because of the unique design of the cochlea, the different frequency components

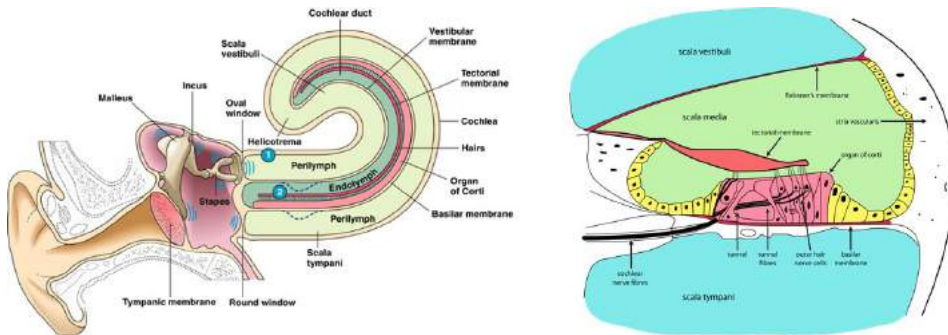


Figure 3. Left. The cochlea showing the tube-like structure and path of the travelling wave in the perilymph of scala vestibuli and scale tympani from oval window to round window. Right. Cross section: in between the scala vestibuli and tympani (in blue) the scala media (in green) is situated with the basilar membrane, tectorial membrane, outer and inner hair cells which are connected to the cochlear nerve.

(from: <http://www1.appstate.edu/~kms/classes/psy3203/Ear/cochlea4.jpg>)

of a complex sound will excite a different and specific location within the, on average, 42 mm long cochlea (Erixon et al. 2009). High frequency sounds generate a wave on the basilar membrane with a peak amplitude close to the base of the cochlea; consequently, these sounds excite hair cells at the base of the cochlea. On the other hand, low frequency sounds excite hair cells preferentially at the apex of the cochlea. This spatial organization of frequencies is called ‘tonotopy’. This tonotopy is found throughout the whole central auditory system (Figure 4).

SOUND LOCALIZATION

For sound localization in the horizontal plane, the auditory system relies on small differences in both arrival time and in loudness of sounds arriving at both ears. For frequencies below 3 kHz interaural time differences (ITDs) are the dominant cue to localize the source; above 3 kHz, interaural intensity differences (ILDs) become dominant. Humans can detect interaural time differences as short as 10 μ s. The longest time differences are in the order of only 700 μ s, which is the width of the head divided by the speed of sound in air (~340 m/s). In order to decode these subtle differences, highly specialized synapses, like the calyx synapse, are employed in the central auditory system. At frequencies above approximately 2 kHz the head progressively becomes an acoustical obstacle; the wavelength of the sound is too short to bend around it. The sound intensity at the ear closest to the source will therefore be higher than at the other ear. Our head thus creates an acoustic ‘shadow’ effect that can be detected by the MNTB and the Lateral Superior Olive (LSO). The LSO receives ipsilateral excitatory, glutamatergic input from the cochlear nucleus and inhibitory, glycinergic input

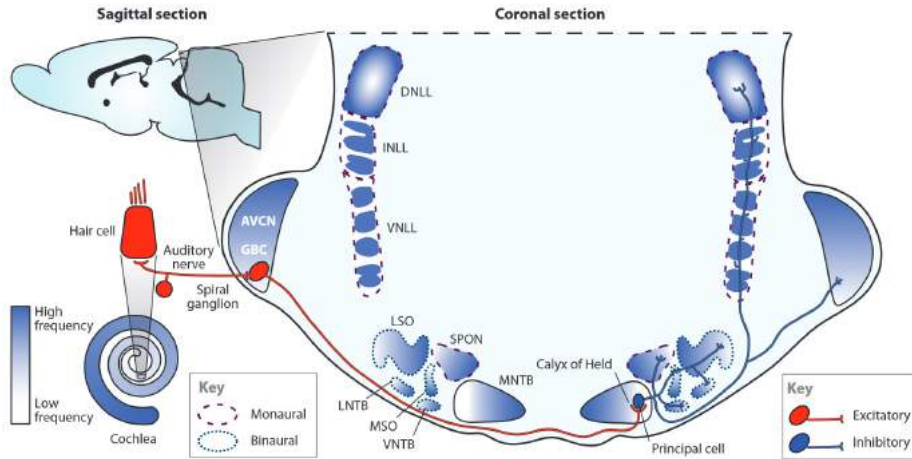


Figure 4. Central auditory pathway of a rat. MNTB is a sign-inverting nucleus: excitatory signal becomes an inhibitory signal towards different other auditory nuclei. The calyx of Held is a giant axosomatic synapse within the MNTB. Tonotopy is seen throughout the whole central auditory nuclei. (Borst and Soria van Hoeve 2012)

from the contralateral MNTB. The calyx of Held synapse thus acts as a fast sign-inverting relay synapse. On the side nearest to the stimulus the excitatory input typically exceeds the inhibitory input, allowing the LSO neurons to fire, whereas on the other side the neurons are inhibited (Figure 4). Figure 4 also illustrates that the LSO is not the only target of the principal neurons of the MNTB, but that the MNTB projects to most other ipsilateral auditory nuclei in the brainstem, including to nuclei that are not involved in sound localization.

IMPACT OF ELECTRICAL ACTIVITY ON THE DEVELOPMENT OF THE AUDITORY SYSTEM

The development of the auditory brainstem is determined by both electrical activity-dependent and activity-independent factors. Several morphogenetic processes do not need electrical activity and are activity independent, whereas finetuning of synaptic connections is dependent of electrical activity, either spontaneous or evoked by sound. Activity-dependent and activity-independent factors interact during the formation and maturation of the synaptic connections of the rodent auditory system (for review: (Friauf and Lohmann 1999)). The first 14 postnatal days of a rodent mark a period where the central auditory nuclei in the brainstem are relatively sensitive to activity-dependent changes. Deprivation of activity during this period can have substantial consequences. For example, unilateral cochlear ablation of wild type mouse at P5 results in ~60% loss of neurons in the anterior ventral cochlear nucleus

(AVCN), but only 1% at P14 (Mostafapour et al. 2000). Cochlear ablation also changes neurotransmitter, receptor and amino acid levels in the cochlear nucleus (Godfrey et al. 2014), and modifies inhibition in the inferior colliculus (IC) (Vale et al. 2004). Cochlear ablation is a drastic procedure, which affects both spontaneous and sensory-evoked activity. In an aural deprivation model, in which an ear is plugged, only sensory-evoked activity is reduced or blocked. Aural deprivation can distort tonotopic maps, disrupt binaural integration, reorganize the neural network and change synaptic transmission in the primary auditory cortex or at lower levels of the auditory system (Chen and Yuan 2015). When only one ear is plugged, the acoustical input is attenuated and delayed, thereby changing the ILDs and ITDs corresponding to each spatial location. Studies in developing barn owls (Knudsen et al. 1984; Gold and Knudsen 2000) and ferrets (Keating et al. 2015) show a shift of neuronal sensitivity in a way that the effect of the monaural occlusion is compensated, but only within a certain critical period. These studies show that after the end of this critical period, the changes are mostly irreversible (Takesian and Hensch 2013). However, the closure time of the critical period is plastic and can be stretched by activity and stimulation, and also depends on the formation of structures like perineuronal nets (PNNs). PNNs are specialized extracellular matrix structures that are thought to contribute to the closure of the critical period in for example mouse barrel cortex, in developing amygdala and also in visual cortex (McRae et al. 2007; Levelt and Hubener 2012; Takesian and Hensch 2013). PNNs are found mostly at parvalbumin-containing interneurons; they can capture the homeoprotein Otx2, which is a regulator of cortical plasticity in amongst others the visual and auditory cortex (Spatazza et al. 2013). Knocking down Otx2 synthesis can reactivate plasticity at the visual cortex even after closure of the critical period (Spatazza et al. 2013). Since Otx2 is also available at the auditory cortex, it could be equally important in managing critical periods in the auditory system. Other molecular markers have an influence on critical periods as well. Growth factors like neurotrophins are present in the MNTB and therefore may play a role in the survival of synapses in the period before hearing onset (Hafidi et al. 1996). Three types of neurotrophic tyrosine kinase receptors (TrkA, TrkB and TrkC) are expressed in the MNTB (Hafidi et al. 1996). Because TrkB immunoreactivity is strong, especially before hearing onset, it has been suggested that it could be involved in the modulation or maintenance of postsynaptic physiology (Hafidi et al. 1996).

The phenomenon that duration of critical periods can be stretched by stimulation is important in the assessment of humans with severe hearing loss. Adults with congenital deafness who have worn a conventional hearing aid, are more likely to obtain better speech perception outcomes with a cochlear implant (CI) compared to adults with a non-stimulated auditory system (Caposecco et al. 2012). Due to the stimulation the auditory system's ability to adapt is maintained, and the patient will be able to adapt better to hearing with a CI. Therefore, it is better to start intracochlear stimulation as soon as possible, especially in congenitally deaf subjects (Kral 2013). Early electrical stimulation allows the auditory system to stay closer to its normal developmental trajectory.

SHORT TERM PLASTICITY

In a system with high temporal precision such as the sound localization circuitry of the auditory system, ideally, every action potential is transmitted the exact same way and transmission is independent of recent history. To meet these demands, the synapse contains a readily releasable pool (RRP) of neurotransmitter vesicles (Liley and North 1953; Rizzoli and Betz 2005; Habets and Borst 2007). Release probability (P_r) is a measure for the ‘eagerness’ of the vesicles to be released. The Pr of vesicles in the RRP is not uniform, and ‘reluctant’ and ‘willing’ vesicles can be discriminated (Neher 1998a; Wu and Borst 1999). Additional parameters that are important for short-term plasticity (STP) are the number of vesicles (N) and the quantal size (q), which is the size of the postsynaptic response following the release of a single vesicle (or quantum). The size of the EPSP depends on the number of vesicles (N) and the probability of release of such a vesicle (P_r) and the quantal size as follows:

$$\text{EPSP} = N \cdot P_r \cdot q$$

When either of these parameters is affected, the EPSP size will be altered. Activity-dependent changes in the size of the EPSP can thus be used to quantify STP (Figure 5). A decrease of synaptic strength is called “short-term depression” and the opposite is called “short-term facilitation” (Zucker 1989). An important, presynaptic cause of synaptic depression is depletion of the vesicle pool due to sustained activity (Zucker 1989; Neher 1998b; Schneggenburger et al. 2002). The opposite can be seen as well. At short intervals after an action potential, the presynaptic $[Ca^{2+}]$ has not yet returned to its basal level. This so-called ‘residual’ calcium may bind to a high-affinity calcium sensor that is separate from the low-affinity calcium sensor triggering release, and thus facilitate vesicle release (Jackman et al. 2016).

The calyx of Held synapse acts as a sign-inverting relay synapse; a presynaptic action potential is typically followed by a postsynaptic action potential with only occasionally a failure (Lorteije et al. 2009). Nevertheless it is possible to induce synaptic depression by stimulating the synapse in a brain slice at a high frequency (Forsythe 1994; Borst et al. 1995; Lorteije et al. 2009). STP can also be observed *in vivo*, although there are few studies that study STP in a quantitative manner. In this thesis, STP in the developing MNTB is studied around hearing onset. The hearing onset is a defining moment in development; many different processes change around hearing onset (Figure 6) such as the number of active zones (Sätzler et al. 2002; Taschenberger et al. 2002; Dondzillo et al. 2010), or a decrease in NMDA receptor expression (Futai et al. 2001). The expression of proteins that regulate calcium buffering, like the slow binding protein parvalbumin is thought to change as well (Lohmann and Friauf 1996). Since parvalbumin is studied in Chapter 4 of this thesis, a short introduction is given in the following section.

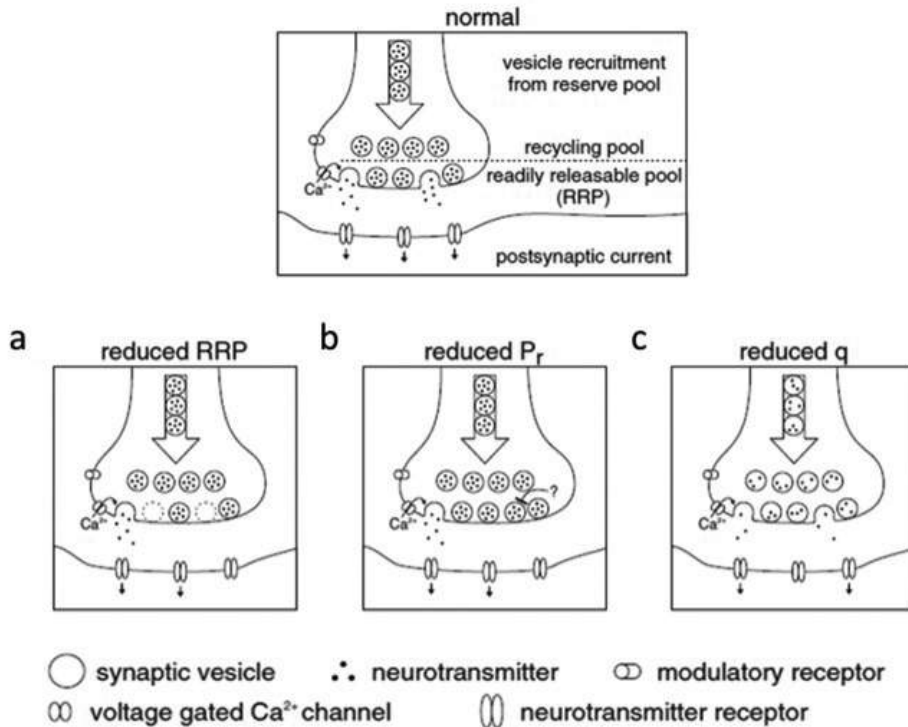


Figure 5. Synaptic depression. Normal situation compared to situation with reduced N, P_r or q. Reduction in either N, P_r or q leads to depression.

(modified from: Friauff et al. Synaptic Plasticity in the Auditory System: a Review. 2015. DOI 10.1007/s00441-015-2176-x)

PARVALBUMIN

One of the proteins that buffer calcium ions in neurons is parvalbumin. Parvalbumin is a slow calcium-binding protein that can prevent build-up of residual calcium, thus contributing to keeping the $[Ca^{2+}]$ low and reducing synaptic facilitation. In skeletal muscles, parvalbumin has a role in the performance of rapid, phasic movements (Schwaller et al. 1999). Although parvalbumin is abundantly available in fast-contracting and -relaxing skeletal muscles, a parvalbumin KO-mouse has a mild phenotype with respect to the contraction-relaxation cycle of fast-twitch muscle fibers (Schwaller et al. 1999). Parvalbumin is also present in the MNTB. After P8 parvalbumin is present in the somata of MNTB cells and also in cochlear nucleus and in other nuclei of the superior olivary complex of rats (Lohmann and Friauf 1996). No distinction between presynaptic terminal and postsynaptic principal cell was made. In this thesis we have the possibility to distinguish the pre- and postsynaptic compartment using immunofluorescence and confocal imaging, as described in the Methods section.

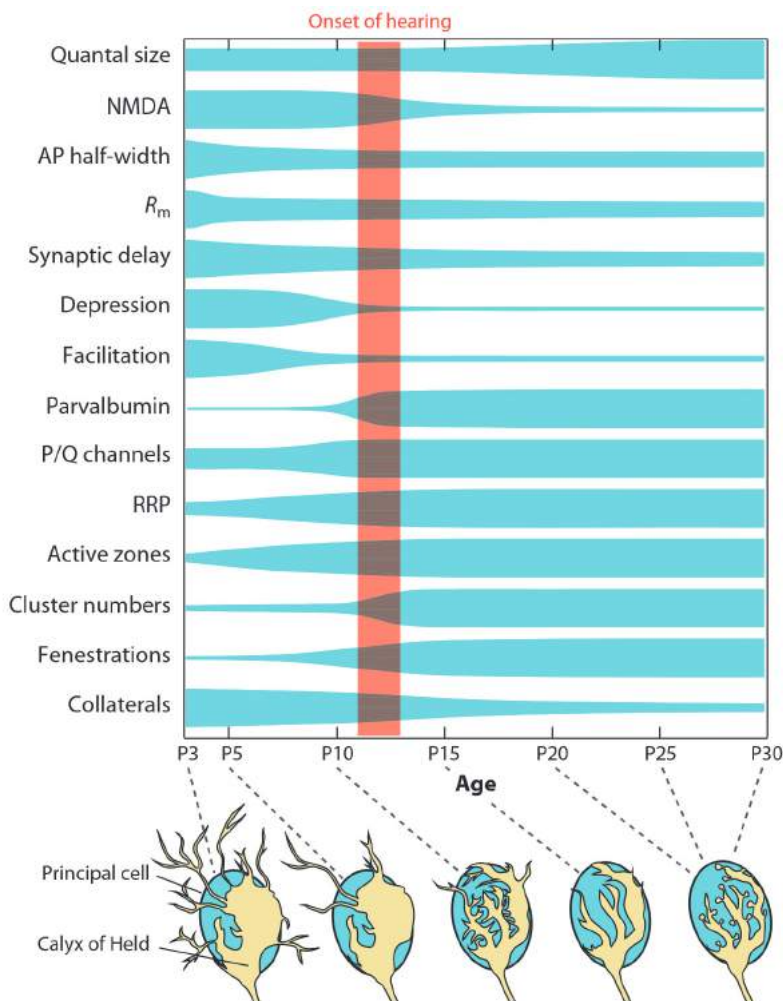


Figure 6. Developmental changes in the calyx of Held synapse. Next to the morphological changes, many other processes change during the first 2 to 3 weeks postnatally. From: (Borst and Soria van Hoeve 2012)

METHODS

Several methods to study STP are available. In this thesis the extracellular recording will be mainly used, and a brief introduction to this method is therefore provided below.

In the section about “measuring parvalbumin” it is explained how parvalbumin can be visualized by the use of a combination of immunocytochemistry and laser scanning confocal microscopy.

MEASURING NEURONAL ACTIVITY AND SHORT TERM PLASTICITY: EXTRACELLULAR RECORDING

A ventral approach was developed to gain access to the ventral part of the brainstem, where the MNTB is located, in isoflurane-anesthetized neonatal rat pups (Rodriguez-Contreras et al. 2008; Rodriguez-Contreras et al. 2014). To reach the skull base, the larynx must be removed and the remaining distal end of the trachea is intubated. During the remaining part of the experiment, the animal is mechanically ventilated. In the skull base a small craniotomy can be made to visualize the basilar artery and the anterior inferior cerebellar artery (AICA). Typically, the MNTB can be found 400-500 μm rostrally from the AICA and 400-500 μm laterally from the basilar artery.

Once access has been obtained surgically, a glass micropipette can be lowered into the ventral brainstem, and placed very close to the cell. This so-called juxtacellular recording is used to gather information about the synapse without interfering with the intracellular environment (Lorteije et al. 2009). It is a fast and relatively straightforward method that allows the researcher to record multiple cells sequentially with the same pipette. Especially in the MNTB it is a very useful recording method because of the size of the presynaptic terminal, which allows to record characteristic complex waveforms (Guinan and Li 1990; Lorteije et al. 2009). This waveform consists of three distinct parts: a prespike, an excitatory postsynaptic potential (EPSP) and an action potential (AP) (Figure 7).

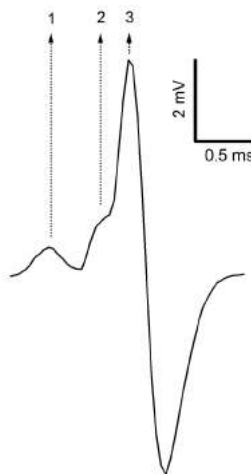


Figure 7. Complex waveform. 1: prespike; 2: Excitatory Postsynaptic Synaptic Potential (EPSP); 3: postsynaptic action potential.

The shape of the waveform can provide much information about the synaptic transmission. Reliability of the synaptic transmission can be studied by measuring the fraction of transmission failures (Lorteije et al. 2009). For this thesis, firing patterns at different ages, changes in the characteristics of the waveform and the influence of recent activity on the shape of the waveform were studied. For instance, by plotting the EPSP against inter-spike-interval, the recovery from synaptic depression can be visualized.

MEASURING PARVALBUMIN: IMMUNOFLOURESCENCE AND CONFOCAL IMAGING

To study the subcellular localization of parvalbumin in a brainstem slice, high resolution microscopy is necessary. In this thesis parvalbumin was studied using immunofluorescent dyes and laser scanning confocal microscopy. An advantage of confocal microscopy is the ability to reduce blur by reducing background signal away from the focal plane. Therefore, thick specimens, like brainstem slices through the MNTB, can be studied more easily and a clear distinction between pre- and postsynaptic part can be made. The brightness of the fluorescence signal can give an indication of the concentration of the labelled protein, but quantification of these data is difficult and comparison between different slices is somewhat tricky. Therefore, immunocytochemical methods can only provide an indicative estimate of the parvalbumin concentration at the MNTB.

SCOPE OF THE THESIS

The main focus of this thesis is to study the maturation of the central auditory pathway, and, more specifically, the developmental changes in synaptic transmission in the Medial Nucleus of the Trapezoid Body. We are interested to find out how the calyx of Held synapse becomes a reliable relay synapse.

In Chapter 2 the origin of the spontaneous activity in the auditory system is studied. We study a group of cells in the cochlea that acts as an activity-generator and the relation between the firing pattern at the level of the auditory brainstem and in the cochlea.

In Chapter 3 the developmental changes in spontaneous activity are studied. We study synaptic transmission and short term plasticity at the calyx synapse using *in vivo* juxtacellular electrophysiological recordings in rats and with whole-cell recordings in slices at different ages before and after hearing onset.

Chapter 4 gives insight into the role of parvalbumin in synaptic transmission and its possible role in short-term synaptic plasticity. We compare parvalbumin KO mice (Schwaller et al. 1999) and wild-type littermates in *in vivo* electrophysiological experiments. The expression of parvalbumin is studied with the use of immunohistology on brainstem slices of the MNTB and confocal fluorescence microscopy. The question to what extent parvalbumin plays an important role in the changes in STP around the onset of hearing is addressed. We

quantify the amount of parvalbumin before and directly after hearing onset and at a young-adult age in the calyx synapse of both rat and mouse.

Chapter 5 contains a general discussion about the studies and their limitations. The possibilities for future studies are highlighted.

REFERENCES

1. Bergsman JB, De Camilli P and McCormick DA (2004). Multiple large inputs to principal cells in the mouse medial nucleus of the trapezoid body. *J Neurophysiol* **92**: 545-552 http://www.ncbi.nlm.nih.gov/entrez/query.fcgi?cmd=Retrieve&db=PubMed&opt=Citation&list_uids=15212444.
2. Blatchley BJ, Cooper WA and Coleman JR (1987). Development of auditory brainstem response to tone pip stimuli in the rat. *Brain-Res* **429**: 75-84 [http://dx.doi.org/10.1016/0165-3806\(87\)90140-4](http://dx.doi.org/10.1016/0165-3806(87)90140-4).
3. Borst JGG, Helmchen F and Sakmann B (1995). Pre- and postsynaptic whole-cell recordings in the medial nucleus of the trapezoid body of the rat. *J Physiol* **489**: 825-840 <http://dx.doi.org/10.1113/jphysiol.1995.sp021095>.
4. Borst JGG and Sakmann B (1996). Calcium influx and transmitter release in a fast CNS synapse. *Nature* **383**: 431-434 <http://www.nature.com/nature/journal/v383/n6599/pdf/383431a0.pdf>.
5. Borst JGG and Soria van Hoeve J (2012). The calyx of Held synapse: from model synapse to auditory relay. *Annual Review of Physiology* **74**: 199-224 <http://dx.doi.org/10.1146/annurev-physiol-020911-153236>.
6. Bredberg G (1968). Cellular pattern and nerve supply of the human organ of Corti. *Acta Otolaryngol* **236**: Suppl 236:231+ <http://dx.doi.org/10.1001/archotol.1965.00760010464003>.
7. Caposecco A, Hickson L and Pedley K (2012). Cochlear implant outcomes in adults and adolescents with early-onset hearing loss. *Ear Hear* **33**: 209-220 <http://dx.doi.org/10.1097/AUD.0b013e31822eb16c>.
8. Chen Z and Yuan W (2015). Central plasticity and dysfunction elicited by aural deprivation in the critical period. *Front Neural Circuits* **9**: 26 <http://dx.doi.org/10.3389/fncir.2015.00026>.
9. Cooper E (1948). The development of the human auditory pathway from the cochlear ganglion to the medial geniculate body. *Acta Anat* **5**: 99-122.
10. Dondzillo A, Sätzler K, Horstmann H, Altmann WD, Gundelfinger ED and Kuner T (2010). Targeted three-dimensional immunohistochemistry reveals localization of presynaptic proteins Bassoon and Piccolo in the rat calyx of Held before and after the onset of hearing. *J Comp Neurol* **518**: 1008-1029 <http://dx.doi.org/10.1002/cne.22260>.
11. Englitz B, Tolnai S, Tytlt M, Jost J and Rübsamen R (2009). Reliability of synaptic transmission at the synapses of Held in vivo under acoustic stimulation. *PLoS One* **4**: e7014 <http://dx.doi.org/10.1371/journal.pone.0007014>.
12. Erixon E, Hogstrop H, Wadin K and Rask-Andersen H (2009). Variational Anatomy of the Human Cochlea: Implications for Cochlear Implantation. *Otology & Neurotology* **30**: 14-22.
13. Forsythe ID (1994). Direct patch recording from identified presynaptic terminals mediating glutamatergic EPSCs in the rat CNS, *in vitro*. *J Physiol* **479**: 381-387 <http://dx.doi.org/10.1113/jphysiol.1994.sp020303>.
14. Friauf E and Lohmann C (1999). Development of auditory brainstem circuitry. Activity-dependent and activity-independent processes. *Cell Tissue Res* **297**: 187-195.
15. Futai K, Okada M, Matsuyama K and Takahashi T (2001). High-fidelity transmission acquired via a developmental decrease in NMDA receptor expression at an auditory synapse. *J Neurosci* **21**: 3342-3349 <http://www.jneurosci.org/cgi/content/full/21/10/3342>.

16. Geal-Dor M, Freeman S, Li G and Sohmer H (1993). Development of hearing in neonatal rats: air and bone conducted ABR thresholds. *Hear Res* **69**: 236-242 [http://dx.doi.org/10.1016/0378-5955\(93\)90113-F](http://dx.doi.org/10.1016/0378-5955(93)90113-F).
17. Godfrey DA, Jin YM, Liu X and Godfrey MA (2014). Effects of cochlear ablation on amino acid levels in the rat cochlear nucleus and superior olive. *Hear Res* **309**: 44-54 <http://dx.doi.org/10.1016/j.heares.2013.11.005>.
18. Gold JI and Knudsen EI (2000). Abnormal auditory experience induces frequency-specific adjustments in unit tuning for binaural localization cues in the optic tectum of juvenile owls. *J Neurosci* **20**: 862-877 <http://www.jneurosci.org/content/20/2/862.long>.
19. Guinan JJ, Jr. and Li RY-S (1990). Signal processing in brainstem auditory neurons which receive giant endings (calyces of Held) in the medial nucleus of the trapezoid body of the cat. *Hearing Research* **49**: 321-334 [http://dx.doi.org/10.1016/0378-5955\(90\)90111-2](http://dx.doi.org/10.1016/0378-5955(90)90111-2).
20. Habets RLP and Borst JGG (2007). Dynamics of the readily releasable pool during post-tetanic potentiation in the rat calyx of Held synapse. *J Physiol* **581**: 467-478 http://www.ncbi.nlm.nih.gov/entrez/query.fcgi?cmd=Retrieve&db=PubMed&dopt=Citation&list_uids=17363387
21. Hafidi A, Moore T and Sanes DH (1996). Regional distribution of neurotrophin receptors in the developing auditory brainstem. *J Comp Neurol* **367**: 454-464 <http://www.ncbi.nlm.nih.gov/htbin-post/Entrez/query?db=m&form=6&dopt=r&uid=8698904>.
22. <http://www.ncbi.nlm.nih.gov/htbin-post/Entrez/query?db=m&form=6&dopt=r&uid=8698904>.
23. Held H (1893). Die centrale Gehörleitung. *Archiv für Anatomie und Physiologie, Anatomie Abtheil.* 201-248.
24. Hoffpauir B, Grimes J, Mathers P and Spirou G (2006a). Synaptogenesis of the Calyx of Held: Rapid Onset of Function and One-to-One Morphological Innervation. *the Journal of Neuroscience* **26**: 5511-5523.
25. Hoffpauir BK, Grimes JL, Mathers PH and Spirou GA (2006b). Synaptogenesis of the calyx of Held: rapid onset of function and one-to-one morphological innervation. *J Neurosci* **26**: 5511-5523 <http://www.jneurosci.org/cgi/content/full/26/20/5511>.
26. Hoffpauir BK, Kolson DR, Mathers PH and Spirou GA (2010). Maturation of synaptic partners: functional phenotype and synaptic organization tuned in synchrony. *J Physiol* **588**: 4365-4385 <http://onlinelibrary.wiley.com/doi/10.1113/jphysiol.2010.198564/full>
27. also see: <http://onlinelibrary.wiley.com/doi/10.1113/jphysiol.2010.200089/full>.
28. Jackman SL, Turecek J, Belinsky JE and Regehr WG (2016). The calcium sensor synaptotagmin 7 is required for synaptic facilitation. *Nature* **529**: 88-91 <http://dx.doi.org/10.1038/nature16507>.
29. Jean-Baptiste M and Morest DK (1975). Transneuronal changes of synaptic endings and nuclear chromatin in the trapezoid body following cochlear ablations in cats. *J. Comp. Neur.* **162**: 111-134 <http://www3.interscience.wiley.com/cgi-bin/fulltext/109685039/PDFSTART>.
30. Kandler K and Friauf E (1993). Pre- and postnatal development of efferent connections of the cochlear nucleus in the rat. *Journal of Comparative Neurology* **328**: 161-184 <http://www3.interscience.wiley.com/cgi-bin/fulltext/109692752/PDFSTART>.
31. Keating P, Dahmen JC and King AJ (2015). Complementary adaptive processes contribute to the developmental plasticity of spatial hearing. *Nat Neurosci* **18**: 185-187 <http://dx.doi.org/10.1038/nn.3914>.
32. Kil J, Kageyama GH, Semple MN and Kitzes LM (1995). Development of ventral cochlear nucleus projections to the superior olivary complex in gerbil. *J Comp Neurol* **353**: 317-340 <http://www3.interscience.wiley.com/cgi-bin/fulltext/109693965/PDFSTART>.
33. Knudsen EI, Esterly SD and Knudsen PF (1984). Monaural occlusion alters sound localization during a sensitive period in the barn owl. *J Neurosci* **4**: 1001-1011 <http://www.jneurosci.org/content/4/4/1001.long>.
34. Kral A (2013). Auditory critical periods: a review from system's perspective.

- Neuroscience* **247**: 117-133 <http://dx.doi.org/10.1016/j.neuroscience.2013.05.021>.
35. Lavigne-Rebillard M and Pujol R (1987). Surface aspects of the developing human organ of Corti. *Acta Otolaryngol Suppl* **436**: 43-50 <http://dx.doi.org/10.3109/00016488709124975>.
 36. Lavigne-Rebillard M and Pujol R (1988). Hair cell innervation in the fetal human cochlea. *Acta Otolaryngol* **105**: 398-402 <http://dx.doi.org/10.3109/00016488809119492>.
 37. Levelt CN and Hubener M (2012). Critical-period plasticity in the visual cortex. *Annu Rev Neurosci* **35**: 309-330 <http://dx.doi.org/10.1146/annurev-neuro-061010-113813>.
 38. Liley AW and North KAK (1953). An electrical investigation of effects of repetitive stimulation on mammalian neuromuscular junction. *Journal of Neurophysiology* **16**: 509-527.
 39. Lohmann C and Friauf E (1996). Distribution of the calcium-binding proteins parvalbumin and calretinin in the auditory brainstem of adult and developing rats. *J Comp Neurol* **367**: 90-109 [http://dx.doi.org/10.1002/\(SICI\)1096-9861\(19960325\)367:1<90::AID-CNE7>3.0.CO;2-E](http://dx.doi.org/10.1002/(SICI)1096-9861(19960325)367:1<90::AID-CNE7>3.0.CO;2-E).
 40. Lorteije JAM, Rusu SI, Kushmerick C and Borst JGG (2009). Reliability and precision of the mouse calyx of Held synapse. *J Neurosci* **29**: 13770-13784 <http://dx.doi.org/10.1523/JNEUROSCI.3285-09.2009>.
 41. Maricich SM, Xia A, Mathes EL, Wang VY, Oghalai JS, Fritzsche B and Zoghbi HY (2009). *Atoh1*-lineal neurons are required for hearing and for the survival of neurons in the spiral ganglion and brainstem accessory auditory nuclei. *J Neurosci* **29**: 11123-11133 <http://www.jneurosci.org/content/29/36/11123.long>.
 42. Mc Laughlin M, van der Heijden M and Joris PX (2008). How secure is *in vivo* synaptic transmission at the calyx of Held? *J Neurosci* **28**: 10206-10219 <http://dx.doi.org/10.1523/JNEUROSCI.2735-08.2008>.
 43. McRae PA, Rocco MM, Kelly G, Brumberg JC and Matthews RT (2007). Sensory deprivation alters aggrecan and perineuronal net expression in the mouse barrel cortex. *J Neurosci* **27**: 5405-5413 <http://dx.doi.org/10.1523/jneurosci.5425-06.2007>.
 44. Moore J and Linthicum F (2001). Myelination of the human auditory nerve: Different time courses for Schwann cell and glial myelin. *Ann Otol Rhinol Laryngol* **110**: 655-661.
 45. Moore JK and Linthicum FH, Jr. (2007). The human auditory system: a timeline of development. *Int J Audiol* **46**: 460-478 <http://dx.doi.org/10.1080/14992020701383019>.
 46. Morest DK (1968). The collateral system of the medial nucleus of the trapezoid body of the cat, its neuronal architecture and relation to the olivo-cochlear bundle. *Brain Research* **9**: 288-311 [http://dx.doi.org/10.1016/0006-8993\(68\)90235-7](http://dx.doi.org/10.1016/0006-8993(68)90235-7).
 47. Mostafapour SP, Cochran SL, Del Puerto NM and Rubel EW (2000). Patterns of cell death in mouse anteroventral cochlear nucleus neurons after unilateral cochlea removal. *J Comp Neurol* **426**: 561-571.
 48. Neher E (1998a). Usefulness and limitations of linear approximations to the understanding of Ca^{2+} signals. *Cell Calcium* **24**: 345-357 http://www.ncbi.nlm.nih.gov/entrez/query.fcgi?cmd=Retrieve&db=PubMed&dopt=Citation&list_uids=10091004.
 49. Neher E (1998b). Vesicle pools and Ca^{2+} microdomains: new tools for understanding their roles in neurotransmitter release. *Neuron* **20**: 389-399.
 50. O'Rahilly R (1963). The early development of the otic vesicle in staged human embryos. *J Embryol Exp Morphol* **11**: 741-755 <http://dev.biologists.org/content/11/4/741.abstract>.
 51. Pasic TR, Moore DR and Rubel EW (1994). Effect of altered neuronal activity on cell size in the medial nucleus of the trapezoid body and ventral cochlear nucleus of the gerbil. *J Comp Neurol* **348**: 111-120 <http://dx.doi.org/10.1002/cne.903480106>.
 52. Pujol R and Lavigne-Rebillard M (1985). Early stages of innervation and sensory cell differentiation in the human fetal organ of Corti. *Acta Otolaryngol Suppl* **423**: 43-50 <http://dx.doi.org/10.3109/00016488509122911>.

53. Rizzoli SO and Betz WJ (2005). Synaptic vesicle pools. *Nat Rev Neurosci* **6**: 57-69 http://www.ncbi.nlm.nih.gov/entrez/query.fcgi?cmd=Retrieve&db=PubMed&dopt=Citation&list_uids=15611727
54. Rodrigues ARA and Oertel D (2006). Hyperpolarization-activated currents regulate excitability in stellate cells of the mammalian ventral cochlear nucleus. *J Neurophysiol* **95**: 76-87 http://www.ncbi.nlm.nih.gov/entrez/query.fcgi?cmd=Retrieve&db=PubMed&dopt=Citation&list_uids=16192334.
55. Rodriguez-Contreras A, Shi L and Fu BM (2014). A method to make a craniotomy on the ventral skull of neonate rodents. *J Vis Exp* <http://dx.doi.org/10.3791/51350>.
56. Rodriguez-Contreras A, van Hoeve JS, Habets RLP, Locher H and Borst JGG (2008). Dynamic development of the calyx of Held synapse. *Proc Natl Acad Sci U S A* **105**: 5603-5608 <http://dx.doi.org/10.1073/pnas.0801395105>.
57. Sätzler K, Söhl LF, Bollmann JH, Borst JGG, Frotscher M, Sakmann B and Lübke JHR (2002). Three-dimensional reconstruction of a calyx of Held and its postsynaptic principal neuron in the medial nucleus of the trapezoid body. *J Neurosci* **22**: 10567-10579 <http://www.jneurosci.org/cgi/content/full/22/24/10567>.
58. Schneggenburger R, Sakaba T and Neher E (2002). Vesicle pools and short-term synaptic depression: lessons from a large synapse. *Trends Neurosci* **25**: 206-212 <http://www.ncbi.nlm.nih.gov/htbin-post/Entrez/query?db=m&form=6&dopt=r&uid=11998689>.
59. Schwaller B, Dick J, Dhoot G, Carrolls, Vrbova G, Nicotera P, Pette D, Wyss A, Bluethmann H, Hunziker W and Celio MR (1999). Prolonged contraction-relaxation cycle of fast-twitch muscles in parvalbumin knockout mice. *Am J Physiol* **276**: C395-403 <http://ajpcell.physiology.org/content/276/2/C395.long>.
60. Spatazza J, Lee HH, Di Nardo AA, Tibaldi L, Joliot A, Hensch TK and Prochiantz A (2013). Choroid-plexus-derived Otx2 homeoprotein constrains adult cortical plasticity. *Cell Rep* **3**: 1815-1823 <http://dx.doi.org/10.1016/j.celrep.2013.05.014>.
61. Streeter G (1906). On the development of the membranous labyrinth and the acoustic and facial nerves in the human embryo. *Am J Anat* **6**: 139-165.
62. Takesian AE and Hensch TK (2013). Balancing plasticity/stability across brain development. *Prog Brain Res* **207**: 3-34 <http://dx.doi.org/10.1016/B978-0-444-63327-9.00001-1>.
63. Taschenberger H, Leão RM, Rowland KC, Spirou GA and von Gersdorff H (2002). Optimizing synaptic architecture and efficiency for high-frequency transmission. *Neuron* **36**: 1127-1143 [http://dx.doi.org/10.1016/S0896-6273\(02\)01137-6](http://dx.doi.org/10.1016/S0896-6273(02)01137-6).
64. Toyoshima M, Sakurai K, Shimazaki K, Takeda Y, Shimoda Y and Watanabe K (2009). Deficiency of neural recognition molecule NB-2 affects the development of glutamatergic auditory pathways from the ventral cochlear nucleus to the superior olivary complex in mouse. *Dev Biol* **336**: 192-200 <http://dx.doi.org/10.1016/j.ydbio.2009.09.043>.
65. Vale C, Juiz JM, Moore DR and Sanes DH (2004). Unilateral cochlear ablation produces greater loss of inhibition in the contralateral inferior colliculus. *Eur J Neurosci* **20**: 2133-2140 <http://dx.doi.org/10.1111/j.1460-9568.2004.03679.x>.
66. von Gersdorff H and Borst JGG (2002). Short-term plasticity at the calyx of Held. *Nature Reviews Neuroscience* **3**: 53-64 <http://dx.doi.org/10.1038/nrn705>.
67. Wu LG and Borst JGG (1999). The reduced release probability of releasable vesicles during recovery from short-term synaptic depression. *Neuron* **23**: 821-832 [http://dx.doi.org/10.1016/S0896-6273\(01\)80039-8](http://dx.doi.org/10.1016/S0896-6273(01)80039-8).
68. Zucker RS (1989). Short-term synaptic plasticity. *Annual Review of Neuroscience* **12**: 13-31.



chapter **TWO**

Calcium action potentials in hair cells pattern auditory neuron activity before hearing onset

Nicolas X. Tritsch^{1,*}, Adrián Rodríguez-Contreras^{2,*}, Tom T.H. Crins^{2,3},
Han Chin Wang¹, J. Gerard G. Borst² & Dwight E. Bergles^{1,4}

¹The Solomon H. Snyder Department of Neuroscience, Johns Hopkins School of Medicine,
Baltimore, MD 21205, USA

²Department of Neuroscience, Erasmus MC, University Medical Center Rotterdam,
Rotterdam, The Netherlands

³Department of Otolaryngology, Erasmus MC, University Medical Center Rotterdam,
Rotterdam, The Netherlands

⁴Department of Otolaryngology-Head and Neck Surgery, Johns Hopkins School of Medicine,
Baltimore, MD 21205, USA

* Present address: Department of Biology, City College of New York, New York, NY 10031, USA
(ARC), Department of Neurobiology, Harvard Medical School, Boston, MA 02115, USA (NXT).

* These authors contributed equally to this work

Nature Neuroscience. 2010;13(9):1050-1052

ABSTRACT

We found rat central auditory neurons to fire action potentials in a precise sequence of mini-bursts prior to hearing onset. This stereotyped pattern was initiated by hair cells within the cochlea, which trigger brief bursts of action potentials in auditory neurons each time they fire a Ca^{2+} spike. By generating theta-like activity, hair cells may limit the influence of synaptic depression in developing auditory circuits and promote consolidation of synapses.

INTRODUCTION

Developing sensory systems rely on intrinsically-generated electrical activity to guide the maturation of circuits required for processing sensory information¹. In all sensory modalities examined, this spontaneous activity occurs in the form of discrete bursts of action potentials separated by long periods of quiescence^{1,2}, yet the mechanisms by which burst firing influences diverse aspects of development are largely unknown. In mature circuits, plasticity is enabled by distinct forms of activity^{3,4}, raising the possibility that developing circuits also initiate stereotyped patterns of activity to promote efficient induction of certain signal transduction cascades.

Atrial mammals are born deaf and do not respond to sound until the second postnatal week. Nevertheless, auditory neurons fire bursts of action potentials during the prehearing period^{5,6} that are likely initiated within the developing cochlea. Indeed, recent studies indicate that ATP is released spontaneously from supporting cells in the developing cochlea, which depolarizes inner hair cells (IHCs) and eventually induces trains of action potentials in spiral ganglion neurons (SGNs)^{7,8}.

MATERIALS, METHODS & RESULTS

To define the patterns of activity exhibited by SGNs during this period, we made extracellular recordings from SGNs in cochleae isolated from prehearing rats. Spontaneous activity in SGNs was clustered into discrete bursts that lasted 2.6 ± 0.3 s, contained 15.8 ± 1.8 action potentials and occurred at a frequency of 2.6 ± 0.4 min⁻¹ ($n = 27$; Fig. 1a). In bursts, action potentials did not occur randomly, but were grouped into discrete “mini-bursts” of one to six action potentials (average: 1.6 ± 0.1) that repeated every 100–300 ms (Fig. 1b,c), suggesting

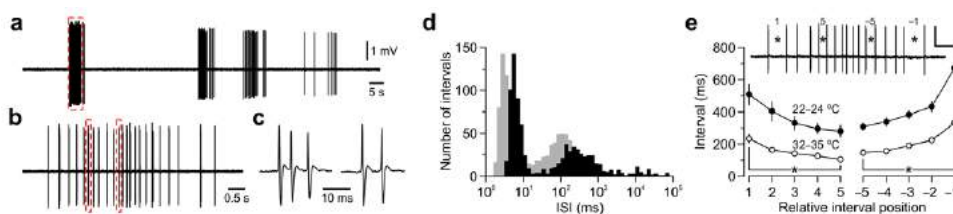


Figure 1. SGNs fire patterned action potential bursts during the prehearing period. (a) *In vitro* extracellular recording from a SGN at room temperature. (b) Detail of dashed red box in a. (c) Detail of mini-bursts highlighted in b. (d) Overlaid log-binned ISI histograms for the neuron in a (black) and a representative cell at near-physiological temperature (32–35 °C, gray). (e) Mean duration (\pm s.e.m.) of intervals separating mini-bursts as a function of their relative position within a burst, for recordings performed at 22–24 °C ($n = 302$ bursts in 23 cochleae) and 32–35 °C ($n = 191$ bursts in 8 cochleae). Inset: Example of relative mini-burst interval position at the beginning (1 and 5) and end (-1 and -5) of a spontaneous burst. Scale: 0.5 mV, 0.4 s. * $P < 0.001$, paired t-test.

that SGNs are under the influence of a pacemaker. This firing pattern was consistent over time and similar between SGNs; inter-spike interval (ISI) histograms had three peaks: one near 10 ms, one between 100 and 300 ms and one broad peak near 10 s ($n = 31$; Fig. 1d and Supplementary Fig. 1), representing the intervals separating action potentials within mini-bursts, intervals separating mini-bursts and long intervals separating bursts, respectively. Another conspicuous feature of this activity was that intervals between mini-bursts consistently decreased and then increased during each burst (Fig. 1e). Similar burst patterns were observed at near physiological temperature ($n = 8$) and in cochleae acutely-isolated from prehearing rats ($n = 10$; Fig. 1d,e and Supplementary Fig. 2). Notably, efferent input was not required to initiate rhythmic activity in SGNs, as this discharge pattern was not altered upon blocking cholinergic transmission at efferent synapses (Supplementary Fig. 3).

To determine the mechanisms responsible for these patterns, we made whole-cell current-clamp recordings from IHCs. Release of ATP from supporting cells periodically depolarized IHCs, which often triggered trains of Ca^{2+} spikes with ISIs of 361 ± 26 ms ($n = 7$) (Fig. 2a,b), similar to the delay between action potentials within mini-bursts in SGNs (356 ± 39 ms, $n = 27$; $P = 0.9$, two-sample t-test). Notably, intervals between Ca^{2+} spikes progressively decreased and then increased during these events (Fig. 2a,c). To determine if IHC Ca^{2+} spikes were sufficient to induce SGN mini-bursts, we recorded simultaneously from IHCs and their synaptically-connected SGNs (Supplementary Fig. 4). Slow depolarization of IHCs triggered trains of Ca^{2+} spikes in IHCs and discrete bursts of action potentials in SGNs ($n = 11$ pairs) (Fig. 2d,e). The vast majority of Ca^{2+} spikes (92 %; $n = 1,634$ spikes) elicited postsynaptic mini-bursts of 2.1 ± 0.1 action potentials (Fig. 2f) separated by 8.0 ± 0.7 ms ($n = 11$), similar to the first peak in ISI histograms (Fig. 1d). Furthermore, intervals separating IHC Ca^{2+} spikes and SGN action potential mini-bursts were indistinguishable (Fig. 2g,h). Thus, IHC Ca^{2+} spikes act as pacemakers to set the timing of action potentials in peripheral auditory neurons before hearing.

To determine whether activity patterns initiated within the cochlea propagate through central auditory nuclei, we made extracellular recordings *in vivo* from principal neurons in the medial nucleus of the trapezoid body (MNTB) (Supplementary Fig. 5), a relay nucleus in the brainstem involved in sound localization⁹. Spontaneous activity in most MNTB neurons ($n = 31/34$, 91 %) in postnatal day (P) 4–8 rats (before hearing), consisted of discrete bursts of action potentials similar to those recorded from SGNs: bursts lasted for 2.6 ± 0.4 s, occurred at a frequency of 3.2 ± 0.3 min⁻¹ and contained 16.5 ± 2.7 action potentials (Fig. 3a). Action potentials within bursts were typically clustered into discrete mini-bursts containing 1.5 ± 0.1 action potentials (Fig. 3b,c), and ISI histograms had distinct peaks near 10 ms, 100–300 ms and 10 s (Fig. 3d and Supplementary Fig. 1). In addition, the intervals between mini-bursts progressively decreased and then increased during each burst (Fig. 3e), a characteristic feature of SGN activity. This firing pattern was observed as early as P1 and was prevalent for most of the postnatal prehearing period (Supplementary Fig. 1). In recordings where pre-

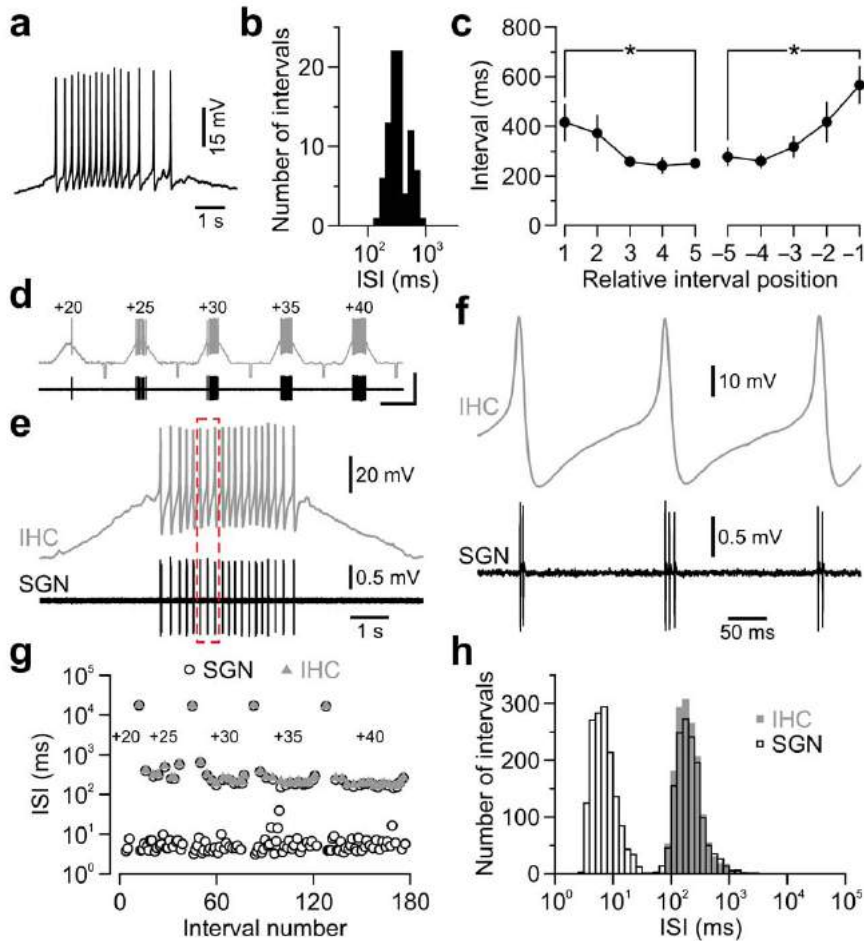


Figure 2. IHC Ca^{2+} spikes initiate action potential mini-bursts in SGNs before hearing onset. (a) Spontaneous burst of Ca^{2+} spikes recorded from an IHC (22–24 °C). (b) Log-binned histogram of intervals separating Ca^{2+} spikes within spontaneous bursts ($n = 7$ IHCs). (c) Mean duration (\pm s.e.m.) of intervals separating Ca^{2+} spikes vs. relative position within a burst. * $P < 0.05$. (d–g) Simultaneous recording from an IHC (whole-cell; gray) and a synaptically-connected SGN (extracellular; black). (d) Continuous paired recording upon 5 consecutive depolarizing current injections of increasing amplitude (20–40 pA). Small hyperpolarizing current steps (–10 pA) were injected every 20 s. Scale bars: 50/2 mV; 10 s. (e) Top: IHC membrane potential ($V_{\text{rest}} = -80$ mV). Bottom: Corresponding postsynaptic SGN firing pattern. (f) Detail of dashed red box in e. (g) Plot of consecutive intervals (log scale) separating IHC Ca^{2+} spikes and SGN action potentials from the recording in d. (h) Superimposed log-binned ISI histograms for all IHC Ca^{2+} spikes and SGN action potentials pooled from 11 paired recordings. Long intervals separating current injections were excluded for clarity.

two

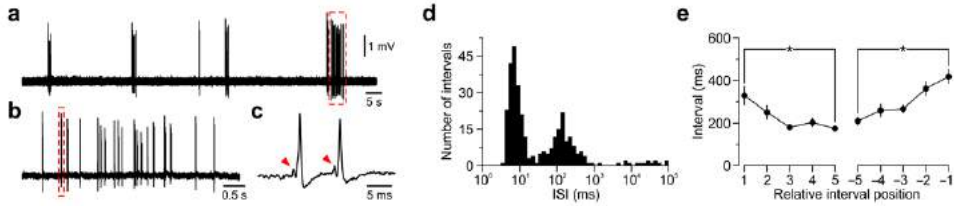


Figure 3. MNTB fire patterned action potential bursts during the prehearing period. (a) *In vivo* extracellular recording from a P5 MNTB neuron. (b) Detail of dashed red box in a. (c) Detail of the mini-burst highlighted in b. Arrowheads indicate pre-spikes. (d) Log-binned ISI histograms for the cell in a. (e) Mean duration (\pm s.e.m.) of mini-burst intervals within bursts ($n = 216$ bursts in 19 units). * $P < 0.003$, paired t-test.

spikes were visible ($n = 16/31$), all action potentials were preceded by a pre-spike in 14 cells (Fig. 3c), and in the remaining two cells, 97 % of action potentials were preceded by a pre-spike, indicating that this activity was induced by synaptic input from the cochlear nucleus¹⁰. Moreover, spontaneously active MNTB neurons were not observed when the contralateral cochlea was removed ($n = 6$; Supplementary Fig. 6), indicating that the patterns of activity exhibited by MNTB neurons *in vivo* are initiated within the cochlea.

To explore whether neurons in other auditory centers exhibit similar activity, we made *in vivo* extracellular recordings from the central nucleus of the inferior colliculus (CIC), a major midbrain nucleus that integrates ascending auditory information. Most recordings from CIC were composed of multiple units that exhibited highly correlated activity ($n = 92/120$ recordings, 77 %), consisting of bouts of action potentials lasting several seconds (Supplementary Fig. 7); the remaining recordings contained either a few isolated spikes or regularly discharging units. The high degree of synchrony among CIC neurons *in vivo* is consistent with ATP-mediated events in the cochlea, which initiate synchronous activity in groups of IHCs in the same region of the organ of Corti^{7,8}. In recordings where action potentials from individual bursting units could be discriminated ($n = 21$), CIC neurons displayed firing patterns similar to those recorded from SGNs and MNTB neurons: action potentials were clustered in discrete bursts of 8.5 ± 1.1 action potentials, which lasted 1.7 ± 0.2 s and occurred at 2.9 ± 0.4 min⁻¹. Although extended mini-bursts were not as frequent, ISI histograms had distinct peaks near 100–300 ms and 10 s, and intervals between mini-bursts progressively shortened and then lengthened during each burst (Supplementary Figs. 1 and 7). Moreover, burst activity in CIC neurons was abolished following bilateral cochlear ablation (Supplementary Fig. 8), providing further evidence that the characteristic activity patterns initiated by Ca²⁺ spikes in cochlear hair cells before hearing propagate through central auditory circuits (see Supplementary Discussion).

Pioneering studies in newborn cats have shown that auditory neurons fire rhythmically in small groups of one to several action potentials every 100–300 ms upon exposure to

loud sound¹². Unexpectedly, the periodicity of this activity was influenced by the intensity but not the frequency of the stimulus, in marked contrast to sharply-tuned, sustained responses observed in adults. Our results suggest that the rhythmic nature of this activity arises from generation of Ca^{2+} spikes in IHCs, which promote transmitter release from immature ribbon synapses¹³, but impose strict limitations on the timing of action potentials in auditory neurons.

Calyceal synapses in the auditory pathway of prehearing animals undergo pronounced synaptic depression in response to repetitive, high frequency stimulation, which eventually prevents EPSPs from inducing action potentials^{9,14}. Thus, clustering activity in mini-bursts is a more efficient means of propagating activity through these developing circuits. Notably, the patterns of activity that occur in the developing auditory system are similar to exogenous stimulation protocols, such as theta burst that reliably induce long-term potentiation of excitatory synapses¹⁵. Repeated initiation of this patterned activity by subsets of IHCs at similar locations within the cochlea could therefore promote the formation and maintenance of tonotopically-arranged connections in auditory centers of the brain.

Note: Supplementary information is available on the Nature Neuroscience website.

ACKNOWLEDGEMENTS

This work was supported by grants from FP6, European Union (EUSynapse, LSHM-CT-2005–019055) and SenterNovem, The Netherlands (Neuro-Bsik, BSIK 03053) to J.G.G.B., and the NIH (DC008860 and DC009464) to D.E.B.

REFERENCES

- Blankenship, A.G. & Feller, M.B. *Nat Rev Neurosci* **11**, 18–29 (2010).
- Ben-Ari, Y. *Trends Neurosci* **24**, 353–360 (2001).
- Malenka, R.C. & Bear, M.F. *Neuron* **44**, 5–21 (2004).
- Zhang, W. & Linden, D.J. *Nat Rev Neurosci* **4**, 885–900 (2003).
- Jones, T.A. *et al. J Neurophysiol* **98**, 1898–1908 (2007).
- Sonntag, M., Englitz, B., Kopp-Scheinpflug, C. & Rübsamen, R. *J Neurosci* **29**, 9510–9520 (2009).
- Tritsch, N.X. *et al. Nature* **450**, 50–55 (2007).
- Tritsch, N.X. & Bergles, D.E. *J Neurosci* **30**, 1539–1550 (2010).
- von Gersdorff, H. & Borst, J.G.G. *Nat Rev Neurosci* **3**, 53–64 (2002).
- Guinan, J.J., Jr. & Li, R.Y. *Hear Res* **49**, 321–334 (1990).
- Oertel, D. *Annu Rev Physiol* **61**, 497–519 (1999).
- Walsh, E.J. & Romand, R. in *Development of auditory and vestibular systems 2* (ed. R. Romand) 161–210 (Elsevier, Amsterdam, 1992).
- Johnson, S.L., Marcotti, W. & Kros, C.J. *J Physiol* **563**, 177–191 (2005).
- Brenowitz, S. & Trussell, L.O. *J Neurosci* **21**, 9487–9498 (2001).
- Larson, J., Wong, D. & Lynch, G. *Brain Res* **368**, 347–350 (1986).

Supplementary Information

SUPPLEMENTARY METHODS

two

All experimental procedures used in this study were performed in strict accordance with protocols approved by the Animal Care and Use Committees at Erasmus MC and Johns Hopkins University.

***In vitro* SGN and IHC recordings.** Cochlear turns of postnatal day (P) 0–7 Sprague-Dawley rats were isolated in ice-cold, sterile-filtered HEPES-buffered ACSF containing (in mM): 130 NaCl, 2.5 KCl, 10 HEPES, 1 NaH_2PO_4 , 1.3 MgCl_2 , 2.5 CaCl_2 , 11 D-glucose (290 mmol.kg^{-1}), pH 7.4, supplemented with 10 U/ml penicillin (Sigma). Explants were plated on Cell-Tak (BD Biosciences) coated glass coverslips and maintained for 1 to 7 days *in vitro* in F-12/DMEM (Invitrogen) containing 1% fetal bovine serum and 10 U/ml penicillin in a 37 °C, 5% CO_2 humidified incubator. Some experiments (Fig. 2a–c, and Supplementary Fig. 2h–n) were performed using cochlear turns acutely isolated from P4–9 rats, as described previously^{1,2}. For recording, coverslips were continually superfused with bicarbonate-buffered ACSF composed of (in mM): 119 NaCl, 5 KCl, 1.3 CaCl_2 , 1.3 MgCl_2 , 1 NaH_2PO_4 , 26.2 NaHCO_3 , and 6 D-glucose (290 mmol.kg^{-1}), saturated with 95% O_2 /5% CO_2 , at 22–24 °C. Some experiments were performed with ACSF heated to 32–35 °C by passing it through a feedback-controlled in-line heater (Warner Instruments) prior to entering the chamber. Electrodes for loose-patch SGN recordings had a tip resistance of 0.7–1.5 M Ω when filled with HEPES-buffered ACSF and action potential waveforms were detected with patch resistances of 5–15 M Ω . Whole-cell current-clamp recordings from IHCs were obtained using 5–9 M Ω patch pipettes filled with internal solution composed of (in mM): 120 KCH_3SO_3 , 20 HEPES, 10 EGTA, 1 MgCl_2 , 2 Na_2ATP and 0.2 Na_2GTP (290 mmol.kg^{-1}), pH 7.3.

Paired IHC-SGN recordings were performed in cultured cochlear explants superfused with bicarbonate-buffered ACSF containing 2.5 mM KCl and 11 mM D-glucose. Most SGNs only contacted one IHC (see Supplementary Fig. 4); cells that received input from multiple IHCs were excluded from analysis. Currents and potentials were recorded with pClamp9 software using a Multiclamp 700A amplifier, low-pass filtered at 2–10 kHz, and digitized at 10–50 kHz with a Digidata 1322A analog-to-digital converter (MDS Analytical Technologies).

***In vivo* MNTB recordings.** Wistar rat pups (P0–8) were anesthetized with isoflurane (1.5%) delivered via a mouse ventilator. The MNTB was accessed using a ventral craniotomy as described previously³. Recordings were made at a depth of 300–400 μm from the pial surface using patch pipettes (5–8 M Ω) filled with artificial cerebrospinal fluid (ACSF) containing (in mM): 125 NaCl, 2.5 KCl, 1 MgSO_4 , 2 CaCl_2 , 1.25 NaH_2PO_4 , 0.4 ascorbic acid, 3 myo-inositol, 2 pyruvic acid, 25 D-glucose, 25 NaHCO_3 (310 mmol.kg^{-1}), pH 7.4 when saturated with 95% O_2 /5% CO_2 , or intracellular solution containing (in mM): 126 K-gluconate, 20 KCl, 10 Na_2 -phosphocreatine, 4 MgATP , 0.3 Na_2GTP , 0.5 EGTA and 10 HEPES (310 mmol.kg^{-1}), pH 7.2.

Extracellular potentials were detected in the loose-patch configuration (10–50 M Ω). Potentials were recorded with pClamp9 software using an Axopatch 200B amplifier, filtered at 2–5 kHz and sampled at 20 kHz with a Digidata 1440A (MDS Analytical Technologies). Inclusion of Alexa Fluor 594 (0.012%, Invitrogen) in pipette solutions allowed *post hoc* confirmation of extracellular recording sites within MNTB in paraformaldehyde-fixed brainstem sections (Supplementary Fig. 5). To test whether the burst pattern observed in the MNTB originated in the cochlea, the contralateral cochlea of P4–8 rat pups was ablated using a ventral approach ($n = 8$). After opening the bulla and removing its contents, a hole in the ventral surface of the cochlea was made and the organ of Corti was disrupted with tweezers. In each case, prior to ablating the cochlea, we confirmed the location of the MNTB by recording from bursting units with complex waveforms and by post mortem histology. To confirm that silent units included principal cells, we stimulated the afferent fibers at the midline of ablated animals with 0.1 ms, 0.2 – 1 mA current pulses using a bipolar Tungsten electrode (0.1 M Ω impedance; tip separation 250 μ m; MicroProbes for Life Science, Gaithersburg, MD).

***In vivo* CIC recordings.** Sprague-Dawley rat pups (P4–7) were anesthetized with either isoflurane (0.5–1.5%) or intraperitoneal injection of ketamine (15 μ g/g) and xylazine (0.23 μ g/g). After stabilizing the skull using a small custom-made metal plate and dental cement, a craniotomy was performed in the interparietal bone overlaying the inferior colliculus and filled with low melting point agarose (type IB, 1.5% in HEPES-buffered ACSF) to minimize brain motion. Multi-unit recordings were obtained at a depth of 200–1000 μ m below the pia using glass electrodes (3–10 M Ω) filled with HEPES-buffered ACSF. Extracellular potentials were recorded with pClamp9 software using an Axopatch 1D amplifier, band-pass filtered at 5–5000 Hz and sampled at 20 kHz with a Digidata 1322A (MDS Analytical Technologies). For bilateral cochlear ablations the cochlea was accessed laterally following crude dissection of the bulla caudal to the pinna and removal of middle ear mesenchyme using fine forceps. After cauterizing the stapedial artery, the otic capsule was opened and the contents of the cochlea were entirely removed using vacuum-assisted suction. Complete bilateral ablation was verified after each experiment with cochlear dissections. The sham-operated group is composed of animals with unilateral or incomplete bilateral ablation. To minimize selection biases, recordings in control and ablated animals were standardized for penetration steps (100–150 μ m) and time allotted per recording site (>3 min).

Data Analysis. Data were analyzed off-line using Clampfit 9.2 (MDS Analytical Technologies), Origin (Microcal Software) or custom procedures written in the NeuroMatic environment (version 2.0, kindly provided by Dr. J. Rothman, University College London) within Igor Pro 6 (WaveMetrics). Data are expressed as mean \pm standard error of the mean (s.e.m.). Statistical tests are noted in text (significance: $\alpha < 0.05$).

Burst identification and separation. Extracellular action potentials were identified by an amplitude threshold criterion. Cells were operationally classified as bursting if inter-spike intervals (ISIs) ranged from values <50 ms to values >1 s. A common measure of ISI variability within a given recording is the coefficient of variation (CV_{ISI}), defined as the ratio of the ISI standard deviation and ISI mean. Randomly-firing units have CV_{ISI} values close to 1. On the other hand, non-stochastic or irregularly-firing units typically display CV_{ISI} values greater than 1; the CV_{ISI} of all ‘bursting’ MNTB units in this study (4.0 ± 0.2 , $n = 50$) was significantly larger than the CV_{ISI} of the ‘non-bursting’ group (1.2 ± 0.3 , $n = 18$, $P < 0.001$, two-sample t-test). Similarly, CV_{ISI} of all bursting IC units averaged 3.2 ± 0.2 ($n = 21$). To objectively identify peaks in SGN and MNTB ISI histograms we obtained two boundary values – one in the 5–50 ms range (to separate first and second peaks) and one in the 1–10 s range (to separate the second and third peaks) – by calculating for each spike CV_b , defined as:

$$CV_b = \frac{2|\Delta t_{i+j} - \Delta t_i|}{\Delta t_{i+j} + \Delta t_i}$$

where Δt_i is the i ’th ISI, with $i=1, 2, \dots$ and Δt_{i+j} is the next interval in the same interval class, with $j=1, 2, \dots$. For the calculation of CV_b each ISI was paired (if possible) with the next ISI belonging to the same interval class. To find the matching interval, intervals belonging to a class with smaller intervals are skipped. If an interval belonging to a class with a larger interval came before the next same-class interval, the value for CV_b is not obtained for that spike. The mean of all obtained CV_b values will be a measure for the overall within-class homogeneity. Bursts were separated by finding the two boundary values for which mean CV_b was minimal. Lower boundaries were on average 31.8 ± 2.6 ms (range: 8.1–50.3 ms), 38.5 ± 1.5 ms (range: 14.8–49.7 ms) and 46.3 ± 0.9 ms (range: 34.4–49.7 ms) for *in vitro* SGN ($n = 35$ room and physiological temperature), *in vivo* MNTB ($n = 50$) and *in vivo* CIC ($n = 21$) recordings, respectively, and higher boundaries were 2.0 ± 0.2 s (range: 1.0–5.2 s), 2.2 ± 0.2 s (range: 1.0–7.6 s) and 3.1 ± 0.6 s (range: 1.0–10.1 s), respectively. For comparison of ISI histograms across many recordings (Supplementary Fig. 1), log-binned ISI histograms for each cell were normalized to the maximum number of intervals measured in any bin.

Mini-burst distribution within bursts. To characterize the progressive shortening and lengthening of intervals separating mini-bursts at the onset and end of each burst, a custom routine was written in Igor 6.0 to identify and number successive inter-mini-burst intervals within bursts in each recording using boundary values obtained with the CV_b analysis. We limited our analysis to bursts composed of a minimum of 10 mini-burst intervals and to recordings containing at least 5 such bursts. For each cell, the first and last 5 mini-burst intervals of each burst were aligned to the beginning and end of each burst, respectively and the mean duration of mini-burst intervals at each position was calculated.

SUPPLEMENTARY DISCUSSION

Comparison of the spontaneous activity of auditory neurons in the brain and the cochlea indicate that immature auditory circuits have a remarkable ability to preserve the overall discharge patterns imposed by IHCs. Although there have been few physiological studies of these developing circuits, anatomical studies in adult cats indicate that globular bushy cells (GBCs), which innervate MNTB neurons with a single, giant axo-somatic terminal known as the calyx of Held⁴ receive dozens of converging auditory nerve inputs (5 to 69, mean = 23)^{5,6}. If a similar convergence exists during the prehearing period, it would likely disrupt IHC-generated activity patterns unless inputs to GBCs fire synchronously or there is one dominant suprathreshold input. Although the degree of 8th nerve convergence has not been determined in rodents before the onset of hearing, it appears to be much smaller in adult mice (4 to 7)⁷ than in cats, and physiological studies of bushy cells in the ventral division of cochlear nucleus do not distinguish between spherical and globular bushy cells^{8,9}, suggesting that both cell types may receive one dominant input. Moreover, there is evidence that multiple synaptic endings on GBCs can originate from the same branched auditory nerve fiber^{6,10}. The disruptive effect of convergence would be further reduced if the SGNs that project to each GBC receive inputs from the same IHC (as each IHC is innervated by as many as 30 SGNs). Further experiments will be required to determine the extent of convergence onto GBCs before the onset of hearing.

Despite the remarkable similarity in discharge patterns exhibited by SGNs *in vitro* and central auditory neurons *in vivo*, some notable differences exist. In particular, discharge patterns in MNTB and CIC neurons *in vivo* were often more similar to the activity of SGNs recorded at room temperature than at near-physiological temperatures; mean firing rates were significantly higher and intervals separating action potentials within mini-bursts were considerably shorter in SGNs at physiological temperature compared to MNTB and CIC neurons. It is possible that these differences arise from the properties of intervening synapses in the developing cochlear nucleus or superior olivary complex. It is also possible that these differences are simply due to technical limitations that arise from comparing activity between *in vivo* and *ex vivo* preparations. Specifically, *in vivo* recordings were performed in the presence of anesthetics, which can affect excitability, firing rates and synaptic release probabilities. In addition, the organ of Corti normally exists within a privileged environment – exposed on one side to high potassium containing endolymph, and on the other to perilymph – that cannot be mimicked *in vitro*. Studies in isolated cochleae are typically performed in extracellular saline enriched in potassium (5–6 mM), although it is unclear whether this condition mimics the endogenous environment of IHCs in the neonatal cochlea.

In addition, some differences were apparent between the discharge patterns of MNTB and CIC neurons recorded under similar conditions *in vivo*: CIC neurons fired bursts that were shorter in duration and contained fewer action potentials, and intervals

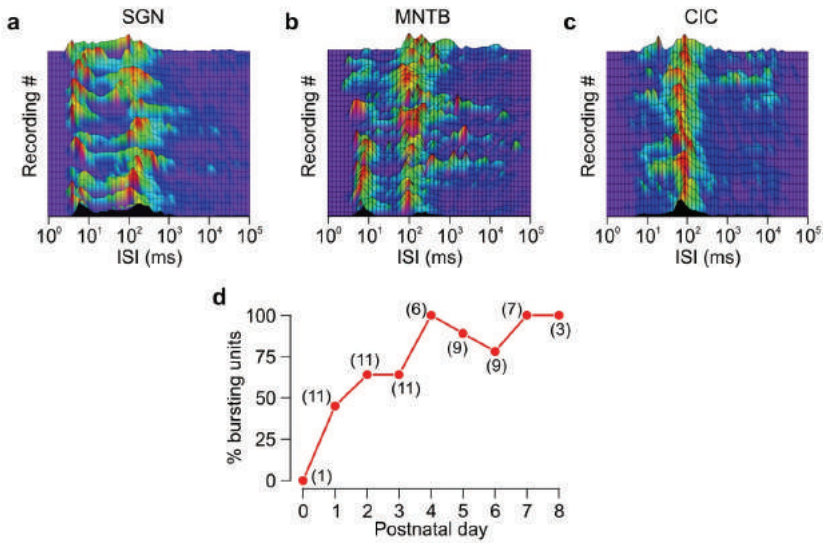
separating action potentials within mini-bursts also appeared longer. These discrepancies presumably arise from the anatomical and functional differences between these auditory centers. While principal neurons in the MNTB are part of a pathway specialized for preserving auditory nerve input patterns from one ear⁴, CIC is a major relay nucleus that integrates ascending excitatory and inhibitory inputs from more than ten ipsi- and contralateral brainstem auditory nuclei, as well as descending modulatory projections from auditory cortex¹¹. The complex intervening circuitry between the cochlea and CIC, as well as inhibitory networks within the CIC, may both limit the propagation of burst activity and shape the timing of action potentials within each burst. It will be important to determine which elements in these developing circuits modify propagation of cochlea-initiated patterns during the pre-hearing period.

SUPPLEMENTARY REFERENCES

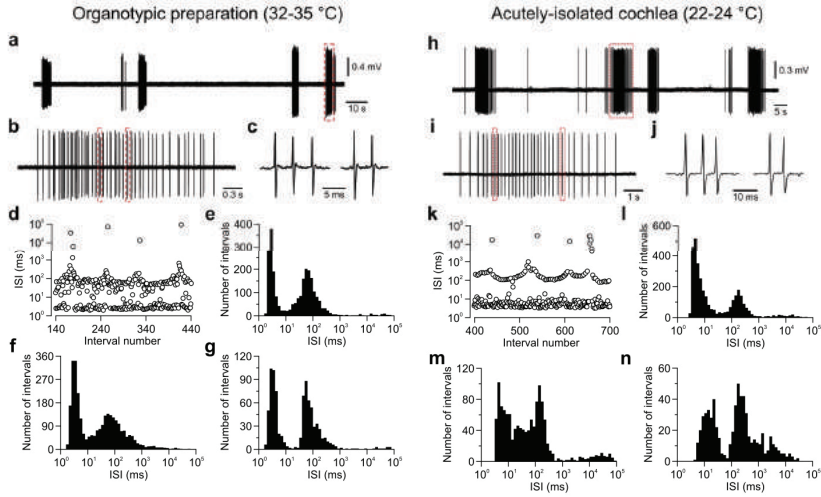
1. Tritsch, N.X., Yi, E., Gale, J.E., Glowatzki, E. & Bergles, D.E. *Nature* **450**, 50-55 (2007).
2. Tritsch, N.X. & Bergles, D.E. *J Neurosci* **30**, 1539-1550 (2010).
3. Rodriguez-Contreras, A., van Hoes, J.S., Habets, R.L.P., Locher, H. & Borst, J.G.G. *Proc Natl Acad Sci USA* **105**, 5603-5608 (2008).
4. von Gersdorff, H. & Borst, J.G.G. *Nat Rev Neurosci* **3**, 53-64 (2002).
5. Spirou, G.A., Rager, J. & Manis, P.B. *Neuroscience* **136**, 843-863 (2005).
6. Liberman, M.C. *J Comp Neurol* **313**, 240-258 (1991).
7. Oertel, D. *J Acoust Soc Am* **78**, 328-333 (1985).
8. Isaacson, J.S. & Walmsley, B. *J Neurophysiol* **73**, 964-973 (1995).
9. Oleskevich, S., Clements, J. & Walmsley, B. *J Physiol* **524 Pt 2**, 513-523 (2000).
10. Rouiller, E.M., Cronin-Schreiber, R., Fekete, D.M. & Ryugo, D.K. *J Comp Neurol* **249**, 261-278 (1986).
11. Malmierca, M.S. *Neuroembryol Aging* **3**, 215-229 (2004).
12. Elgoyhen, A.B., Johnson, D.S., Boulter, J., Vetter, D.E. & Heinemann, S. *Cell* **79**, 705-715 (1994).

SUPPLEMENTARY FIGURES

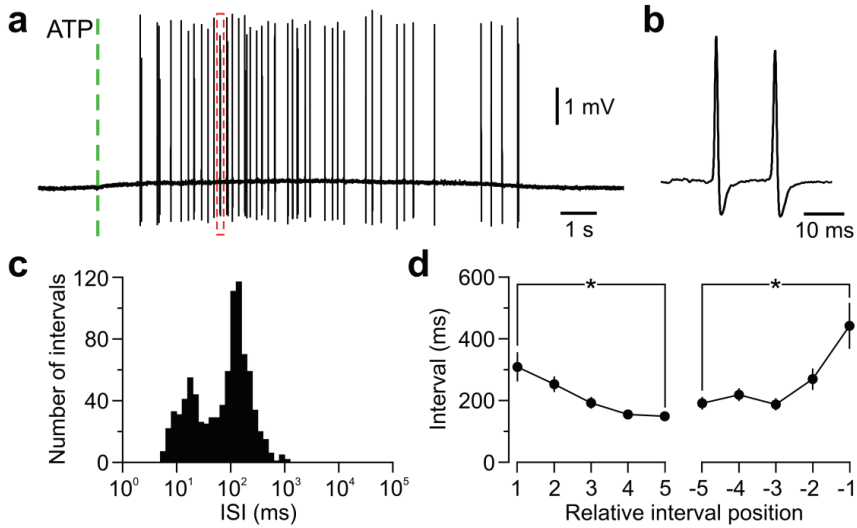
two



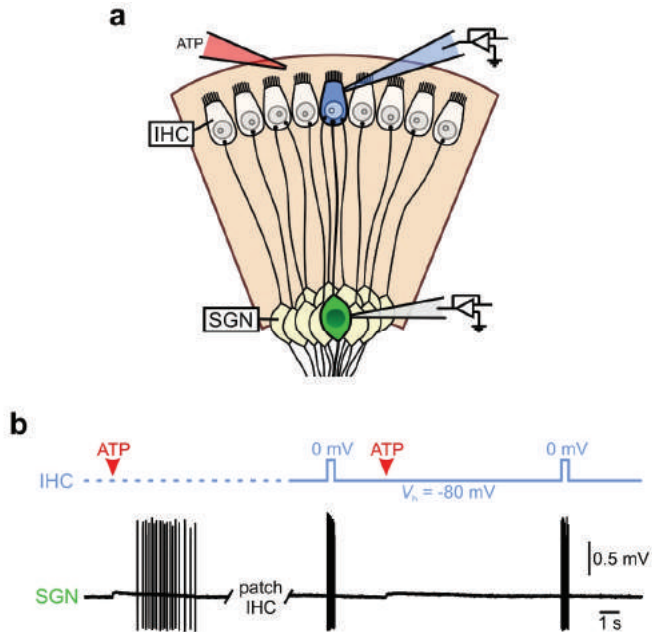
Supplementary Figure 1. Firing patterns of SGNs *in vitro*, and MNTB and CIC neurons *in vivo*, before the onset of hearing. (a) Normalized log-binned ISI frequency distributions of action potentials recorded from 27 SGNs (distributed along the ordinate) in prehearing cochlear explants at room temperature. Warmer colors indicate more frequently observed intervals. (b,c) Normalized log-binned ISI frequency distributions of action potentials recorded from 34 MNTB neurons in P4–8 rats (b) and 21 CIC neurons at P4–7 (c). (d) Percentage of all MNTB units displaying burst firing *in vivo* as a function of postnatal age (in days). Number of recordings indicated in parentheses.



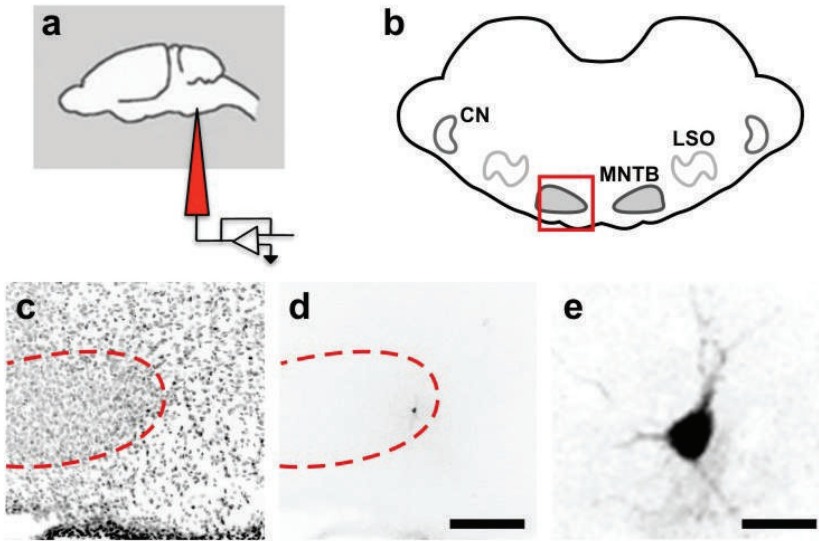
Supplementary Figure 2. SGNs display similar firing patterns in cochlear explants and in acutely-isolated cochleae. (a) Extracellular action potentials recorded from an SGN at 32–35 °C, from a P6 cochlea maintained for 2 days *in vitro*. (b) Burst within dashed red box in a shown on expanded time scale. (c) Detail of two mini-bursts within dashed red boxes in b. (d,e) Plot of 300 consecutive ISI intervals (log scale, d) and log-binned ISI histogram (e) for the cell in a. (f,g) Log-binned ISI histograms for two additional extracellular SGN recordings performed at 32–35 °C. (h–l) Same as in (a–e) for a SGN recorded at room temperature in a cochlea acutely isolated from a P9 rat. (m,n) Log-binned ISI histograms for another P9 (m) and a P5 (n) SGN in acutely-isolated cochleae at room temperature. P5 recordings were performed in extracellular solution containing 2.5 mM K⁺; all other recordings were performed in extracellular solution containing 6 mM K⁺.



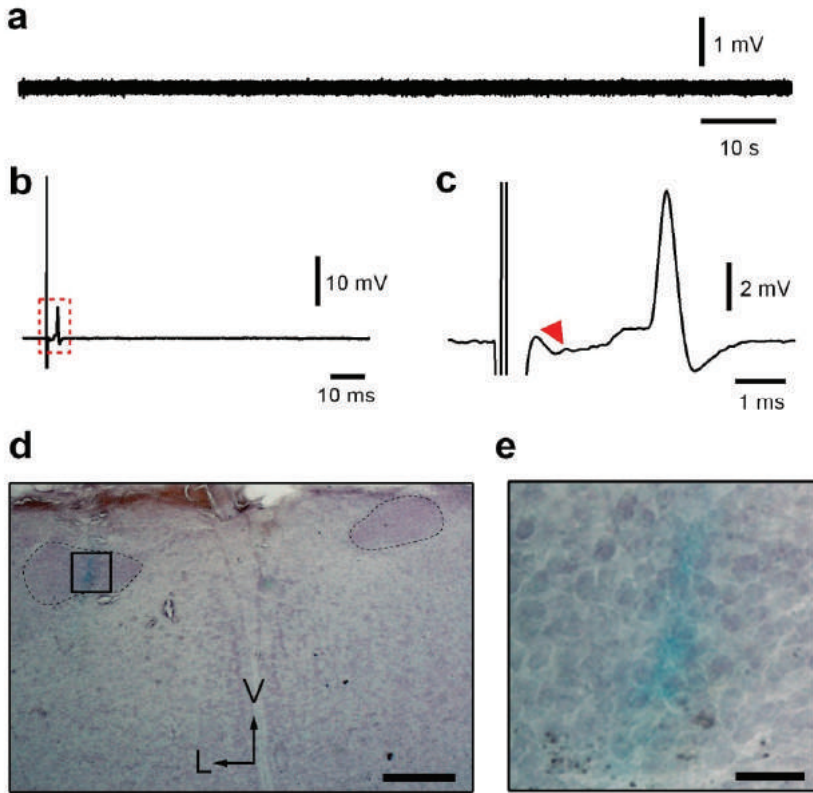
Supplementary Figure 3. Stimulation of an IHC with ATP triggers a train of action potential mini-bursts in the postsynaptic SGN. (a) Extracellular action potentials recorded from an SGN in response to application of ATP (10 μ M, 50 ms, 5 psi; dashed green line) to its presynaptic IHC. (b) Detail of a mini-burst outlined by the dashed red box in a. (c) Log-binned histogram of all SGN action potentials evoked in response to ATP (10 μ M) application ($n = 900$ action potentials in 5 SGNs). (d) Mean duration (\pm s.e.m.) of intervals separating mini-bursts vs. relative mini-burst position within a burst ($n = 19$ bursts in 5 SGNs). * $P < 0.005$, paired t-test. Recordings in a–d were performed in the presence of strychnine (1 μ M), an $\alpha 9/\alpha 10$ acetylcholine receptor antagonist¹², indicating that efferent input to prehearing IHCs is not required to initiate patterned bursts of action potentials in SGNs.



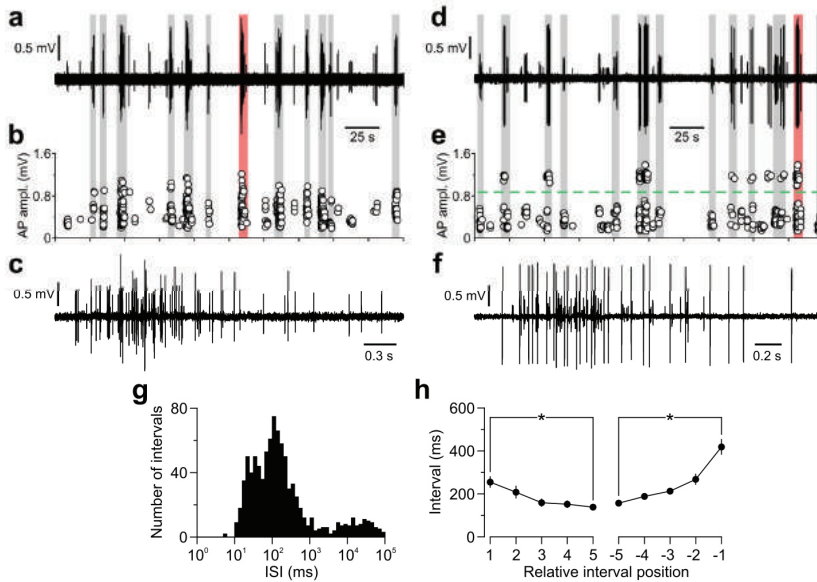
Supplementary Figure 4. Sequence used to identify SGNs that receive input from a single IHC. (a) Diagram of the paired IHC-SGN recording configuration in an organotypic preparation. Once a stable extracellular recording was established from a SGN (labeled in green), we identified the region in the organ of Corti innervated by this neuron using small ATP puffs (10–100 μ M, 5 psi; red pipette) delivered to IHCs. Upon identification of the presynaptic region, several IHCs were patched until the presynaptic cell (indicated in blue) was found. (b) Representative recording illustrating the protocol employed to ensure that each SGN only received synaptic inputs from a single IHC. *Top*. Command voltage (V_h) applied to the presynaptic IHC. Dashed line indicates time period prior to obtaining whole-cell recording from the presynaptic IHC. *Bottom*. Extracellular recording from a SGN (obtained first). The small positive deflections induced by ATP application to IHCs represent source waves resulting from inward currents in supporting cells'. Depolarization of the presynaptic IHC to 0 mV triggered a burst of action potentials in the recorded SGN, but exogenous ATP (red arrowheads) was unable to elicit a burst of action potentials when the presynaptic IHC was voltage-clamped at -80 mV, indicating that this SGN did not receive synaptic inputs from surrounding IHCs.



Supplementary Figure 5. Morphological and anatomical identification of MNTB neurons recorded from *in vivo*. (a) Experimental configuration. A patch electrode filled with a fluorescent dye was advanced into the ventral side of the brainstem according to anatomical landmarks and a whole-cell (not in this paper) or extracellular recording was obtained. After perfusion fixation, coronal 50 μm thick brain sections were obtained, the tissue was counterstained with DAPI and then mounted onto coverslips. (b) Schematic of the cochlear nucleus (CN), MNTB and lateral superior olive (LSO) in a coronal brainstem slice. Red box indicates the area shown in panels (c) and (d). (c) Example of a DAPI counterstained P1 brain section at the level of the MNTB (circled by dashed red line). (d) Same region as in (c) indicating the position of the Alexa594-filled principal cell. MNTB outline is indicated by dashed red line. Scale bar: 200 μm . (e) Higher magnification view of the dye-filled principal neuron shown in panel (d). Scale bar: 15 μm .

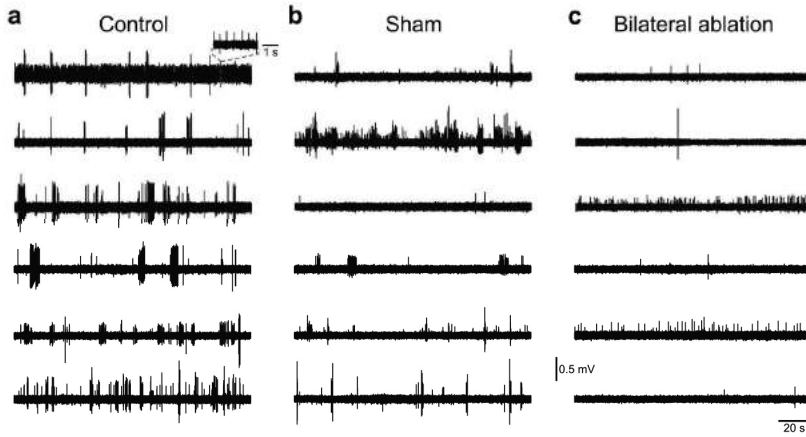


Supplementary Figure 6. Cochlear ablation silences MNTB neurons *in vivo*. (a) Continuous recording from a unit in a P5 animal following ablation of the contralateral cochlea. No action potentials were observed in 68 extracellular recordings from putative MNTB principal neurons in six animals (> 6 units/animal); in each animal bursting activity from a unit with a complex waveform was recorded before ablation. A single bursting unit was observed in each of two additional animals; however, after further cochlear dissection, all MNTB neurons (15 units/animal) were silent in these rats, suggesting that the cochlea had been incompletely ablated. (b) Response of a unit in the same animal shown in **a** to afferent stimulation at the midline after cochlea ablation. The complex waveform indicates that this was an MNTB principal neuron. Stimulus artifact is partially truncated. Note the lack of spontaneous activity preceding and following the electrically-evoked complex waveform. Similar results were obtained in a total of six units from four different animals. (c) Enlargement of the boxed area in **b**. The red arrowhead marks the pre-spike. (d) Section containing the ventral brainstem showing the presence of blue dye within the MNTB (outlined with dashed black line) injected at the same site as units illustrated in **a–c**. Scale bar: 200 μ m. L, lateral; V, ventral. Vertical arrow indicates the midline. (e) Magnification of boxed area shown in **d**. Scale bar: 50 μ m.



two

Supplementary Figure 7. CIC neurons fire correlated bursts of patterned action potentials before hearing onset. (a) *In vivo* multi-unit extracellular recording from CIC in a P5 pup. (b) Scatter plot of peak action potential amplitude vs. spike time for the recording shown in a. Bursts (highlighted in gray) are composed of action potentials with widely varying amplitudes, indicating coincident discharge of groups of neighboring neurons. (c) Detail of the multi-unit burst highlighted in red in a. (d–f) Same as a–c for another recording obtained in a P7 animal. Note in e that one unit is clearly distinguishable from others (dashed green line), offering the possibility to define its pattern. (g) Log-binned ISI histograms for the largest unit in d. (h) Mean duration (\pm s.e.m.) of mini-burst intervals within bursts ($n = 110$ bursts in 9 units). * $P < 0.005$, paired t-test.



Supplementary Figure 8. Spontaneous correlated bursts of action potentials in CIC originate in the cochlea. (a–c) Spontaneous multi-unit activity recorded in CIC from six control (a), sham-operated (b) or ablated (c) animals (P4–7). Spontaneous bursting activity was recorded from most electrode tracks in which action potentials were detected in control ($n = 36/43$, 84 % in 13 pups) and sham-operated animals ($n = 8/11$, 73% of electrode tracks in 6 pups), but was never observed in animals in which both cochleae had been removed ($n = 0/20$ electrode tracks in which action potentials were detected in 7 pups). Recordings with sparse activity or regularly-discharging units were observed in all animals, indicating that the source of this activity is extrinsic to the cochlea.



chapter **THREE**

Developmental changes in short-term plasticity at the rat calyx of Held synapse

Tom T.H. Crins^{1,2}, Silviu I. Rusu¹, Adrian Rodríguez-Contreras^{1,*}, J. Gerard G. Borst¹.

¹ Department of Neuroscience, Erasmus MC,
University Medical Center Rotterdam, The Netherlands.

² Department of Otorhinolaryngology - Head and Neck Surgery, Erasmus MC,
University Medical Center Rotterdam, The Netherlands.

* Present address: Department of Biology, City College of New York, New York, NY 10031, USA.

ABSTRACT

The calyx of Held synapse of the medial nucleus of the trapezoid body (MNTB) functions as a relay synapse in the auditory brainstem. *In vivo* recordings have shown that this synapse displays low release probability and that the average size of synaptic potentials does not depend on recent history. We used a ventral approach to make *in vivo* extracellular recordings from the calyx of Held synapse in rats aged postnatal day 4 (P4) to P29 to study the developmental changes that allow this synapse to function as a relay. Between P4 and P8, we observed evidence for the presence of large short-term depression, which was counteracted by short-term facilitation at short intervals. Major changes occurred in the last few days before the onset of hearing for air-borne sounds, which happened at P13. The bursting pattern changed into a primary-like pattern, the amount of depression and facilitation decreased strongly and the decay of facilitation became much faster. Whereas short-term plasticity (STP) was the most important cause of variability in the size of the synaptic potentials in immature animals, its role became minor around hearing onset and afterwards. Similar developmental changes were observed during stimulation experiments both in brain slices and *in vivo* following cochlear ablation. Our data suggest that the strong reduction in release probability and the speedup of the decay of synaptic facilitation that happen just before hearing onset are important events in the transformation of the calyx of Held synapse into an auditory relay synapse.

INTRODUCTION

The medial nucleus of the trapezoid body (MNTB) functions as an inverting relay in the auditory brainstem. The synaptic transmission across the MNTB has to be both fast and reliable. These requirements are met by a giant, excitatory axosomatic synapse: each principal neuron is contacted by a single calyx of Held, which originates from globular bushy cells in the anteroventral cochlear nucleus (Schneggenburger and Forsythe, 2006). By virtue of its many release sites, the adult calyx can drive its principal neuron at high frequencies for sustained periods (Guinan and Li, 1990). Even though there are activity-dependent changes in, for example, the synaptic delay (Mc Laughlin et al., 2008; Tolnai et al., 2009), these changes are typically small compared to upstream changes (Lorteije and Borst, 2011).

Because of the large size of this synapse, juxtacellular (loose-patch) recordings from principal neurons are characterized by the presence of a complex waveform, which consists of a prespike that signals the presynaptic action potential and a postsynaptic waveform, which consists of the extracellularly recorded EPSP (eEPSP) and, when the eEPSP is suprathreshold, the extracellularly recorded postsynaptic action potential (eAP; Guinan and Li, 1990; Lorteije et al., 2009). We previously showed that the eEPSP provides a measure for the strength of synaptic transmission. Using both *in vivo* juxtacellular and whole-cell recordings from the mouse calyx of Held synapse, we found that this synapse shows little or no evidence for the presence of short-term plasticity (STP) (Lorteije et al., 2009).

Even though this finding was in agreement with the tonic, relay aspect of its function, it was nevertheless unexpected. Because of the accessibility of the presynaptic terminal and its postsynaptic partner to patch-clamp recordings in slices (Forsythe, 1994; Borst et al., 1995), synaptic transmission at the calyx of Held synapse has been well studied. One of the main findings was that this synapse displays several forms of STP, including short-term facilitation and short-term depression, and the mechanisms underlying these different forms of STP have been well characterized (von Gersdorff and Borst, 2002). The large discrepancy between results obtained *in vivo* and *in vitro* is incompletely understood. One contributing factor is that the release probability of the mature calyx of Held synapse is much lower *in vivo* than previous *in vitro* estimates (Lorteije et al., 2009). The developmental decrease of release probability (Taschenberger and von Gersdorff, 2000; Iwasaki and Takahashi, 2001; Taschenberger et al., 2002), the lower calcium concentration *in vivo* (Lorteije et al., 2009) and tonic depression owing to spontaneous activity (Hermann et al., 2007) may all contribute to this discrepancy. Even though the low release probability provides an explanation for the apparent lack of short-term depression, it does not explain why high-frequency activity does not lead to pronounced short-term facilitation under these circumstances (Borst et al., 1995). To better understand the synaptic mechanisms that allow the calyx of Held synapse to be both precise and reliable, we studied changes in firing pattern, synaptic speed, reliability and STP between postnatal day 4 (P4) and P29.

MATERIALS AND METHODS

Methods

Animals. All experiments were conducted in accordance with the European Communities Council Directive and approved by the animal ethics committee of the Erasmus MC.

The day of birth is defined as postnatal day 0 (P0). A total of 79 Wistar rats of either sex were anesthetized with isoflurane (induction at 5%, maintenance at approximately 1%) and placed in the supine position. Rectal temperature was maintained between 37 and 38 °C with a homeothermic blanket system (Stoelting). In post-hearing animals, the external ear canal was filled with silicone gel to reach maximal conductive hearing loss. Following laryngectomy, the animal was intubated and mechanically ventilated. Animals between P4 and P15 were ventilated with a MiniVent (type 845; Harvard Apparatus, March-Hugstetten, Germany) at a frequency of ~80/min; stroke volume was 7 µl/gram bodyweight. Animals between P16 and P29 were ventilated with a Small Animal Ventilator (KTR-5; Harvard Apparatus) at a frequency of 64/min; end inspiratory pressure was ~12 cm H₂O (max. 20 cm H₂O); the inspiration-expiration ratio was 44:56. Arterial oxygen saturation and heart rate were monitored using a MouseOx (STARR Life Sciences Corp.). The left MNTB was reached via a ventral approach, as previously described (Rodriguez-Contreras et al., 2008). Typically, the location of the MNTB was 400-500 µm rostrally from the left anterior inferior cerebellar artery and 400-450 µm laterally from the basilar artery. In some experiments with relatively large surface movements, agar was applied on the surface before recording.

In vivo electrophysiology. In vivo juxtacellular (loose-patch) recordings were made as previously described (Lorteije et al., 2009). Glass micropipettes (3.5-5.0 MΩ) were filled with a solution containing in mM: 135 NaCl, 5.4 KCl, 1 MgCl₂, 1.8 CaCl₂ and 5 HEPES (pH 7.2). When passing the brain surface high positive pressure (~300 mBar) was used, which was lowered to ~12 mBar when searching for cells and to 0 mBar during recordings.

In vivo stimulation experiments were performed as previously described (Tritsch et al., 2010). Briefly, the location of the MNTB was first ascertained by making a juxtacellular recording from a spontaneously active unit with a complex waveform. Subsequently, spontaneous activity was abolished by mechanically ablating the contralateral cochlea with tweezers after drilling a hole in the bulla and, in the case of the youngest animals, removing the mesenchyme in the bullar cavity. A bipolar Pt/Ir electrode (MicroProbes for Life Science, Gaithersburg, MD) was inserted at the contralateral side, below the basilar artery. Afferent fibers were stimulated (<0.5 mA, 0.1 ms) using a stimulus isolator (A385, World Precision Instruments). The stimulus protocol consisted of paired-pulse stimuli with intervals ranging from 2 to 2400 ms, which was repeated between 6 - 10 times, or a custom made in-vivo-like stimulation protocol resembling the spontaneous firing pattern of a P5 animal. The in-vivo-like stimulation protocol consisted of a randomized sequence of 450 intervals ranging from 3 ms to 9 sec, which were drawn from three lognormal distributions with preferred intervals

at about 10, 100 and 1000 ms (Figure 6A, B). The protocol was applied once and had a total duration of approximately 4 min.

Data were acquired with an Axopatch 200B amplifier (MDS Analytical Technologies) in fast current-clamp mode, filtered with a low-pass 4-pole Bessel filter and sampled at an interval of 20 μ s with a Digidata 1320A.

three

Auditory Brainstem Response. Prior to surgery the Auditory Brainstem Response (ABR) was measured to obtain hearing thresholds in 17 animals at 4, 8, 16 and 32 kHz as described previously (van Looij et al., 2004). Rats were anesthetized with ketamine/xylazine (0.08 ml/10 gram bodyweight of a solution containing 0.12% xylazine and 0.8% ketamine in 0.9% NaCl). Tone repetition rate was 80 Hz. Maximum tone pip intensities were 120 dB SPL at 4-16 kHz and 105 dB SPL at 32 kHz.

In vitro whole cell slice recordings. MNTB slices were prepared as described previously (Habets and Borst, 2007; Lorteije et al., 2009). In short, P4-6 or P13-16 Wistar rats were decapitated under deep isoflurane anesthesia and the isolated brainstem was submerged in ice cold oxygenated artificial cerebrospinal fluid (aCSF), containing (in mM): 125 NaCl, 2.5 KCl, 3 MgSO_4 , 0.1 CaCl_2 , 1.25 NaH_2PO_4 , 0.4 ascorbic acid, 3 myo-inositol, 2 pyruvic acid, 25 D-glucose, 25 NaHCO_3 (Merck), pH 7.4 with carbogen. Coronal slices containing the MNTB were cut at a thickness of 150-200 μ m. After incubation for 30 min at 37 °C, slices were transferred to the recording chamber of an upright microscope (BX-50, Olympus). Recordings were performed at physiological temperature (35-37 °C) and slices were continuously perfused with carbogenated aCSF with the same composition as the slicing solution, except that the concentration of CaCl_2 was either 0.6 or 1.2 mM and the MgSO_4 concentration was 1 mM. MNTB afferents were stimulated using a bipolar electrode (FHC Inc, Bowdoin, ME) positioned at the midline or half-way between the midline and the MNTB. In whole cell experiments, borosilicate glass electrodes (2.5-5.5 M Ω) were filled with intracellular solution containing (in mM): K-gluconate 125, KCl 20, Na_2 -phosphocreatine 10, Na_2 -GTP 0.3, Mg-ATP 4, EGTA 0.5, HEPES 10, pH 7.2; extracellular electrodes were filled with aCSF. Voltages were compensated for the liquid junction potential (-11 mV) between the pipette solution and the aCSF. Holding potential was -80 mV. Series resistance (<15 M Ω) was compensated by 95-98 % with a lag of 7-10 μ s during voltage clamp recordings. Voltage and current-clamp data were acquired using an Axopatch 200B amplifier and filtered at 2-10 kHz with a low-pass 4-pole Bessel filter. Data were digitized at intervals of 16-25 μ s.

The same 2 stimulus protocols were used in the slice electrophysiology as in the in vivo electrophysiology described above. The paired-pulse protocol was run in voltage-clamp mode; the in-vivo-like protocol both in voltage-clamp and in current-clamp mode. These three configurations were tested at both 1.2 and 0.6 mM calcium, for a total of up to 6 different stimulus protocols on the same cell, depending on the stability of the recording.

To determine the origin of the extracellular waveform at the rat calyx of Held synapse, we made simultaneous intra- and extracellular slice recordings in P6-9 rats as described previously (Lorteije et al., 2009). Correlation between amplitudes of postsynaptic events in whole-cell voltage or current clamp and extracellular current clamp recording was calculated from the responses evoked by afferent stimulation with stimulus trains ranging from 10 to 200 Hz.

Analysis

Data were analyzed with custom-written Igor procedures (Igor Pro 6.0.2.0, WaveMetrics, Inc. Lake Oswego, OR, USA) running within the NeuroMatic environment (version 2.00, kindly provided by Dr. J. Rothman, University College London, London, UK).

Measuring EPSC amplitudes. EPSC amplitudes were measured as the difference between peak and baseline. To estimate the baseline, a double exponential function was fitted to the decay phase of each EPSC. The extrapolated value of the fitted function at the time of the next EPSC peak was taken as the baseline. In case the amplitude of the stimulus artifact at the start of the EPSC was >5% of the peak EPSC amplitude, a double exponential fit to the decay phase of the stimulus artifact was used instead to estimate the baseline.

Analysis of complex waveforms. Complex waveforms were analyzed as previously described (Lorteije et al., 2009). Whole-cell current clamp recordings were differentiated before analysis. The minimum signal-to-noise ratio, which was defined as the ratio of the mean EPSP amplitude and the standard deviation of the baseline, was 7. On average it was 20 ± 2 ($n = 63$) in the spontaneous in vivo recordings.

Short-term plasticity model. The relation between the size of the eEPSP and inter-EPSP interval was described with a simple model for STP (Varela et al., 1997). In the presence of both facilitation and depression, the eEPSP amplitude depended on the availability of a depletion factor, D , which was constrained to be between 0 and 1, and a facilitation factor, F . With each event, the depletion factor depleted with fraction d , which was also constrained to be between 0 and 1:

$$D \rightarrow dD \quad (1)$$

Following the event, D recovered exponentially from depletion with time constant τ :

$$\tau_d dD/dt = 1 - D \quad (2)$$

With each event, the facilitation factor, F increased with a certain amount f :

$$F \rightarrow F + f \quad (3)$$

Following the event, F recovered exponentially analogously to D .

The amplitude A of the eEPSP depended in a multiplicative fashion on the availability of the two resources:

$$A = A_{inf} F D \quad (4)$$

three

where A_{inf} is the amplitude of the eEPSP after a very long interval. All EPSP amplitudes from a given experiment were fit at once to incorporate cumulative effects. Fits were evaluated by plotting predicted against measured sizes to look for systematic deviations. Especially in the *in vivo* spontaneous data before hearing onset, the interval distributions were inhomogeneous. We therefore used inverse probability weighting (Horvitz and Thompson, 1952); events were weighted by the square root of the local sparseness. For each event, its local sparseness was defined as the inverse of the total number of events in the neighborhood of each event. We defined 0.5 decade for the logarithmically transformed intervals as the neighborhood. To evaluate the goodness-of-fit of the three models, facilitation alone, depression alone and both facilitation and depression, Pearson's r between fitted and measured amplitudes was calculated. Its square, r^2 , sometimes called the coefficient of determination, is a measure for the proportion of the amplitude variance that is accounted for by the STP model. We accepted an extra component (e.g. facilitation) if the explained variance increased by at least 2.5%.

EPSP amplitudes were linearly detrended before fitting the STP model if a linear regression could explain >10% of the variance in their amplitudes (5.9% of fits).

To estimate the recovery from spike depression, the same model was used, except there was no facilitation factor and no weighting (Lorteije et al., 2009). In contrast to Lorteije et al. (2009), recovery from depression was set to start instantaneously.

In ten cells which had postsynaptic failures and showed both facilitation and depression we estimated the impact of synaptic facilitation on reliability by calculating the increase in spike failures after subtracting the estimated contribution of facilitation. This estimate was obtained from the fit of the measured eEPSP amplitudes with the model that included both facilitation and depression. The fit function calculates predicted amplitudes for each measured eEPSP. In addition, we calculated what the predicted amplitudes would be for the same model parameters, except that the facilitation was omitted. For each measured eEPSP, the difference between the amplitude prediction with and without facilitation provides an estimate for the contribution of facilitation, given the interval history of that eEPSP. We then calculated the percentage of eEPSPs that became subthreshold after subtraction of these estimates from the measured amplitudes. An uncertainty in this procedure is the threshold for triggering an AP, since there were generally no failures at short intervals, when synaptic facilitation has the largest impact. We therefore assumed that the threshold that was measured at longer intervals could also be used at short event intervals in the same cell. This assumption neglects the (opposite) effects of spike depression and EPSP summation (Lorteije et al., 2009).

Statistical analysis. Data are given as mean \pm standard error, except when noted otherwise. Differences between two means were assessed by Student's *t* test.

three

RESULTS

Hearing onset occurs at about P13

We studied developmental changes in synaptic transmission at the rat calyx of Held synapse between postnatal day 4 (P4) and P29. To be able to relate developmental changes in firing pattern and synaptic transmission to the maturation of the peripheral auditory system, we assessed the status of the external auditory meatus by visual inspection at the start of each experiment. In all 42 animals in the age range P4-12 the external auditory meatus was still closed, whereas in 2 of 5 P13 animals and all 32 animals in the age range P14-29, including 3 P14 animals, it had opened. In addition, we measured the responses to air-borne sounds using auditory brainstem responses (ABR) in 17 animals in the age range P6-18 before surgery. No responses were found in P6-P11 animals ($n = 7$). At P13 the two animals with the closed external auditory meatus showed responses only at 4 kHz and only at very high intensities (100-115 dB SPL). Two other P13 animals showed responses not only at 4 kHz, but also at both 8 and 16 kHz; thresholds ranged from 85-115 dB. At P14, thresholds were 80-100 dB at 4-16 kHz; still no responses were measured at 32 kHz ($n = 3$). At P17-18, thresholds at 4-16 kHz were 20-50 dB; at 32 kHz they were 45-80 dB ($n = 3$). Our data thus indicate that onset of air-borne sound hearing starts around P13, in general agreement with previous studies in the rat, which found hearing onset to occur between P10 and P14 (Jewett and Romano, 1972; Uziel et al., 1981; Blatchley et al., 1987; Rybak et al., 1992; Geal-Dor et al., 1993). The opening of the ear canal was a good predictor for hearing onset, especially at 8-16 kHz, even though other factors such as the maturation of the middle ear and the endocochlear potential may be functionally more important (Jewett and Romano, 1972; Woolf and Ryan, 1988; Rybak et al., 1992).

Firing pattern changes from bursting to primary-like just before hearing onset

To study the developmental changes in synaptic transmission at the rat calyx of Held synapse, rats were anesthetized and the MNTB was reached via a ventral approach. All in vivo recordings were made in the juxtacellular (loose-patch) configuration, allowing unambiguous identification of single-unit recordings from principal neurons based on their characteristic complex waveform (Figures 1A-C, 2A). Before hearing onset, principal neurons fired bursts of action potentials (Figure 1A; Sonntag et al., 2009); these bursts were triggered by spontaneous calyceal inputs at preferred intervals of about 10, 100-300 and >1000 ms (Figure 1A), in agreement with our previous findings (Tritsch et al., 2010). At P11, just before hearing onset, cells still showed a bursting firing pattern, but long intervals became rare

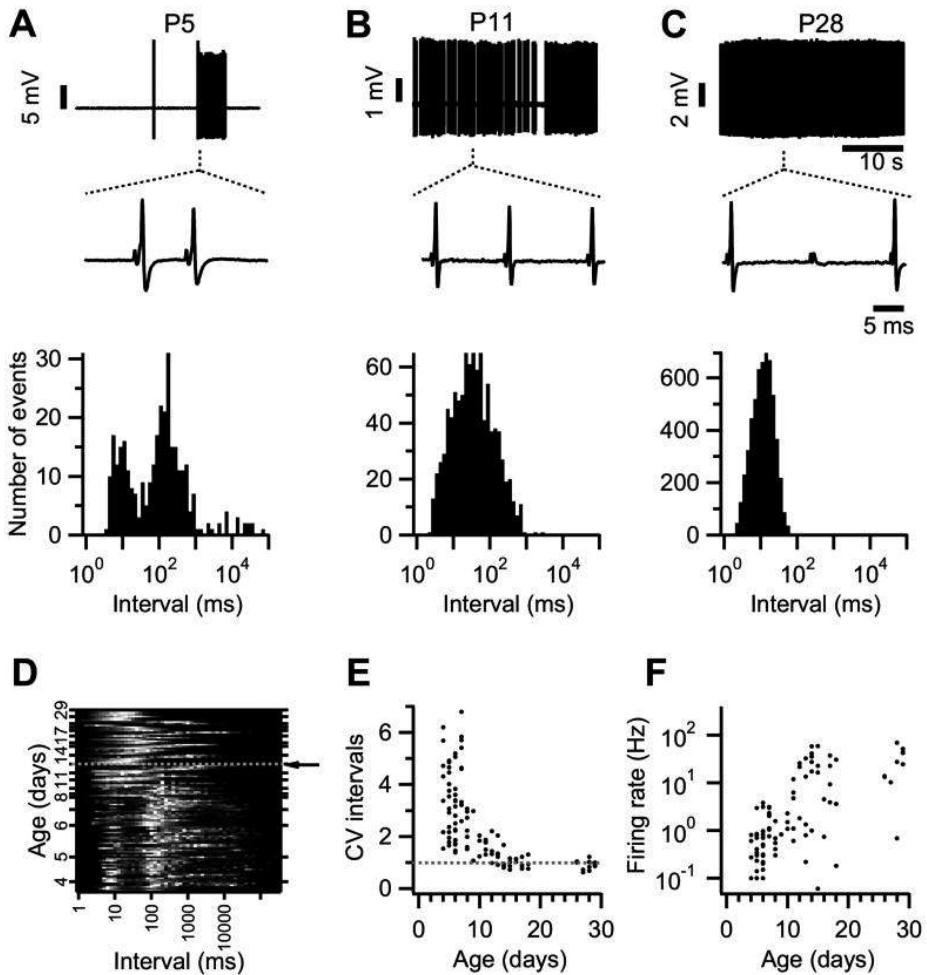


Figure 1. Developmental changes in firing pattern. **A**, Example of bursting firing pattern of a principal neuron from the MNTB of a P5 rat during an in vivo juxtacellular recording. Lower panel shows complex waveforms at higher time resolution, consisting of a prespike, followed by an EPSP (eEPSP) and the postsynaptic action potential (eAP). Lower panel shows the inter-event interval histogram. Preferred intervals cluster around 10 ms, a few hundred ms and 10 seconds. **B**, As **A**, except age of the rat was P11. The interval histogram shows lack of very long intervals. **C**, As **A**, except age of the rat was P28. Middle panel shows three complex waveforms; the middle one lacks an eAP. The lower panel shows the interval histogram showing smaller and less variable intervals than at the younger ages. **D**, Surface plot showing the age dependence of the event interval distribution in a total of 142 units. Sixty-three cells from Tritsch et al. (2010) within the P4-8 range have been included. In each cell the histogram is normalized to its largest value. Dashed gray line and arrow indicate hearing onset at P13. **E**, Developmental decrease in coefficient of variation (CV) of event intervals. **F**, Developmental increase in average firing rate.

(Figure 1B). The adult spontaneous, primary-like firing pattern is illustrated in Figure 1C. An overview of the spontaneous firing patterns of 140 cells between P4 and P29 is shown in Figure 1D, illustrating the transition from a bursting pattern before hearing onset to a primary-like firing pattern in the young-adult, which largely happened between P9 and P11, i.e. before hearing onset. In most units the signal-to-noise ratio was sufficient to verify that all postsynaptic events were preceded by a prespike, suggesting that the calyx drove the spontaneous activity of principal neurons throughout this developmental period. The developmental decrease in the variability was reflected by a decrease in the coefficient of variation (CV) of the event intervals (Figure 1E). In 4-6-day-old animals the CV was on average 3.06 ± 0.30 ($n = 20$), whereas in young-adult animals (P26-29), it had decreased to a value of 0.90 ± 0.05 ($n = 12$), close to the prediction for a primary-like firing pattern (Heil et al., 2007). The mean firing rates were on average 0.69 ± 0.11 Hz ($n = 42$) in recordings from 4-6-day-old animals (Figure 1F); after hearing onset mean frequencies were quite variable (Kopp-Scheinflug et al., 2008), but generally much higher than before hearing onset. Average firing frequencies in young-adult animals (P26-29) were 21.8 ± 8.6 Hz ($n = 12$). Several factors are probably responsible for the observed changes, including maturation of the electrical and release properties of the hair cells (Kros et al., 1998; Beutner and Moser, 2001) and the regression of Kölliker's organ (Tritsch and Bergles, 2010), which drives the action potentials in the hair cells before hearing onset (Tritsch et al., 2007).

Synaptic transmission becomes faster, but not more reliable during development

Figure 2A shows an overlay of the first complex waveform shown in Figure 1A and in Figure 1C (*middle panel*), illustrating that synaptic transmission in the MNTB became much faster during development. The halfwidth of the extracellularly recorded postsynaptic action potential (eAP) decreased from 0.31 ± 0.02 ms ($n = 20$) at P4-6 to 0.16 ± 0.015 ms ($n = 12$) in young-adult rats (Figure 2B). The delay between the pre- and the postsynaptic spike also showed a large developmental change, decreasing from 1.83 ± 0.16 ms ($n = 17$) at P4-6 to 0.67 ± 0.04 ms ($n = 7$) in young-adult rats (Figure 2C).

At short intervals between events, the eAP became smaller (Figure 1A, 2D, *inset*). In young animals, the amount of depression was much larger at short intervals and spike depression recovered much more slowly (Figure 2D). To allow a quantitative comparison of the time course of recovery from spike depression, we fitted a model with a single recovery time constant to the data, as detailed in the Methods. Even though the fit with a single component was not always optimal (Figure 2E; Lorteije et al., 2009), the model could account for as much as $74 \pm 3\%$ ($n = 20$) of the variance in the AP amplitudes in P4-6 animals. The use of only a single component also had the advantage that it facilitated a comparison between all cells. In cells from P4-6 animals, the time constant for recovery of depression was 323 ± 132 ms ($n = 20$); on average spikes depressed by $15 \pm 2\%$ per AP. After hearing onset, most cells showed little spike depression during spontaneous firing. In cells between P15-29 in which the fit could

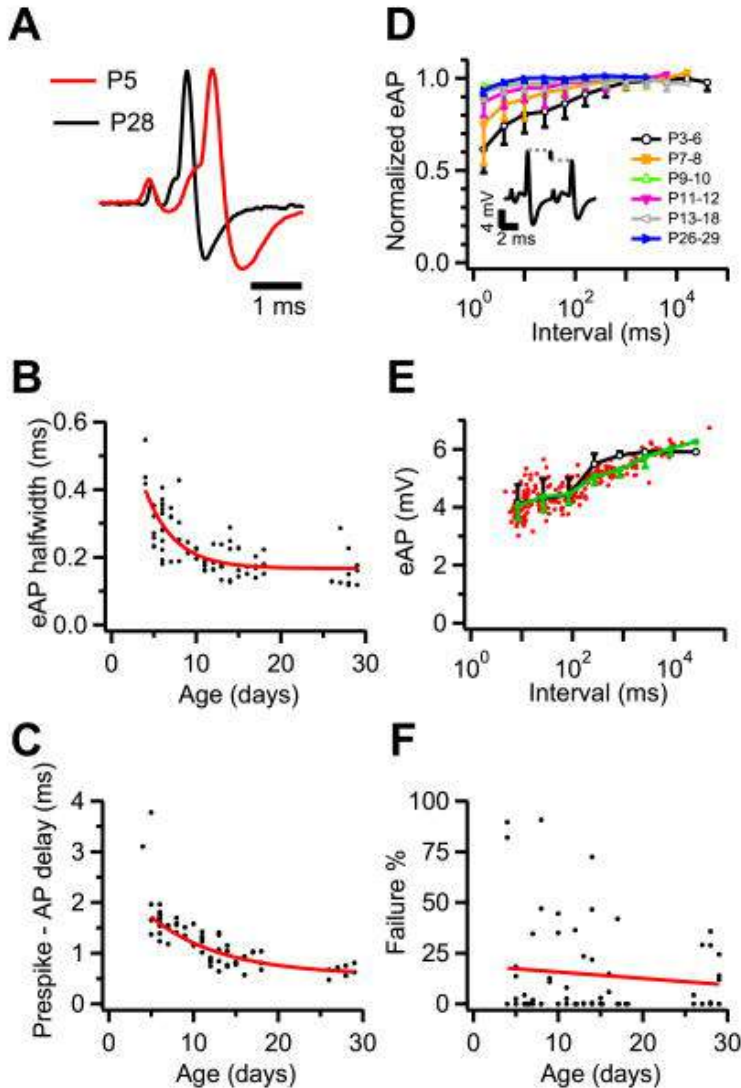


Figure 2. Developmental changes in timing and reliability of synaptic transmission. **A**, The first complex waveform of the lower panel of Figure 1A and **E** are aligned on the prespike and scaled to the same peak amplitude to illustrate the difference in the time course of the complex waveform at P5 and at P28. **B**, Developmental changes in eAP halfwidth. Solid line is an exponential fit with time constant 4 days. **C**, Developmental changes in latency between prespike and eAP. Solid line is exponential fit on the data starting at P5, with time constant 8 days. **D**, Depression of eAP size as a function of eAP interval. eAP sizes from individual recordings ($n = 57$) were log-binned and normalized to the average of the 3 bins with the longest intervals before averaging within the different age groups. Inset shows example of depression of eAP size at short intervals in a P5 rat. **E**, Relation between eAP size and log-interval. Green trace shows binned average with standard deviation. Black trace shows model fit with single recovery time constant of 320 ms. **F**, Percentage of subthreshold eEPSPs per cell as a function of age. Red line shows linear regression ($r = -0.1$; $p > 0.4$).

account for at least 10% of the variance in eAP amplitudes, the time constant for recovery was on average only 1.0 ± 0.1 ms ($n = 4$). Despite the much slower recovery from spike depression at young ages, the reliability of the synaptic transmission did not change greatly during development; both before and after hearing onset about half of the cells showed transmission failures during spontaneous activity (Figure 2F). Interestingly, before hearing onset almost all failures were observed at inter-spike intervals larger than 20 ms.

Developmental changes in short-term plasticity during spontaneous activity in vivo

The observation that before hearing onset the reliability of the calyx of Held synapse depended on recent history suggested a contribution of STP to synaptic strength. The excellent signal-to-noise ratio of the juxtacellular recordings allowed us to quantify interval-dependent changes in the size of the extracellular recorded EPSP (eEPSP). We previously showed that the size of the eEPSP or the maximum amplitude of its first derivative recorded from the young-adult mouse principal neurons provide a measure for the strength of synaptic transmission (Lorteije et al., 2009); by making simultaneous whole-cell and juxtacellular recordings we confirmed that this also held true in slice recordings from principal neurons of young (P6-9) rats ($n = 8$, results not shown). Figure 3A illustrates that before hearing onset the mean amplitude of eEPSPs clearly depended on interval. On average, amplitudes were larger both at very short and at very long intervals, creating a U-shaped relation between eEPSP amplitude and (log) interval (Figure 3B). We interpret the increase at short intervals as evidence for synaptic facilitation and the increase at very long intervals as evidence for the presence of recovery from synaptic depression. The failures were only present at the intermediate intervals, when facilitation had decayed, but depression had not yet recovered, illustrating the impact that STP could have on the transmission reliability before hearing onset. To quantify the time course of both types of STP, we fitted the relation between the eEPSP amplitude and its interval after the previous event with a model that took the accumulating effects of both synaptic facilitation and depression and their interaction into account (Varela et al., 1997), as detailed in the Methods. For each recording we compared three different configurations: depression alone, facilitation alone, and a combination of synaptic depression and facilitation. To evaluate the goodness-of-fit, we calculated the value of Pearson's correlation coefficient r between model and measured values. Its square, r^2 , sometimes called the coefficient of determination, provides an estimate of the fraction of the variance in the eEPSP amplitudes that can be explained by the model. A comparison of average measured and fitted eEPSP amplitudes for the model with both facilitation and depression suggests that this model provided an adequate description of the interval-dependent changes in the eEPSP amplitudes (Figure 3B). For this recording, 70.7% of the variance could be explained by a combination of synaptic depression and facilitation, whereas this was 62.8% for a model with only depression. A fit with a model with only facilitation was not possible. To choose between the different models, we evaluated the

three fits for each recorded cell, setting a minimum increase of 2.5% explained variance per component, with each component contributing two extra free parameters. The fit of the data shown in Figure 3B indicated for the facilitation process a 95% increase per AP, decaying with a time constant of 125 ms and for the depression a decrease of 37% per AP, recovering with a time constant of 1.0 s. Shortly before hearing onset, the contribution of STP decreased dramatically. An example of a recording from a P11 rat is shown in Figure 3C. This cell also showed evidence for both facilitation and depression. The amount of facilitation was smaller (62%) and its decay time course was much faster (12.7 ms) than in

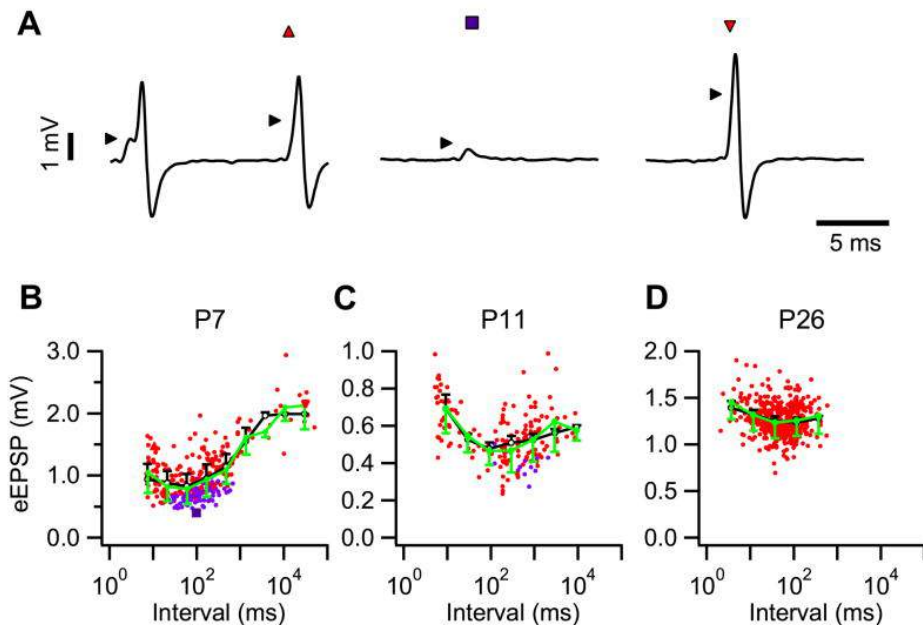


Figure 3. Short-term plasticity changes during development. **A**, Illustration of complex waveforms from a P7 rat showing synaptic facilitation at short intervals (*left*), depression at intermediate intervals leading to a postsynaptic failure (*middle*) and recovery from depression at long intervals (*right*). Symbols above the waveforms refer to events shown in **B**. **B**, Dependence of eEPSP size on inter-event interval. Red dots show individual suprathreshold eEPSP amplitudes, purple dots subthreshold eEPSP amplitudes, individual square, triangle and inverted triangle refer to examples shown in **A**. Green symbols show binned averages with standard deviation and black circles indicate fit with an STP model with both facilitation and depression. Fit parameters were amplitude 2.0 mV, 95% facilitation per AP, decaying with a time constant of 125 ms, 38% depression per AP, decaying with a time constant of 1.0 s. The fit could account for 71% of the variance in the eEPSP amplitudes. **C**, as **B**, except P11 animal. Fit parameters were amplitude 0.6 mV, 62% facilitation per AP, decaying with a time constant of 12.7 ms, 2.9% depression per AP, decaying with a time constant of 4.4 s. The fit could account for 32% of the variance in the eEPSP amplitudes. **D**, as **B**, except P26 animal. Fit parameters were amplitude 1.25 mV, 11% facilitation per AP, decaying with a time constant of 11.5 ms. There was no depression. The fit could account for 5.2% of the variance in the eEPSP amplitudes.

the recording shown in Figure 3B. In addition, the amount of depression was much lower, without an obvious change in its recovery time course. The model could account for 32% of the variance in the eEPSP amplitudes. Figure 3D shows the results of a cell from a young-adult animal (P26). Facilitation again decayed fast (11.5 ms). In this cell there was no clear contribution of synaptic depression and the model could account for only 5.2% of the total variance.

Figure 4 summarizes the dramatic developmental changes in both the kinetics and amount of STP. Between P4 and P8, all recordings showed STP; 18 of 21 cells showed evidence for the presence of both facilitation and depression; in the other 3 cells depression dominated. In contrast, at P26-29 only 1 cell showed evidence for depression. In 6 out of 12 cells there was evidence for facilitation; in 5 cells no evidence for either facilitation or depression was observed. Especially around hearing onset, the decay of facilitation became much faster, from a value of 123 ± 14 ms ($n = 12$) at P4-6, 71 ± 13 ms ($n = 8$) at P7-9, 12.5 ± 2.3 ms ($n = 11$) at P13-18, to a value of only 11.4 ± 3.0 ms ($n = 6$) at P26-29 (Figure 4A). The time constant for facilitation did not significantly differ between P13-18 and P26-29 ($p = 0.8$). The amount of facilitation gradually decreased, from $189 \pm 32\%$ increase per AP at P4-6 ($n = 12$), to $23 \pm 4\%$ at P13-18 ($n = 14$) and only $12 \pm 6\%$ at P26-29 ($n = 11$; Figure 4B). The amount of facilitation did not differ significantly between P13-18 and P26-29 ($p = 0.1$).

Around the same time the amount of synaptic depression decreased strongly. In the age range P4-6, all cells (14/14) showed evidence for depression, whereas this was the case in only 1 of 12 cells at P26-29. The amount of depression decreased from $38 \pm 4\%$ per AP at P4-6 ($n = 14$) to only $3 \pm 1\%$ at P13-P18 ($n = 20$; Figure 4D). In most cells the recovery from depression was slow and there were no obvious changes in the time course of the recovery from depression, although the estimates of the recovery time constant were not very reliable as a result of the paucity of very long intervals in most cells after hearing onset (Figure 4C). In a few cells the recovery time constant for synaptic depression was only about 100 ms. In the cells from immature animals these short time constants appeared to be genuine and not caused by a fit bias owing to a lack of longer intervals. They may be a reflection of the short, Ca-dependent recovery time constants that have been observed in slice recordings (Wang and Kaczmarek, 1998; Sakaba and Neher, 2001).

Figure 4E shows how much of the variance in the eEPSP amplitudes could be accounted for by the model, showing that this contribution decreased from an average of $51 \pm 5\%$ at P4-6 ($n = 14$) to only $3 \pm 1\%$ in the young-adults (P26-29; $n = 12$). In Figure 4E, cells without significant facilitation or depression have 0% explained variance. Even though our criterion for accepting additional components was quite lenient, it is of course hard to exclude that a contribution of STP was somehow missed. However, it is unlikely that this contribution was very large in the young-adult animals, since the explained variance increased on average by only $0.5 \pm 0.1\%$ if we would have used the fit with both facilitation and depression in each experiment, irrespective of the parameter outcome (e.g. negative facilitation). This

illustrates that whatever model selection criterion would be chosen, the contribution of STP to the variability in the spontaneous eEPSP amplitudes rapidly becomes quite small after hearing onset. A comparison of Figures 1H and 4E shows that the changes in the firing pattern and the changes in STP happened around the same time. Indeed, the CV of the

three

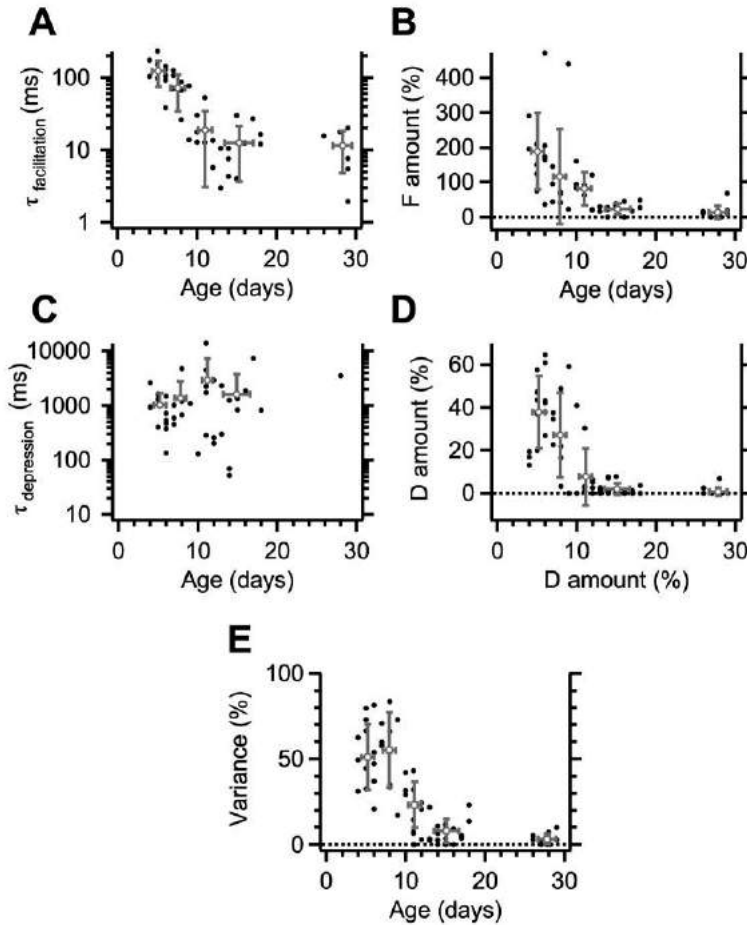


Figure 4. Developmental changes in STP. **A**, Developmental decrease in time constant of facilitation, as obtained from the fit with an STP model. Only cells which showed significant facilitation are included (45 of 65 cells). Gray symbols show binned averages with standard deviations. **B**, As **A**, showing the developmental changes in the amount of facilitation (53 of 65 cells). All cells are included, except when they showed only depression. Cells without significant facilitation are included as 0%. **C**, Age dependence of the time constant for recovery from depression as obtained from the fit in cells with significant depression (42 of 65 cells). **D**, Developmental decrease in the amount of depression. Cells without significant depression are included as 0%. **E**, Developmental decrease in the percentage of variance that can be explained by the model fit (coefficient of determination). Cells without both significant facilitation and depression are included as 0%.

event intervals and the amount of variance explained by the STP fit model showed a good correlation ($r = 0.81$), even though individual cells could show synaptic maturation without already having the adult firing pattern. For example, in Figure 3C a P11 unit is illustrated that showed little depression and a rapid decay of facilitation, yet still had retained the bursting firing pattern (the CV of its event intervals was 1.8). The large impact of STP on the EPSP variability was also evident from the CV of the eEPSP amplitudes, which decreased from 0.35 ± 0.02 at P4-8 ($n = 19$), to 0.18 ± 0.01 at P26-29 ($n = 12$). The eEPSP amplitude CV was well correlated with the variance explained by the fit model ($r = 0.79$; $n = 65$). After subtraction of the variance in the eEPSPs that could be explained by the fit from the total variance, the CV for P4-8 animals decreased to only 0.16 ± 0.01 , i.e. even below the value after hearing onset. As the signal-to-noise ratio was good in each of the recordings that are included in Figure 4, this indicates that stochastic fluctuations in the number of released vesicles are the dominant source for amplitude fluctuations at the rat calyx of Held synapse after hearing, whereas STP is the most important contributor to amplitude fluctuations before hearing onset.

To get an estimate of the impact that short-term facilitation might have on the transmission reliability before hearing onset, we adjusted the measured amplitudes in cells which showed both significant facilitation and failures as if there were no facilitation, as explained in the Methods. In the absence of synaptic facilitation, the estimated percentage of failures increased by $17.9 \pm 3.3\%$, from a value of $39.9 \pm 11.3\%$ to $61.4 \pm 9.2\%$ ($n = 10$). Our data thus suggest that the presence of synaptic facilitation played a substantial role in counteracting the effects of synaptic depression in immature synapses.

Developmental changes in short-term plasticity in slice recordings

Our finding that the contribution of STP to the variability in spontaneous transmission decreases dramatically just before hearing onset raises the question whether the observed changes are due to a change in synaptic properties, or whether they are a direct consequence of changes in the electrical input pattern, the extracellular milieu, or the postsynaptic voltage-dependent ion channels. To discriminate between these different possibilities, we measured the time course and magnitude of both facilitation and depression in slices from P4-6 or P13-16 animals during paired-pulse stimulation. The results obtained in slices were in general agreement with the results obtained during spontaneous activity in vivo. At an extracellular calcium concentration of 1.2 mM, which is close to the in vivo concentration (reviewed in Borst, 2010), both facilitation and depression of EPSCs were generally observed. An example cell from a P5 rat is shown in Figure 5A. The model fit resulted in a decay time constant of facilitation of 72 ms. It also showed clear depression, of about 25% per AP, which recovered with a time constant of several seconds. At a calcium concentration of 0.6 mM, the EPSCs were much smaller and synaptic depression was no longer present. Facilitation was still observed, which decayed with an estimated time constant of 47 ms (Figure 5B). In contrast, in slices from P13-16 animals synaptic depression was generally greatly reduced or

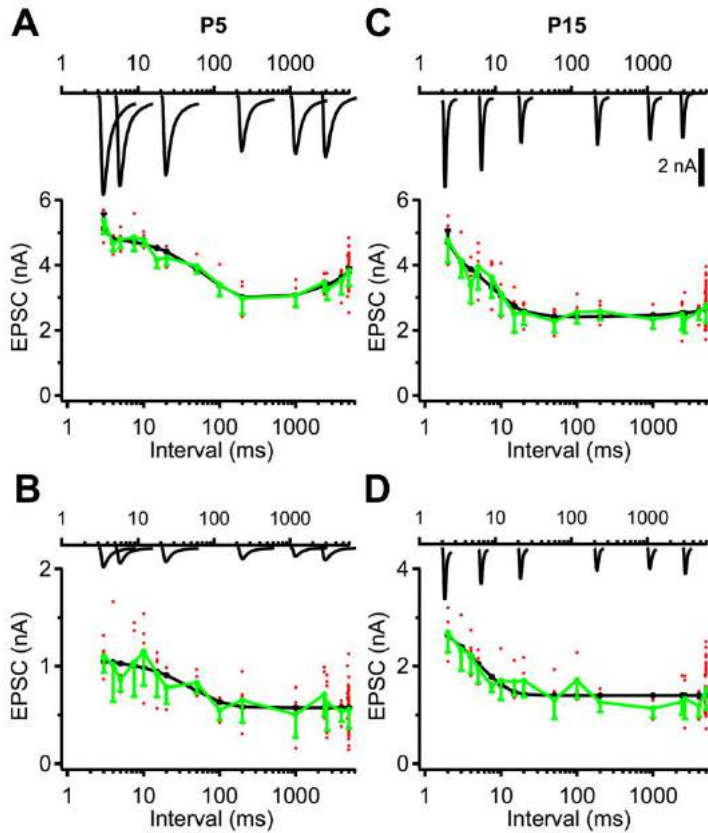


Figure 5. Developmental changes in STP during paired-pulse stimulation in slice recordings. **A**, Top, example EPSCs obtained at the indicated interval in a P5 whole-cell voltage clamp experiment at 1.2 mM calcium. Bottom, red dots show individual EPSC amplitudes, green symbols binned averages with standard deviation and black circles show fit with an STP model with both facilitation and depression. Fit parameters were amplitude 5.2 nA, 74% facilitation per AP, decaying with a time constant of 72 ms, 25% depression per AP, decaying with a time constant of 6.5 s. The fit could account for 68% of the variance in the EPSC amplitudes. **B**, As **A**, except calcium concentration was lowered to 0.6 mM. Fit parameters were amplitude 0.6 nA, 87% facilitation per AP, decaying with a time constant of 47 ms. The fit could account for 43% of the variance in the EPSC amplitudes. **C**, As **A**, except recording was from a P15 neuron. Fit parameters were amplitude 3.4 nA, 104% facilitation per AP, decaying with a time constant of 7.3 ms, 9% depression per AP, decaying with a time constant of 10.9 s. The fit could account for 57% of the variance in the EPSC amplitudes. **D**, As **C**, except that calcium concentration was lowered to 0.6 mM. Fit parameters were amplitude 1.4 nA, 136% facilitation per AP, decaying with a time constant of 4.6 ms. The fit could account for 42% of the variance in the EPSC amplitudes. Scale bar for EPSCs in **C** also pertains to EPSCs shown in **A**, **B** and **D**.

absent and synaptic facilitation decayed much faster. An example is shown in Figure 5C, *D*. EPSCs were much faster than at P4-6, in agreement with previous results (Chuhma and Ohmori, 1998; Taschenberger and von Gersdorff, 2000; Joshi and Wang, 2002; Joshi et al., 2004; Koike-Tani et al., 2005). This cell showed both facilitation and depression at a calcium concentration of 1.2 mM (Figure 5C). The facilitation decayed with a time constant of about 7 ms, much faster than in the P5 cell shown in Figure 5A. This fit also illustrates that the criterion for accepting additional components was lenient, since this recording showed significant depression, even though the amount of depression was quite small. At 0.6 mM only facilitation was present, which had a similar decay time course as at 1.2 mM (Figure 5D).

We also stimulated cells with a protocol with more continuously chosen intervals over a wide range, which was designed to mimic the interval range observed before hearing onset, but which lacked the gaps in the interval distribution that were sometimes observed in the *in vivo* data, as explained in the Methods. A histogram of the interval distribution of this *in-vivo*-like protocol is shown in Figure 6A. The time derivative of the whole-cell current clamp recording is shown in Figure 6B and at higher time resolution in Figure 6C, *D* to illustrate the presence of short-term facilitation at short intervals and short-term depression at intermediate intervals. This recording is from the same cell as illustrated in Figure 5A, *B*. The interval dependence of the rate of rise of the intracellularly recorded EPSPs (iEPSP') at 1.2 mM calcium is shown in Figure 6E, together with the fit with the STP model. The fit indicated a decay time constant for synaptic facilitation of 95 ms and a clear synaptic depression of 33% per AP, which recovered slowly. No postsynaptic failures were observed. At a calcium concentration of 0.6 mM, the average rate of rise of EPSPs was strongly reduced and most EPSPs with a rate of rise <16 V/s failed (Figure 6F). Synaptic depression was no longer apparent, but the EPSPs showed facilitation at short intervals, which decayed with a time constant of about 35 ms. Similar results were obtained in voltage clamp, with both facilitation and depression at 1.2 mM calcium and only facilitation at 0.6 mM (results not shown).

The same cell from a P15 animal that was illustrated in Figure 5D-*F* was also probed with the *in-vivo*-like protocol. Both at 1.2 mM (Figure 6G) and at 0.6 mM (Figure 6H) clear facilitation was observed, which decayed with time constants of 9 and 5 ms, respectively. At 1.2 mM there was also a small depression, similar to Figure 5C. No failures were observed at 1.2 mM calcium, whereas at 0.6 mM most EPSPs with a rate of rise of less than 30 V/s were subthreshold. In the *in-vivo*-like current-clamp stimulus protocol, only 2 of 5 P5 and 1 of 4 P15 cells showed postsynaptic failures at 1.2 mM; at 0.6 mM, 4 of 4 P5 and 3 of 4 P15 cells showed failures. Failures were generally not observed at short intervals, in agreement with the results obtained *in vivo*. The estimated threshold EPSP amplitude, the amplitude at which about half of the EPSPs did not induce an AP, ranged between 16 and 30 V/s at P5 ($n = 4$) and between 30 and 35 V/s at P15 ($n = 3$).

Our *in vitro* data thus confirm the observations made *in vivo* that facilitation becomes faster and depression is reduced during development. There was some variability in the

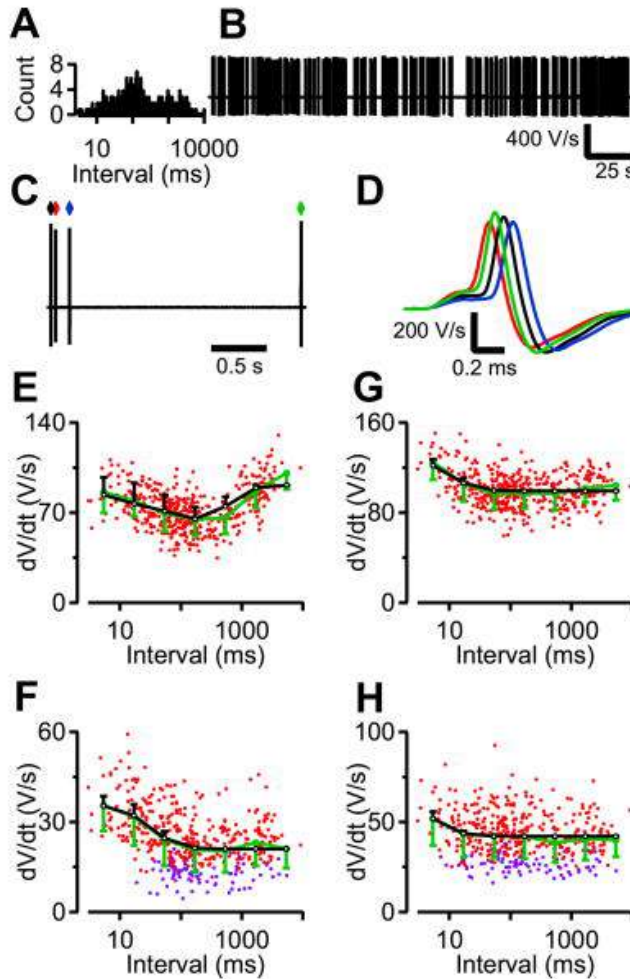


Figure 6. Developmental changes in STP in slices during in-vivo-like stimulation. **A**, Histogram of intervals for stimulus protocol. **B**, Time derivative of whole-cell current clamp responses of a P5 cell to in-vivo-like stimulus protocol. Note the large range and random character of intervals between stimuli. **C**, Small segment of the responses shown in **B**. **D**, Responses shown in **C** aligned at rising phase of the iEPSP'. Colors correspond to markers above trace in **C**. **E**, Interval dependence of iEPSP' maximal amplitude in a P5 cell at 1.2 mM calcium. Green curve indicates binned average. Error bars show standard deviation. Black circles are result of the fit with an STP model, with amplitude 91.4 V/s, 74% facilitation per AP, decaying with a time constant of 95 ms, 33% depression per AP, decaying with a time constant of 0.5 s. The fit could account for 50% of the variance in the iEPSP' amplitudes. **F**, as **E**, except that calcium concentration was 0.6 mM. Red circles are suprathreshold EPSPs, blue subthreshold. Fit parameters were: amplitude 21 V/s, 70% facilitation per AP, decaying with a time constant of 35 ms. The fit accounted for 28% of the amplitude variance. **G**, as **E**, except that recording was from a P15 animal. Fit parameters were: amplitude 103 V/s, 47% facilitation per AP, decaying with a time constant of 10.2 ms. 1% depression per AP, decaying with a time constant of 1.7 s. The fit accounted for 18% of the amplitude variance. **H**, as **G**, except that calcium concentration was 0.6 mM. Fit parameters were: amplitude 42 V/s, 74% facilitation per AP, decaying with a time constant of 5.4 ms. Fit accounted for 4% of the variance.

estimates for the decay of facilitation, ranging for the six different protocols from 21 ms for the in-vivo-like stimulation under voltage clamp at 1.2 mM to 95 ms for the same stimulus under current clamp for the P5 cell and between 5 ms for the paired-pulse protocol at 1.2 mM and 14 ms for the in-vivo-like protocol under voltage clamp at 0.6 mM for the P15 cell. However, there were no systematic differences in the amount or decay time constant of facilitation or of depression obtained with the different protocols across different cells. The lack of systematic differences between these parameters between voltage-clamp and current-clamp recordings and between paired pulse and more random stimulation indicates that the results obtained in vivo can be used as a quantitative measure for the kinetics and amount of STP at the calyx of Held synapse. We therefore averaged the different significant estimates for these parameters to obtain a single estimate per cell. Figure 8 summarizes the averages across cells before and after hearing onset. Facilitation became much faster after hearing onset, with the decay accelerating from 31.6 ± 7.7 ms ($n = 5$; range 6-50 ms) at P4-6 to 6.6 ± 0.8 ms ($n = 5$; range 5-9 ms; $p = 0.03$) at P13-16; in addition the amount of facilitation became smaller ($122 \pm 30\%$ vs. $51 \pm 13\%$; $p = 0.08$). The amount of depression in the presence of 1.2 mM calcium decreased from $27.6 \pm 3.8\%$ ($n = 5$) at P4-6 to only $1.9 \pm 0.8\%$ ($n = 5$; $p = 0.002$) at P13-16, but there was no change in the time constant of the recovery from depression (1.9 ± 0.2 s vs. 1.9 ± 1.0 s; $p > 0.9$). At 0.6 mM, 3 of 5 cells at P5 and none of the 5 cells at P15 showed significant depression. The percentage of the variance in the synaptic potentials or currents during the in-vivo-like stimulation at 1.2 mM that could be ascribed to STP decreased strongly after hearing onset. On average this percentage decreased from $62 \pm 6\%$ at P5 to only $8 \pm 3\%$ at P15 ($n = 5$).

The comparison between the in vivo spontaneous data and the data obtained in slice recordings in Figure 8 shows that despite the large experimental differences between the two approaches, the main developmental changes were consistent. This indicates that these changes were not predominantly the result of changes in firing pattern, postsynaptic voltage-dependent ion channels or the composition of the extracellular environment, even though a contribution of each of these factors cannot be excluded. A difference between both types of experiments was that the time constant for the decay of facilitation was lower in the in vivo spontaneous data than in the age-matched slice experiments (Figure 8A). The cause for this difference is largely unknown. It is unlikely to be due to a cooling of the exposed brain surface in the in vivo experiments, since the delay between the pre- and postsynaptic action potential was not significantly different ($p = 0.09$) in P5-6 animals under both conditions, and in addition the decay of facilitation changes little between 33 and 38°C (Klyachko and Stevens, 2006). A difference between extracellular and intracellular measurements may contribute, since the eEPSP amplitude becomes difficult to measure accurately when it becomes relatively large (Figure 3A; Lorteije et al., 2009). Facilitation can therefore lead to an underestimation at short intervals, and thus to an apparently larger decay of facilitation. An analysis of simultaneous intra- and extracellular recordings showed

that extracellularly measured time constants for the decay of facilitation can be somewhat larger (results not shown), but this effect is limited in its impact. Decay time constants *in vivo* were similar when we used instead of the amplitude the peak of the first time derivative of the eEPSP (results not shown), a measure which is less sensitive to ceiling effects, but more sensitive to confounding effects of the prespike (Lorteije et al., 2009). Also, the magnitude of the facilitation was similar *in vivo* and *in vitro*, arguing against a large underestimation during the *in vivo* experiments. Finally, the difference between *in vivo* and *in vitro* is unlikely to be due to an interaction with depression, since the amount and time course of facilitation were similar at low and at physiological release probabilities in our slice experiments, in agreement with a recent report showing that the decay of facilitation is similar in the presence of depression (Müller et al., 2010).

Developmental changes in short-term plasticity during electrical stimulation *in vivo*

In the *in vivo* experiments, the firing pattern before and after hearing onset differed greatly, whereas in the slice experiments both age groups received the same stimulation protocols. In the *in vivo* situation, long pauses become rare after P11; because of the slow recovery from synaptic depression, the spontaneous activity may therefore tonically depress a synapse (Boudreau and Ferster, 2005; Reig et al., 2006; Hermann et al., 2007; Hermann et al., 2009). To further delineate the differences in STP before and after hearing onset under conditions that approximated the physiological situation as closely as possible, we therefore applied the stimulation protocols used for the slice experiments during *in vivo* recordings. In these experiments, spontaneous activity was completely abolished by ablation of the contralateral cochlea and afferent activity was evoked by placement of a bipolar electrode at the midline, as detailed in the Methods. A limitation of these experiments was that the field potentials could be large because many cells were activated almost simultaneously. If time permitted, both the paired-pulse protocol and the *in-vivo-like* stimulation protocol were tested. We compared the impact of STP at P5-6 and at P26-28. Figure 7A shows examples of electrically evoked eEPSPs at different intervals in a P6 animal. As was also the case for the spontaneous data, before hearing onset the mean eEPSP clearly depended on the interval (Fig. 7B). In young-adult animals, the contribution of STP was much smaller (Fig. 7C). In the young animals, all 3 cells displayed evidence for depression and in 2 of 3 cells there was also facilitation. In the young-adult animals, 1 of 5 cells did not show evidence for STP, in the other 4 cells either facilitation alone, depression or a combination (1 cell) was observed. During development, the time constant of facilitation decreased from 69 ± 20 ms at P5-6 ($n = 3$) to 5.5 ± 1.0 ms at P26-28 ($n = 3$; Fig. 8A). The amount of facilitation decreased from $96 \pm 56\%$ ($n = 3$) at P5-6 to $52 \pm 21\%$ ($n = 4$) in the young-adult animals (Fig. 8B). At the same time, the amount of depression per AP decreased from $22 \pm 8\%$ ($n = 4$) to only $4 \pm 2\%$ ($n = 6$; Fig. 8C), whereas there were no clear changes in the time constant for recovery from depression

(1.4 ± 0.5 vs. 1.5 ± 0.4 s; Fig. 8D). The percentage of variance explained by the best model during the in-vivo-like stimulation decreased from $50 \pm 6\%$ ($n = 3$) to $9 \pm 2\%$ ($n = 6$; Fig. 8E). Despite the limited number of experiments and the more problematic analysis caused by the presence of field potentials, we conclude that the general developmental changes observed both for the spontaneous in vivo and the slice experiments were also observed during electrical stimulation in the silenced in vivo situation.

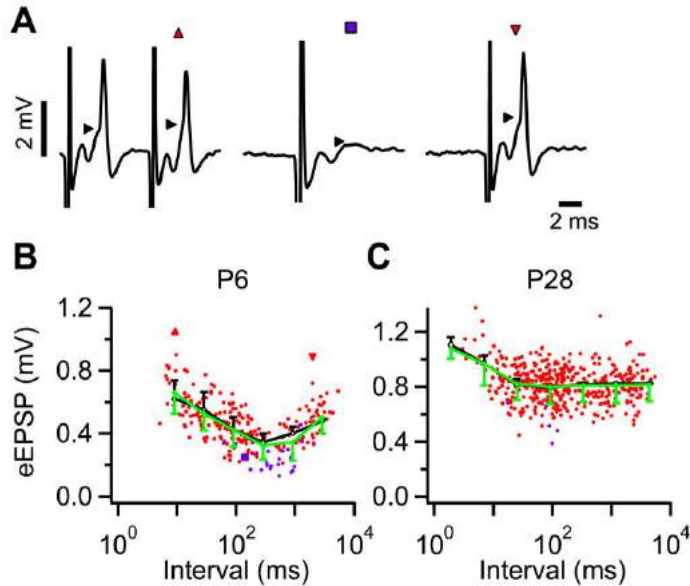


Figure 7. Developmental in vivo changes in STP during electrical stimulation following cochlear ablation. **A**, Illustration of electrically evoked complex waveforms from a P6 rat showing synaptic facilitation at short intervals (*left*), depression at intermediate intervals leading to a postsynaptic failure (*middle*) and recovery from depression at long intervals (*right*) animal. Symbols above the waveforms refer to events shown in **B**. **B**, Dependence of eEPSP size on stimulus interval. Same in-vivo-like protocol was used as in Figure 6. Red dots show individual suprathreshold eEPSP amplitudes, purple dots subthreshold eEPSP amplitudes, individual square, triangle and inverted triangle refer to examples shown in **A**. Green symbols show binned averages with standard deviation and black circles indicate fit with an STP model with both facilitation and depression. Fit parameters were amplitude 0.5 mV, 130% facilitation per AP, decaying with a time constant of 97 ms, 29% depression per AP, decaying with a time constant of 725 ms. The fit could account for 50% of the variance in the eEPSP amplitudes. **C**, as **B**, except P28 animal. Fit parameters were amplitude 0.8 mV, 64% facilitation per AP, decaying with a time constant of 6.8 ms; there was no depression. The fit could account for 15% of the variance in the eEPSP amplitudes.

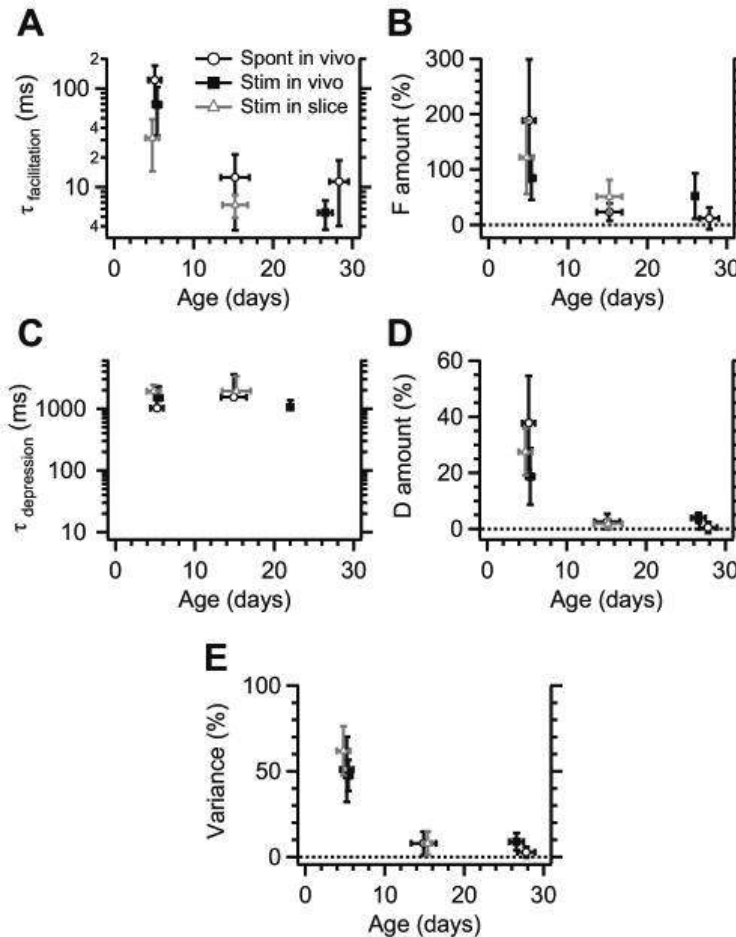


Figure 8. Comparison of developmental changes in STP in vivo and in vitro. Three types of experiments are included: spontaneous in vivo data (open circles; same data as in Figure 4), slice data (open gray triangle) and electrically evoked in vivo data (closed squares). Symbols show binned averages with standard deviations. If multiple protocols from the same cell were applicable, the average from the different protocols was used. **A**, Developmental decrease in time constant of facilitation, as obtained from the fit with an STP model. Only fits which showed significant facilitation are included. **B**, As **A**, showing the developmental changes in the amount of facilitation. Fits showing only depression are not included. **C**, Age dependence of the time constant for recovery from depression as obtained from the fit in cells with significant depression. Fits for slice experiments performed at 0.6 mM were not included to calculate amount or time constant of depression. **D**, Developmental decrease in the amount of depression. Fits without significant depression were included as 0%. **E**, Developmental decrease in the coefficient of determination, the percentage of variance that can be explained by the model fit. For stimulation experiments, only the in-vivo-like protocols were included. Slice experiments performed at 0.6 mM were not included. Fits without both significant facilitation and depression were included as 0%.

DISCUSSION

We studied the developmental changes in short-term plasticity (STP) at the rat calyx of Held synapse during *in vivo* recordings. We found clear evidence for the presence of STP in immature synapses, whereas just before hearing onset the impact of STP greatly decreased or even disappeared. Control experiments, both in slices and *in vivo*, suggested that these differences mostly resulted from presynaptic changes, and not from changes in firing pattern, postsynaptic voltage-dependent ion channels or the composition of the extracellular environment. The observed dramatic changes in STP just before hearing onset are likely to play an essential role in the conversion of the calyx of Held synapse into an auditory relay synapse.

Developmental changes in transmission speed

We observed a gradual increase in speed during postnatal development, with relatively little change after hearing onset. Based on experiments performed in slices, multiple factors contributed to these changes, including faster pre- and postsynaptic action potentials and faster EPSCs (Wu and Oertel, 1987; Chuhma and Ohmori, 1998; Taschenberger and von Gersdorff, 2000; Futai et al., 2001; Joshi and Wang, 2002; Joshi et al., 2004; Koike-Tani et al., 2005; Kushmerick et al., 2006). The faster action potentials are presumably due to an increased density of Kv3 potassium and other voltage-dependent ion channels (reviewed in Johnston et al., 2010).

One other important developmental change was that the principal neurons became much more resistant to spike depression. Voltage clamp measurements from principal neurons in slices have shown a biphasic recovery of sodium currents with a fast recovery time constant of around 1 ms and a slow time constant of around 100 ms at room temperature (Leão et al., 2005); during development, the contribution of the slow time constant decreases. The fast time constant of recovery observed previously in slices was much smaller than the minimum inter-event interval that we generally observed in our *in vivo* experiments before hearing onset, whereas the very slow recovery that we did observe was even slower than the slow time constant measured previously in slices. After hearing onset, when minimum intervals generally became much shorter, we did observe the fast recovery component, whereas the slow recovery component was strongly reduced or even absent, in agreement with the results obtained previously in slices (Leão et al., 2005). The much greater resistance to spike depression is likely to play an essential role in the transformation of the calyx of Held synapse into a fast relay.

Short-term plasticity before hearing onset

We found a large contribution of both short-term facilitation and short-term depression in the immature calyx of Held synapse. Facilitation was not observed in each cell, probably because it can only be uncovered when release probability is not very high (Borst et al.,

1995). The estimated amount and time course of facilitation and depression generally matched previous slice estimates (von Gersdorff et al., 1997; Felmy et al., 2003; Kushmerick et al., 2006; Müller et al., 2007; Müller et al., 2008) and the estimates we obtained both in slices and during in vivo stimulation, except that the decay of facilitation in the immature synapse was somewhat slower in vivo.

three

Mechanisms underlying the developmental decrease in short-term depression

The synaptic depression was most likely predominantly presynaptic, since postsynaptic receptor desensitization or saturation are typically observed only during longer-lasting trains at high frequencies (Neher and Sakaba, 2001; Taschenberger et al., 2002; Wong et al., 2003) and recovery from postsynaptic receptor desensitization is faster than the recovery from synaptic depression observed here (Joshi et al., 2004; Taschenberger et al., 2005). The depression is probably caused by depletion of the readily-releasable pool of vesicles (Schneggenburger et al., 1999; Wu and Borst, 1999) with an additional contribution of presynaptic calcium channel inactivation (Forsythe et al., 1998; Xu and Wu, 2005).

Just before hearing onset, the contribution of STP changed dramatically. The timing of these changes did not indicate a major role for sensory-evoked activity, in agreement with the idea that many aspects of synaptic maturation at the calyx of Held synapse are relatively hard-wired (Erazo-Fischer et al., 2007). The amount of depression decreased strongly without an apparent change in its recovery time course, even though the paucity of long intervals made it hard to estimate this. The most likely explanation for this decrease is a strong decrease in the amount of vesicle depletion. Possible causes include differences in the organization of the release sites, an increase in vesicle pool size, the number of docked vesicles, the number of active zones, exocytotic efficiency (amount of exocytosis per Ca influx), or Ca current facilitation, and a decrease in the release probability (Taschenberger and von Gersdorff, 2000; Iwasaki and Takahashi, 2001; Taschenberger et al., 2002; Kushmerick et al., 2006; Wimmer et al., 2006; Yang et al., 2010). Since quantal analysis suggested release probability to be low in the young-adult calyx of Held (Lorteije et al., 2009), it seems likely that the developmental reduction of release probability made a large contribution to the decreased impact of short-term depression. A developmental reduction of release probability has also been observed elsewhere, for example in cortex (reviewed in Feldmeyer and Radnikow, 2009).

The importance of synaptic facilitation during burst firing in developing synapses

Before hearing onset, the synaptic facilitation played an important role in counteracting the large synaptic depression. The observed characteristic burst pattern, with multiple micro-bursts interspersed by very long intervals (Tritsch et al., 2010), is thus an efficient way of relaying information from the periphery to central synapses. Similar firing patterns

have been observed in the developing mouse MNTB (Sonntag et al., 2009), more peripherally in the auditory system (Brugge and O'Connor, 1984; Walsh and McGee, 1987) and in other developing sensory systems (Blankenship and Feller, 2010), suggesting that synaptic facilitation may have a similar function in these developing synapses. The strong developmental reduction in synaptic depression made the opposing effect of facilitation less opportune and, indeed, we saw a decrease in the amount of facilitation and a much faster decay. As a result, the impact of synaptic facilitation decreased strongly around the same time that the bursting pattern disappeared. A very rapid decay of synaptic facilitation has previously been observed in the endbulb synapse of the cochlear bushy cells and at the cerebellar mossy fibre-granule cell synapse, both of which are also specialized in high-frequency signalling (Saviane and Silver, 2006; Kuenzel et al., 2011).

Mechanisms underlying the developmental acceleration of the decay of facilitation

Synaptic facilitation in the calyx of Held depends on the buildup of residual calcium (Felmy et al., 2003; Müller et al., 2007; Müller et al., 2008). The most likely explanation for the strong increase in the decay speed after the onset of hearing is therefore that the Ca^{2+} concentration in the terminal decays much more rapidly in mature animals. After a presynaptic action potential Ca^{2+} can bind to calcium buffers or be cleared by pumps (reviewed in Neher and Sakaba, 2008). Evidence for a developmental increase in both Ca^{2+} binding capacity and clearance rates have been obtained at the calyx of Held synapse (Chuhma et al., 2001). Whereas the immature calyx has a relatively small calcium buffer capacity (Helmchen et al., 1997), the calyx expresses among others the calcium-binding proteins calretinin and parvalbumin, whose expression increases during development (Lohmann and Friauf, 1996; Felmy and Schneggenburger, 2004). The slow calcium-binding protein parvalbumin has been shown to speed up the decay of short-term facilitation at the calyx of Held synapse (Müller et al., 2007), suggesting that a developmental increase in its concentration may contribute to the observed changes in facilitation. Ca^{2+} is extruded from the calyx by a combination of several pumps (Kim et al., 2005), whose density may increase during development. Morphological changes may also contribute to faster clearance. Around hearing onset the calyx starts to assume its mature, floral-like structure (Kandler and Friauf, 1993; Kil et al., 1995; Ford et al., 2009). By increasing the surface-to-volume ratio, the more fenestrated, open structure may speed up presynaptic calcium clearance.

Replenishment of the readily-releasable pool in the adult calyx

In slice recordings, the recovery from synaptic depression can be biphasic, with the slow time constant matching the recovery observed here in most synapses. The fast time constant is thought to reflect both a calcium-dependent increase in vesicle replenishment and an increase in release probability of 'reluctant', rapidly replenishing vesicles (Wang and Kaczmarek, 1998; Wu and Borst, 1999; Sakaba and Neher, 2001; Hosoi et al., 2007;

Müller et al., 2010). As this rapid recovery phase was not observed in most of the present experiments, the most parsimonious explanation is that apparently the demands on the synapse were not sufficient to prolong the Ca^{2+} decay time course appreciably. Even though we cannot exclude that this rapid phase may become apparent during acoustic stimulation, this was not the case in the mouse calyx of Held synapse or the related gerbil endbulb of Held synapse (Lorteije et al., 2009; Kuenzel et al., 2011). This rapid decay can be expected to considerably limit the time window during which Ca-dependent processes can affect the size or the release probability of the readily-releasable pool. We speculate that the combination of limited depletion owing to low release probability and a short window of increased replenishment immediately following a presynaptic action potential are sufficient to allow the adult calyx to maintain its output even at high frequencies. The timing of these changes suggests that the calyx of Held synapse is ready to assume its relay function when hearing starts.

ACKNOWLEDGEMENTS

We would like to thank Hans van der Burg for advice on stimulation electrodes. Supported by FP6 European Union grant (EUSynapse, LSHM-CT-2005-019055), Heinsius Houbolt fund, ALW-NWO (Moving vesicles, 814.02.004) and SenterNovem, The Netherlands (Neuro-Bsik, BSIK 03053).

REFERENCES

1. Beutner D, Moser T (2001) The presynaptic function of mouse cochlear inner hair cells during development of hearing. *J Neurosci* 21:4593-4599.
2. Blankenship AG, Feller MB (2010) Mechanisms underlying spontaneous patterned activity in developing neural circuits. *Nat Rev Neurosci* 11:18-29.
3. Blatchley BJ, Cooper WA, Coleman JR (1987) Development of auditory brainstem response to tone pip stimuli in the rat. *Brain-Res* 429:75-84.
4. Borst JGG (2010) The low synaptic release probability *in vivo*. *Trends Neurosci* 33:259-266.
5. Borst JGG, Helmchen F, Sakmann B (1995) Pre- and postsynaptic whole-cell recordings in the medial nucleus of the trapezoid body of the rat. *J Physiol (Lond)* 489:825-840.
6. Boudreau CE, Ferster D (2005) Short-term depression in thalamocortical synapses of cat primary visual cortex. *J Neurosci* 25:7179-7190.
7. Brugge JF, O'Connor TA (1984) Postnatal functional development of the dorsal and posteroventral cochlear nuclei of the cat. *J Acoust Soc Am* 75:1548-1562.
8. Chuhma N, Ohmori H (1998) Postnatal development of phase-locked high-fidelity synaptic transmission in the medial nucleus of the trapezoid body of the rat. *J Neurosci* 18:512-520.
9. Chuhma N, Koyano K, Ohmori H (2001) Synchronisation of neurotransmitter release during postnatal development in a calyceal presynaptic terminal of rat. *J Physiol (Lond)* 530:93-104.
10. Erazo-Fischer E, Striessnig J, Taschenberger H (2007) The role of physiological afferent nerve activity during *in vivo* maturation of

- the calyx of Held synapse. *J Neurosci* 27:1725-1737.
11. Feldmeyer D, Radnikow G (2009) Developmental alterations in the functional properties of excitatory neocortical synapses. *J Physiol (Lond)* 587:1889-1896.
 12. Felmy F, Schneggenburger R (2004) Developmental expression of the Ca^{2+} -binding proteins calretinin and parvalbumin at the calyx of Held of rats and mice. *Eur J Neurosci* 20:1473-1482.
 13. Felmy F, Neher E, Schneggenburger R (2003) Probing the intracellular calcium sensitivity of transmitter release during synaptic facilitation. *Neuron* 37:801-811.
 14. Ford MC, Grothe B, Klug A (2009) Fenestration of the calyx of Held occurs sequentially along the tonotopic axis, is influenced by afferent activity, and facilitates glutamate clearance. *J Comp Neurol* 514:92-106.
 15. Forsythe ID (1994) Direct patch recording from identified presynaptic terminals mediating glutamatergic EPSCs in the rat CNS, *in vitro*. *J Physiol (Lond)* 479:381-387.
 16. Forsythe ID, Tsujimoto T, Barnes-Davies M, Cuttle MF, Takahashi T (1998) Inactivation of presynaptic calcium current contributes to synaptic depression at a fast central synapse. *Neuron* 20:797-807.
 17. Futai K, Okada M, Matsuyama K, Takahashi T (2001) High-fidelity transmission acquired via a developmental decrease in NMDA receptor expression at an auditory synapse. *J Neurosci* 21:3342-3349.
 18. Geal-Dor M, Freeman S, Li G, Sohmer H (1993) Development of hearing in neonatal rats: air and bone conducted ABR thresholds. *Hear Res* 69:236-242.
 19. Guinan JJ, Jr., Li RY-S (1990) Signal processing in brainstem auditory neurons which receive giant endings (calyces of Held) in the medial nucleus of the trapezoid body of the cat. *Hear Res* 49:321-334.
 20. Habets RLP, Borst JGG (2007) Dynamics of the readily releasable pool during post-tetanic potentiation in the rat calyx of Held synapse. *J Physiol (Lond)* 581:467-478.
 21. Heil P, Neubauer H, Irvine DRF, Brown M (2007) Spontaneous activity of auditory-nerve fibers: insights into stochastic processes at ribbon synapses. *J Neurosci* 27:8457-8474.
 22. Helmchen F, Borst JGG, Sakmann B (1997) Calcium dynamics associated with a single action potential in a CNS presynaptic terminal. *Biophys J* 72:1458-1471.
 23. Hermann J, Grothe B, Klug A (2009) Modeling short-term synaptic plasticity at the calyx of Held using *in vivo*-like stimulation patterns. *J Neurophysiol* 101:20-30.
 24. Hermann J, Pecka M, von Gersdorff H, Grothe B, Klug A (2007) Synaptic transmission at the calyx of Held under *in vivo*-like activity levels. *J Neurophysiol* 98:807-820.
 25. Horvitz DG, Thompson DJ (1952) A generalization of sampling without replacement from a finite universe. *Journal of the American Statistical Association* 47:663-685.
 26. Hosoi N, Sakaba T, Neher E (2007) Quantitative analysis of calcium-dependent vesicle recruitment and its functional role at the calyx of Held synapse. *J Neurosci* 27:14286-14298.
 27. Iwasaki S, Takahashi T (2001) Developmental regulation of transmitter release at the calyx of Held in rat auditory brainstem. *J Physiol (Lond)* 534:861-871.
 28. Jewett DL, Romano MN (1972) Neonatal development of auditory system potentials averaged from the scalp of rat and cat. *Brain Res* 36:101-115.
 29. Johnston J, Forsythe ID, Kopp-Scheinpflug C (2010) Going native: voltage-gated potassium channels controlling neuronal excitability. *J Physiol (Lond)* 588:3187-3200.
 30. Joshi I, Wang L-Y (2002) Developmental profiles of glutamate receptors and synaptic transmission at a single synapse in the mouse auditory brainstem. *J Physiol (Lond)* 540:861-873.
 31. Joshi I, Shokralla S, Titis P, Wang L-Y (2004) The role of AMPA receptor gating in the development of high-fidelity

- neurotransmission at the calyx of Held synapse. *J Neurosci* 24:183-196.
32. Kandler K, Friauf E (1993) Pre- and postnatal development of efferent connections of the cochlear nucleus in the rat. *J Comp Neurol* 328:161-184.
 33. Kil J, Kageyama GH, Semple MN, Kitzes LM (1995) Development of ventral cochlear nucleus projections to the superior olivary complex in gerbil. *J Comp Neurol* 353:317-340.
 34. Kim M-H, Korogod N, Schneggenburger R, Ho W-K, Lee S-H (2005) Interplay between $\text{Na}^+/\text{Ca}^{2+}$ exchangers and mitochondria in Ca^{2+} clearance at the calyx of Held. *J Neurosci* 25:6057-6065.
 35. Klyachko VA, Stevens CF (2006) Temperature-dependent shift of balance among the components of short-term plasticity in hippocampal synapses. *J Neurosci* 26:6945-6957.
 36. Koike-Tani M, Saitoh N, Takahashi T (2005) Mechanisms underlying developmental speeding in AMPA-EPSC decay time at the calyx of Held. *J Neurosci* 25:199-207.
 37. Kopp-Scheinpflug C, Tolnai S, Malmierca MS, Rübsamen R (2008) The medial nucleus of the trapezoid body: comparative physiology. *Neuroscience* 154:160-170.
 38. Kros CJ, Ruppersberg JP, Rüsch A (1998) Expression of a potassium current in inner hair cells during development of hearing in mice. *Nature* 394:281-284.
 39. Kuenzel T, Borst JGG, van der Heijden M (2011) Factors controlling the input-output relationship of spherical bushy cells in the gerbil cochlear nucleus. *J Neurosci* 31:4260-4273.
 40. Kushmerick C, Renden R, von Gersdorff H (2006) Physiological temperatures reduce the rate of vesicle pool depletion and short-term depression via an acceleration of vesicle recruitment. *J Neurosci* 26:1366-1377.
 41. Leão RM, Kushmerick C, Pinaud R, Renden R, Li G-L, Taschenberger H, Spirou G, Levinson SR, von Gersdorff H (2005) Presynaptic Na^+ channels: locus, development, and recovery from inactivation at a high-fidelity synapse. *J Neurosci* 25:3724-3738.
 42. Lohmann C, Friauf E (1996) Distribution of the calcium-binding proteins parvalbumin and calretinin in the auditory brainstem of adult and developing rats. *J Comp Neurol* 367:90-109.
 43. Lorteije JAM, Borst JGG (2011) Contribution of the mouse calyx of Held synapse to tone adaptation. *Eur J Neurosci* 33:251-258.
 44. Lorteije JAM, Rusu SI, Kushmerick C, Borst JGG (2009) Reliability and precision of the mouse calyx of Held synapse. *J Neurosci* 29:13770-13784.
 45. Mc Laughlin M, van der Heijden M, Joris PX (2008) How secure is *in vivo* synaptic transmission at the calyx of Held? *J Neurosci* 28:10206-10219.
 46. Müller M, Felmy F, Schneggenburger R (2008) A limited contribution of Ca^{2+} current facilitation to paired-pulse facilitation of transmitter release at the rat calyx of Held. *J Physiol (Lond)* 586:5503-5520.
 47. Müller M, Felmy F, Schwaller B, Schneggenburger R (2007) Parvalbumin is a mobile presynaptic Ca^{2+} buffer in the calyx of Held that accelerates the decay of Ca^{2+} and short-term facilitation. *J Neurosci* 27:2261-2271.
 48. Müller M, Goutman JD, Kochubey O, Schneggenburger R (2010) Interaction between facilitation and depression at a large CNS synapse reveals mechanisms of short-term plasticity. *J Neurosci* 30:2007-2016.
 49. Neher E, Sakaba T (2001) Combining deconvolution and noise analysis for the estimation of transmitter release rates at the calyx of Held. *J Neurosci* 21:444-461.
 50. Neher E, Sakaba T (2008) Multiple roles of calcium ions in the regulation of neurotransmitter release. *Neuron* 59:861-872.
 51. Reig R, Gallego R, Nowak LG, Sanchez-Vives MV (2006) Impact of cortical network activity on short-term synaptic depression. *Cereb Cortex* 16:688-695.
 52. Rodríguez-Contreras A, van Hoesen JS, Habets RLP, Locher H, Borst JGG (2008) Dynamic development of the calyx of Held synapse. *Proc Natl Acad Sci U S A* 105:5603-5608.

53. Rybak LP, Whitworth C, Scott V (1992) Development of endocochlear potential and compound action potential in the rat. *Hear Res* 59:189-194.
54. Sakaba T, Neher E (2001) Calmodulin mediates rapid recruitment of fast-releasing synaptic vesicles at a calyx-type synapse. *Neuron* 32:1-13.
55. Saviane C, Silver RA (2006) Fast vesicle reloading and a large pool sustain high bandwidth transmission at a central synapse. *Nature* 439:983-987.
56. Schneggenburger R, Forsythe ID (2006) The calyx of Held. *Cell Tissue Res* 326:311-337.
57. Schneggenburger R, Meyer AC, Neher E (1999) Released fraction and total size of a pool of immediately available transmitter quanta at a calyx synapse. *Neuron* 23:399-409.
58. Sonntag M, Englitz B, Kopp-Scheinpflug C, Rübsamen R (2009) Early postnatal development of spontaneous and acoustically evoked discharge activity of principal cells of the medial nucleus of the trapezoid body: an *in vivo* study in mice. *J Neurosci* 29:9510-9520.
59. Taschenberger H, von Gersdorff H (2000) Fine-tuning an auditory synapse for speed and fidelity: developmental changes in presynaptic waveform, EPSC kinetics, and synaptic plasticity. *J Neurosci* 20:9162-9173.
60. Taschenberger H, Scheuss V, Neher E (2005) Release kinetics, quantal parameters and their modulation during short-term depression at a developing synapse in the rat CNS. *J Physiol (Lond)* 568:513-537.
61. Taschenberger H, Leão RM, Rowland KC, Spiro GA, von Gersdorff H (2002) Optimizing synaptic architecture and efficiency for high-frequency transmission. *Neuron* 36:1127-1143.
62. Tolnai S, Englitz B, Scholbach J, Jost J, Rübsamen R (2009) Spike transmission delay at the calyx of Held *in vivo*: rate dependence, phenomenological modeling, and relevance for sound localization. *J Neurophysiol* 102:1206-1217.
63. Tritsch NX, Bergles DE (2010) Developmental regulation of spontaneous activity in the mammalian cochlea. *J Neurosci* 30:1539-1550.
64. Tritsch NX, Yi E, Gale JE, Glowatzki E, Bergles DE (2007) The origin of spontaneous activity in the developing auditory system. *Nature* 450:50-55.
65. Tritsch NX, Rodríguez-Contreras A, Crins TTH, Wang HC, Borst JGG, Bergles DE (2010) Calcium action potentials in hair cells pattern auditory neuron activity before hearing onset. *Nat Neurosci* 13:1050-1052.
66. Uziel A, Romand R, Marot M (1981) Development of cochlear potentials in rats. *Audiology* 20:89-100.
67. van Looij MA, Liem SS, van der Burg H, van der Wees J, De Zeeuw CI, van Zanten BG (2004) Impact of conventional anesthesia on auditory brainstem responses in mice. *Hear Res* 193:75-82.
68. Varela JA, Sen K, Gibson J, Fost J, Abbott LF, Nelson SB (1997) A quantitative description of short-term plasticity at excitatory synapses in layer 2/3 of rat primary visual cortex. *J Neurosci* 17:7926-7940.
69. von Gersdorff H, Borst JGG (2002) Short-term plasticity at the calyx of Held. *Nature Reviews Neuroscience* 3:53-64.
70. von Gersdorff H, Schneggenburger R, Weis S, Neher E (1997) Presynaptic depression at a calyx synapse: the small contribution of metabotropic glutamate receptors. *J Neurosci* 17:8137-8146.
71. Walsh EJ, McGee J (1987) Postnatal development of auditory nerve and cochlear nucleus neuronal responses in kittens. *Hear Res* 28:97-116.
72. Wang L-Y, Kaczmarek LK (1998) High-frequency firing helps replenish the readily releasable pool of synaptic vesicles. *Nature* 394:384-388.
73. Wimmer VC, Horstmann H, Groh A, Kuner T (2006) Donut-like topology of synaptic vesicles with a central cluster of mitochondria wrapped into membrane protrusions: a novel structure-function

- module of the adult calyx of Held. *J Neurosci* 26:109-116.
74. Wong AY, Graham BP, Billups B, Forsythe ID (2003) Distinguishing between presynaptic and postsynaptic mechanisms of short-term depression during action potential trains. *J Neurosci* 23:4868-4877.
 75. Woolf NK, Ryan AF (1988) Contributions of the middle ear to the development of function in the cochlea. *Hear Res* 35:131-142.
 76. Wu LG, Borst JGG (1999) The reduced release probability of releasable vesicles during recovery from short-term synaptic depression. *Neuron* 23:821-832.
 77. Wu SH, Oertel D (1987) Maturation of synapses and electrical properties of cells in the cochlear nuclei. *Hear Res* 30:99-110.
 78. Xu J, Wu L-G (2005) The decrease in the presynaptic calcium current is a major cause of short-term depression at a calyx-type synapse. *Neuron* 46:633-645.
 79. Yang Y-M, Fedchyshyn MJ, Grande G, Aitoubah J, Tsang CW, Xie H, Ackerley CA, Trimble WS, Wang L-Y (2010) Septins regulate developmental switching from microdomain to nanodomain coupling of Ca^{2+} influx to neurotransmitter release at a central synapse. *Neuron* 67:100-115.

three



chapter **FOUR**

Developmental changes in parvalbumin in the rodent calyx of Held synapse and its role in controlling short-term synaptic plasticity

Tom T.H. Crins^{1,2} and J. Gerard G. Borst¹.

¹ Department of Neuroscience, Erasmus MC,
University Medical Center Rotterdam, The Netherlands.

² Department of Otorhinolaryngology - Head and Neck Surgery, Erasmus MC,
University Medical Center Rotterdam, The Netherlands.

ABSTRACT

four

The calyx of Held synapse in the medial nucleus of the trapezoid body (MNTB) shows a dramatic decrease in the impact of short-term plasticity (STP) immediately before hearing onset, which occurs at about P13 in rodents. This decrease marks the transformation of the calyx of Held synapse into a safe relay synapse. We investigated the possible contribution of the calcium binding protein parvalbumin to this decrease using immunohistochemistry in rats and mice ranging from postnatal day 4 (P4) to adult. In both species the concentration of parvalbumin was low in the principal neurons at P4, and showed a modest, transient increase just before hearing onset. Parvalbumin staining intensities in the rat calyx of Held were similar as in the principal neurons throughout development. In the mouse calyx of Held, presynaptic concentrations were high at young ages (P4-10), but, similar to the situation in the rat, decreased before hearing onset. Based on a comparison with the staining intensities of cerebellar basket cells, we estimate the PV concentrations in the rodent MNTB to be only about 100 μM after hearing onset. *In vivo* juxtacellular recordings of the calyx of Held synapse showed no differences in STP in parvalbumin knock-out mice (PV^{-/-}) compared to wild type littermates. Our data therefore suggest that the calcium binding protein parvalbumin does not play a major role in the developmental decrease in STP at the rodent calyx of Held synapse.

INTRODUCTION

Sound localization in azimuth depends on the precise comparison of the intensities and arrival times of sounds at both ears (Jeffress 1948; Grothe et al. 2010; Ashida and Carr 2011). A specialized circuit in the brainstem with highly specialized synapses is largely dedicated to the analysis of these subtle differences (Masterton et al. 1967; Casseday and Neff 1975; Tollin and Yin 2005). A well-studied example of such a highly specialized synapse is the calyx of Held synapse, which is formed between globular bushy cells and principal neurons of the medial nucleus of the trapezoid body (MNTB). Each principal neuron is contacted by a single, giant, axosomatic terminal, called the calyx of Held (Held 1893; Morest 1968; Guinan and Li 1990). In the adult situation, this synapse functions as a relay synapse, being able to fire reliably at high frequencies (Guinan and Li 1990; Mc Laughlin et al. 2008; Lorteije et al. 2009; Sonntag et al. 2011). Interestingly, in rodents its properties change strongly around hearing onset (Taschenberger and von Gersdorff 2000; Sonntag et al. 2009; Crins et al. 2011), which happens around postnatal day 13 (P13) (Jewett and Romano 1972; Ehret 1976; Uziel et al. 1981; Blatchley et al. 1987; Rybak et al. 1992; Geal-Dor et al. 1993). Around that period there is a strong reduction in the release probability of vesicles in the readily-releasable pool, and the amount of short-term plasticity that can be observed during high-frequency signaling decrease strongly, both in slice recordings (Taschenberger and von Gersdorff 2000; Crins et al. 2011; Rusu and Borst 2011) and *in vivo* (Sonntag et al. 2009; Crins et al. 2011). The mechanisms that underlie this transformation into a relay synapse are still largely unknown. A possible candidate mechanism is the change in the presynaptic concentration of the mobile calcium-binding protein parvalbumin. This protein has relatively slow calcium-binding kinetics, making it a suitable candidate to reduce the so-called residual calcium that is thought to underlie short-term synaptic facilitation. A study of the parvalbumin knockout (KO) mouse indeed found evidence that already before hearing onset (P8-10) parvalbumin accelerates the decay of short-term facilitation in the calyx of Held by accelerating the decay of the presynaptic intracellular calcium concentration (Müller et al. 2007). A low concentration of parvalbumin (100 μM) was sufficient to restore the kinetics in the KO animals. Their findings raise the possibility that developmental changes in the expression of parvalbumin in the calyx of Held contribute to the observed developmental changes in short-term plasticity. Some immunocytochemical evidence for a developmental upregulation of the parvalbumin expression around hearing onset has indeed been obtained. (Lohmann and Friauf 1996) found no staining for parvalbumin in both somata and neuropil in the rat MNTB before P8, a rapid increase between P8 and P10, and intense labeling of fibers in the trapezoid body by P10. Following a further increase at P12 the labeling intensity decreased again. In contrast, (Felmy and Schneggenburger 2004) found evidence for the presence of parvalbumin in both calyces and the soma of the postsynaptic principal cells at all developmental stages they investigated (P8–P33) in rats. In mice, PV staining was already present already in the calyces at P6, with only weak staining in the principal neurons. At P14

(and older), both principal neurons and calyces were positive. These studies are thus not conclusive with regard to the question whether changes in the expression of parvalbumin can contribute to the transformation of the calyx of Held synapse into a relay synapse. Here we therefore revisit this question by studying the developmental changes in the pre- and the postsynaptic expression of parvalbumin and by recording *in vivo* juxtacellular responses from principal neurons of the MNTB in the KO mouse and wild type controls.

MATERIALS AND METHODS

Animals. All experiments were conducted in accordance with the European Communities Council Directive and approved by the Animal Ethics Committee of the Erasmus MC. Parvalbumin knock-out (PV^{-/-}) mice in C57Bl6/6J background (Schwaller et al. 1999) were kindly provided by Dr. B. Schwaller, Fribourg, Switzerland. The day of birth is defined as postnatal day 0 (P0).

Surgery. A total of 13 PV^{-/-} mice and 19 of their wild type littermates of either sex were anesthetized with a mixture of ketamine (60 mg/kg) and xylazine (6 mg/kg) and placed in the supine position. Rectal temperature was maintained between 37 and 38 °C with a homoeothermic blanket system (Stoelting). Via a ventral approach the brainstem was reached as described previously (Rodriguez-Contreras et al. 2008). In short, a medial incision of the skin from sternum to mandibula was made to reach the left medial nucleus of the trapezoid body (MNTB). Typically, the MNTB was found 400-500 µm rostral from the left anterior inferior cerebellar artery and 400-450 µm lateral from the basilar artery. In post-hearing animals, the external ear canal was filled with silicone gel to reach maximal conductive hearing loss. Following laryngectomy, the animal was intubated and mechanically ventilated with a MiniVent (type 845; Harvard Apparatus, March-Hugstetten, Germany) at a frequency of ~90-100/min and stroke volume of 7 µl/gram bodyweight. Arterial oxygen saturation and heart rate were monitored using a MouseOx (STARR Life Sciences Corp.).

Auditory stimulation. Closed-field sound stimulation was presented as described previously (Tan and Borst 2007). Speaker probes were inserted into both ear canals and stabilized with silicone elastomer (Kwik-Cast, WPI). A custom-made program written in MATLAB (version 7.0.4; The MathWorks) controlled auditory stimulus generation with Tucker Davis Technologies hardware (TDT, System 3, RP2.1 processor, PA5.1 attenuator, ED1 electrostatic driver, EC1 electrostatic speaker), which in turn triggered acquisition via Clampex (Axon Instruments). Tones consisted of Gaussian noise band with durations of 500 ms plus 1 ms rise/decay time. The first noise band was followed by a second at variable intervals (2ⁿ * 20 ms; n: 0-7). One run consisted of 80 sweeps with a sweep duration of 4.0 s and a start-

to-start interval of 4.001 s. Sound intensities were calibrated between 0.5 and 64 kHz with a condenser microphone (ACO Pacific type 7017, MA3 stereo microphone amplifier, TDT SigCal) as described previously (Tan and Borst 2007). All *in vivo* experiments were performed in a single walled sound-attenuated chamber (Gretch-Ken Industries; attenuation ≥ 40 dB at 4–32 kHz).

In vivo electrophysiology. A total of 7 PV KO mice (13 cells) were used; P4 (n=2, 4 cells), P7 (n=1, 2 cells), P10 (n=1, 2 cells), P15 (n=1, 2 cells) and P21 (n=1, 3 cells). A total of 6 wild type (WT) littermates (19 cells) were used; P8 (n=1, 4 cells), P11 (n=1, 3 cells), P13 (n=1, 2 cells), P14 (n=1, 1 cell), P21 (n=1, 3 cells) and P40 (n=1, 6 cells). 5 heterozygote (HET) littermates (21 cells) were used; P7 (n=1, 3 cells), P8 (n=3, 15 cells) and P10 (n=1, 3 cells).

four

In vivo juxtacellular (loose-patch) recordings were made as described previously (Lorteije et al., 2009). Glass borosilicate micropipettes with filament (3.5–5.0 M Ω) were filled with a solution containing the following (in mM): 135 NaCl, 5.4 KCl, 1 MgCl₂, 1.8 CaCl₂, and 5 HEPES, pH 7.2. When passing the brain surface, high positive pressure (≈ 300 mbar) was used, which was lowered to ≈ 12 mbar when searching for cells, and to 0 mbar during recordings.

Analysis electrophysiology. Data were analysed with custom-written Igor procedures (Igor Pro 6; WaveMetrics) running within the Neuromatic environment (version 2.00, kindly provided by dr. J. Rothman, University College London, London, U.K.).

Measuring EPSC amplitudes. EPSC amplitudes were measured as the difference between peak and baseline. To estimate the baseline, a double exponential function was fitted to the decay phase of each EPSC. The extrapolated value of the fitted function at the time of the next EPSC peak was taken as the baseline. In case the amplitude of the stimulus artifact at the start of the EPSC was 5% of the peak EPSC amplitude, a double exponential fit to the decay phase of the stimulus artifact was used instead to estimate the baseline.

Analysis of complex waveforms. Complex waveforms were identified on a first-derivative threshold criterion. The level and the minimally acceptable interval were adjusted to ensure that each complex waveform was captured once. For every suprathreshold waveform the so-called inflection point where eEPSP and eAP could be separated was found or, for subthreshold events, the eEPSP itself could be found following a prespike. (Lorteije et al. 2009).

Short-term plasticity model. The relation between the size of the eEPSP and the inter-EPSP interval was described with a simple model for STP (Varela et al., 1997). In the presence of both facilitation and depression, the eEPSP amplitude depended on the availability of a depletion factor, D , which was constrained to be between zero and one, and a facilitation

factor, F . With each event, the depletion factor depleted with fraction d , which was also constrained to be between zero and one, as follows:

$$D \rightarrow dD \quad (1)$$

Following the event, D recovered exponentially from depletion with time constant τ :

$$\tau D \, dD/dt = 1 - D \quad (2)$$

With each event, the facilitation factor F increased with a certain amount f :

$$F \rightarrow F + f \quad (3)$$

Following the event, F recovered exponentially analogously to D . The amplitude A of the eEPSP depended in a multiplicative fashion on the availability of the two resources:

$$A = A_{\text{inf}} FD \quad (4)$$

where A_{inf} is the amplitude of the eEPSP after a very long interval. All EPSP amplitudes from a given experiment were fit at once to incorporate cumulative effects. Fits were evaluated by plotting predicted against measured sizes to look for systematic deviations. Especially in the *in vivo* spontaneous data before hearing onset, the interval distributions were inhomogeneous. We therefore used inverse probability weighting (Horvitz and Thompson 1952); events were weighted by the square root of the local sparseness. For each event, its local sparseness was defined as the inverse of the total number of events in the neighborhood of each event. We defined 0.5 decade for the logarithmically transformed intervals as the neighborhood. To evaluate the goodness-of-fit of the three models, facilitation alone, depression alone, and both facilitation and depression, a Pearson's r value between fitted and measured amplitudes was calculated. Its square, r^2 , sometimes called the coefficient of determination, is a measure for the proportion of the amplitude variance that is accounted for by the STP model. We accepted an extra component (e.g., facilitation) if the explained variance increased by at least 2.5%.

Immunohistochemistry. A total of 16 mice (95 cells) of the following ages were used: P4 (n=1: 5 cells), P6 (n=1: 6 cells), P8 (n=2: 11 cells), P10 (n=2: 9 cells), P13 (n=1: 6 cells), P21 (n=7: 33 cells), P46 (n=1: 3 cells) and P170 (n=1: 3 cells). A total of 8 rats (34 cells) of ages P4 (n=2: 3 cells), P10 (n=2: 9 cells), P14 (n=2: 8 cells) and P22 (n=2: 5 cells) were used. Under anesthesia they were perfused transcardially with 10 ml of cold saline (0.9%) solution followed by at least 10 ml of 4% paraformaldehyde before being immersed in 4% paraformaldehyde for

1 hour to allow sufficiently strong fixation while minimizing epitope-masking (Schneider Gasser et al. 2006). The tissue was cryoprotected by overnight immersion in 10% sucrose solution in 0.1 M phosphate buffer (PB; pH 7.2–7.4) and 30% sucrose solution in 0.1 M PB the following night. Using a freezing microtome, 40 μ m coronal sections were made and collected in 0.1 M Phosphate Buffer (PB). After a 4 x 10 min washing step in 0.1 M TBS (pH 7.6), the sections were preincubated for 1 hour at 4°C in 10% normal goat serum (Vector Laboratories, Burlingame, CA) + 0.5% Triton + TBS. Primary antibodies were incubated for 48–72 hours at 4°C in 2% normal serum + 0.4% Triton + TBS + Guinea Pig(GP)-Vglut1 (1:1000) + GP-Vglut2 (1:000) + Rabbit (R)-Parvalbumin (1:5000). After a 4 x 10 min washing step in TBS, the secondary antibodies diluted in 2% NS + 0.4% Triton + TBS + Alexa GP-633 nm + Alexa R-488 nm (both Invitrogen, La Jolla, CA) were added for 2 hours at room temperature in the dark. After 1 x 10 min washing step in TBS and 1 x 10 min washing step in 0.1 M PB, the Sytox Blue solution containing 3 ml 0.1 M PB + 20 μ l Sytox Blue (nucleic acid stain; Invitrogen) + 30 μ l 10% Triton, was added for 1 min followed by a 3 x 5 min washing step in 0.1 M PB.

The sections were mounted onto glass coverslips using Vectashield without DAPI (H-100; Vector Laboratories).

Confocal imaging. Confocal images were acquired using a LSM700, Axio Observer, confocal microscope (Zeiss) with a $\times 63$ plan-apochromat oil objective with a numerical aperture (NA) of 1.4. Using ZEN-software, pictures were collected of 2048x2048 pixels, 3 channels, 16-bit, no zoom, no averaging and a pixel dwell time of 1.58 μ s. The pinhole of the parvalbumin channel was 41 μ m. All images were acquired using the same settings, only the laser power was adjusted for an optimal dynamic range without saturation. We verified that at the used laser power settings the relation between laser power and fluorescence was linear. AF-488 was excited at 488 nm; emission filter 560–1000 nm. SYTOX Blue was excited at 405 nm; emission short pass filter 555 nm. AF-633 was excited at 639 nm; emission filter 415–735 nm.

Line analysis. A total of 95 cells (mouse) and 34 cells (rat) were analyzed. Images were loaded in ImageJ (NIH, Bethesda, MD) for line analysis. A line with a thickness of 10 pixels was drawn over the calyx, membrane and cytoplasm. Plot profiles were used to distinguish the pre- and postsynaptic part. Inclusion criteria for cells in the MNTB were as follows: - postsynaptic principal cell with an eccentric nucleus in the focal plane; - a calyx of Held covering at least 20% of the postsynaptic cell; - the covered section of the calyx should be at least as thick as the line thickness. The background staining was quantified for each channel: a line was drawn in a 'dark' area with no evident structures. Gray level intensities per point were calculated and deducted from the gray level intensities of the pre- and postsynaptic cell staining. To allow a comparison between images, intensities were normalized to a power of 1.0 (maximal).

Cerebellar basket cells were identified as the PV-positive cells close to the Purkinje cells. Images of MNTB and cerebellum were analysed the same way.

Statistical analysis. Data are given as mean \pm standard deviation (SD), except when noted otherwise.

four

RESULTS

PV concentration in MNTB was markedly lower than in cerebellar basket cells

We studied the developmental changes in PV expression in the MNTB in mice and rats between the age of P4 and P30. An example of the staining of the MNTB of a P10 rat is shown in Figure 1A, B. Antibodies against the vesicular glutamate transporters Vglut 1 and 2 were used as a marker for the presynaptic compartment, and sytox blue, which stains nucleic acids, as a marker for the soma of the principal neuron. By using these markers it became possible to separate the pre- and the postsynaptic PV staining (Figure 1C; (Felmy and Schneggenburger 2004). To get a rough estimate for the absolute concentration of PV in the MNTB, we compared the staining intensities to those of young-adult rat cerebellar basket cells, whose PV concentration have been estimated to be 0.56 mM (Eggermann and Jonas 2012). Somewhat surprisingly, at P22 we found both the pre- and the postsynaptic PV staining intensity in the MNTB to be only 15% and 27%, respectively, of the intensity of the cerebellar basket cells (Figure 2). Assuming linearity and correcting for differences in laser power (see Methods), this would indicate that the PV concentration in both the calyces and the principal neurons of the young-adult MNTB is only about 100 μ M.

We next studied the developmental changes in the rat by quantifying pre- and postsynaptic fluorescence intensities in the MNTB at ages P4, P10, P14 and P22 (Figure 3). At P4, staining intensities were low, both pre- and postsynaptically. At P10 we observed a strong increase in staining intensity both pre- and postsynaptically, which reached levels comparable to those in young-adult cerebellar basket cells. At P14 intensities decreases to much lower levels, and little change was observed at P22 compared to the situation at P14 (Figure 3D). The developmental changes in the staining intensities in mice differed from those in rats. Figure 4A is an example of the staining of the MNTB of a P4 mouse, showing clear calyceal staining, but little postsynaptic staining. The postsynaptic PV staining showed no major developmental changes in the mouse, but, interestingly, the presynaptic staining levels were at their highest levels at P4-6, after which the intensities decreased in a few days to much lower levels (Figure 4). We conclude that the developmental changes in the MNTB of PV differ in rats and mice, but that in both species there is little evidence suggesting that a clear increase in the calyceal PV concentration can contribute to its transformation into a relay synapse.

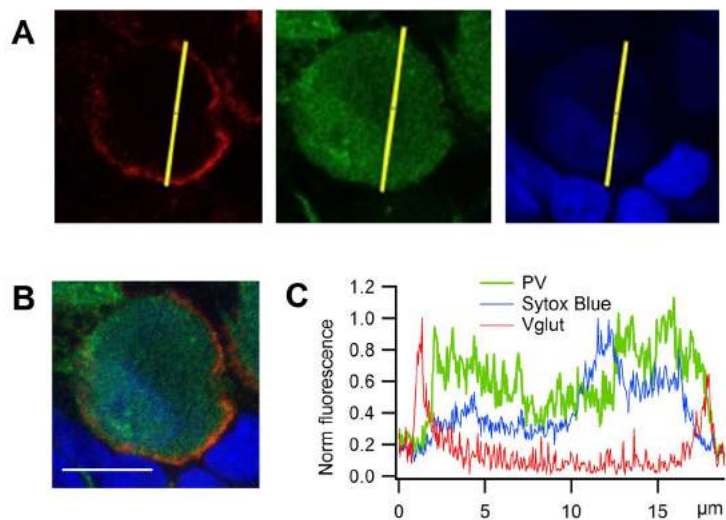


Figure 1. Discriminating between pre- and postsynaptic PV staining in the MNTB.

A, confocal image of staining of MNTB of a P10 rat with antibodies against Vglut1+2 (left, red), PV (middle, green) and Sytox blue (right, blue). **B**, merged image. Scale bar 10 μm . **C**, line scan along yellow line in **A**. Fluorescence levels are normalized to the average fluorescence level in cerebellar basket cells.

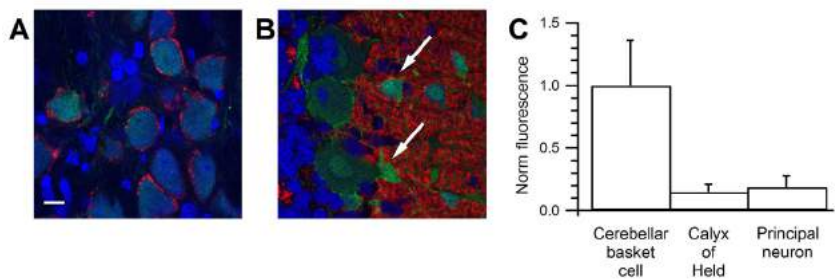


Figure 2. Comparison of PV staining in MNTB with cerebellar basket cells

Stainings in **A** and **B** are from the same P22 rat. **A**, confocal image of staining of MNTB for PV (green), Vglut1+2 (red), and Sytox blue (blue). Scale bar, 10 μm . **B**, as **A**, except showing cerebellum. Arrows indicate basket cells. **C**, Comparison of average fluorescence levels in calyces, principal neurons of the MNTB and basket cells. Fluorescence levels are normalized to the average fluorescence level in the basket cells. Error bars indicate standard deviation.

Electrophysiological properties of the calyx of Held synapse in WT and PV^{-/-} mice are similar

We next compared synaptic transmission at the calyx of Held synapse between WT, HET, and PV KO animals by making juxtacellular recordings from principal neurons in the MNTB in anesthetized animals using a ventral approach, as detailed in the Methods. In this set of experiments we found that in all 11 animals in the age range P4-P11 the external meatus was still closed, and at about P13 the meatus was open in all 6 animals. The MNTB principal neurons could be readily identified by their characteristic complex waveforms (Figure 5). The

four

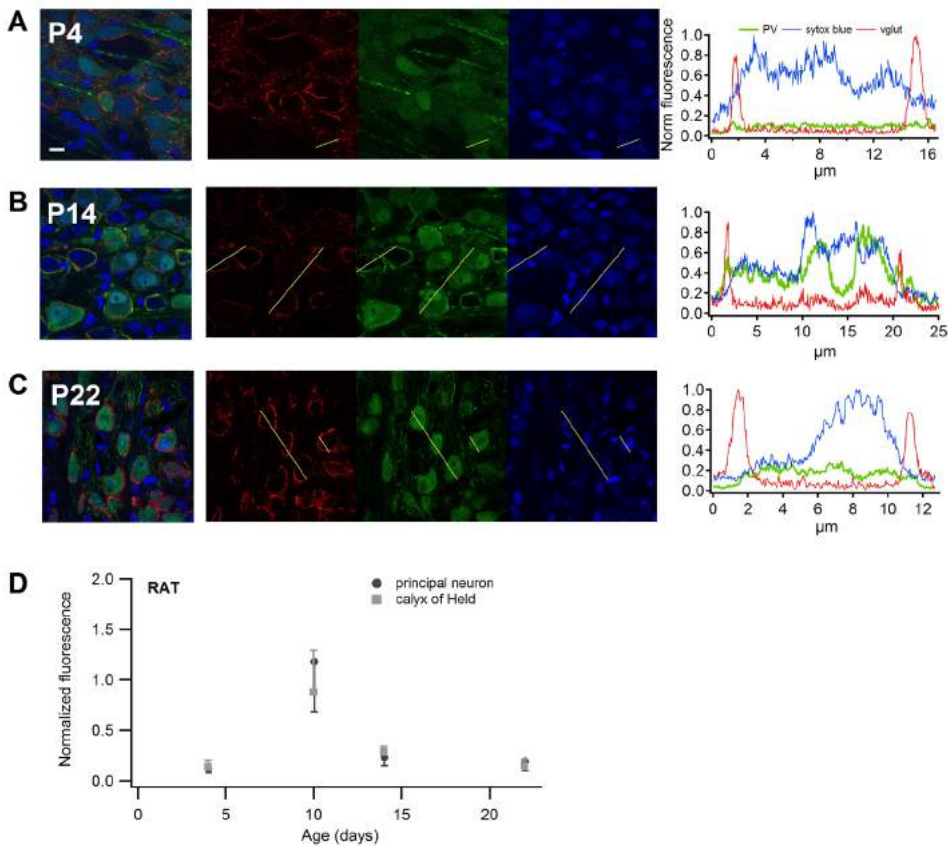


Figure 3. Developmental changes in the expression of PV in the rat calyx of Held synapse.

A, Left, confocal image of staining of MNTB of a P4 rat for PV (green) and Vglut1+2 (red), and Sytox blue (blue). Scale bar, 10 μ m. Left, merged image. Middle, individual channels. Right, line scan along yellow line shown in middle panel. **B**, As **A**, except from a P14 rat. **C**, As **A**, except from a P22 rat. **D**, Summary of developmental changes in pre- and postsynaptic PV staining intensities in the rat. Fluorescence levels are normalized to the average fluorescence level in the basket cells in the case of PV and to the maximum value in the case of Vglut and sytox.

shape of the extracellular waveforms showed large developmental changes: eAP halfwidth and prespike-AP delay decreased considerably (Figure 6A and B) (Taschenberger and von Gersdorff 2000; Sonntag et al. 2009; Crins et al. 2011), but there were no obvious differences between recordings from the different genotypes.

Both WT and PV KO showed a developmental increase in firing frequency and a change to a more primary-like firing pattern just before hearing onset, as seen previously in rats (Crins et al, 2011). Again, there were no obvious differences between genotypes (Figure 5). Note that differences in amplitudes between animals mostly signify differences in seal resistance of the juxtacellular (loose-patch) configuration.

four

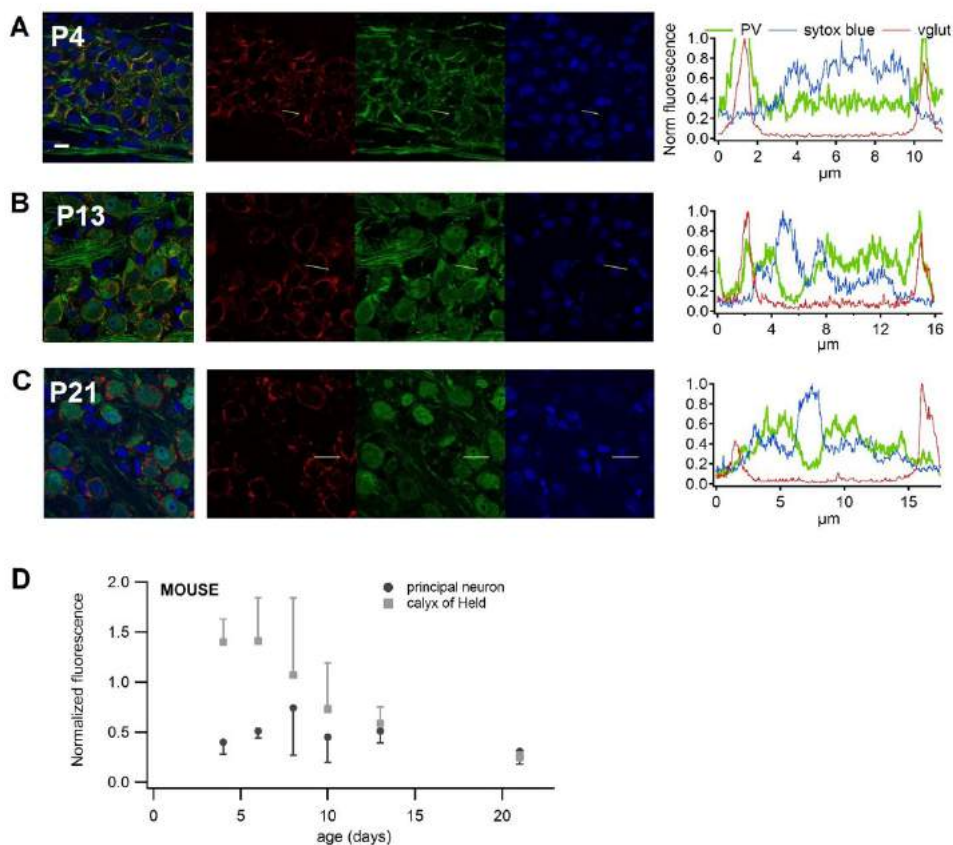


Figure 4. Developmental changes in the expression of PV in the mouse calyx of Held synapse.

A, Left, confocal image of staining of MNTB of a P4 rat for PV (green) and Vglut1+2 (red), and Sytox blue (blue). Scale bar, 10 μ m. Left, merged image. Middle, individual channels. Right, line scan along yellow line shown in middle panel. **B**, As **A**, except from a P13 mouse. **C**, As **A**, except from a P21 mouse. **D**, Summary of developmental changes pre- and postsynaptic PV staining intensities in the mouse. Fluorescence levels are normalized to the average fluorescence level in the basket cells for PV and to the maximum value for Vglut and sytox.

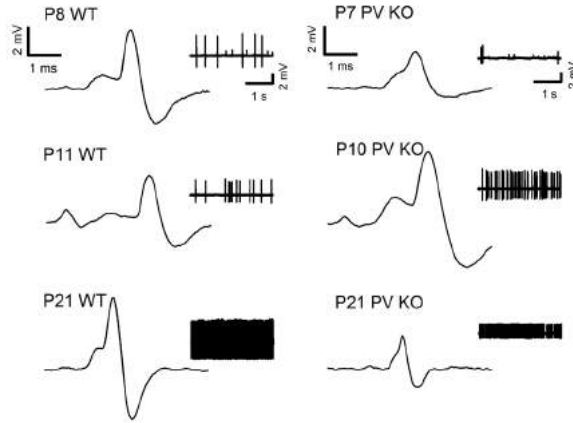


Figure 5. Examples of characteristic complex waveforms at different ages in PV WT and KO animals. PV WT (left column) and KO animals (right column). Insets show firing pattern during 3 seconds.

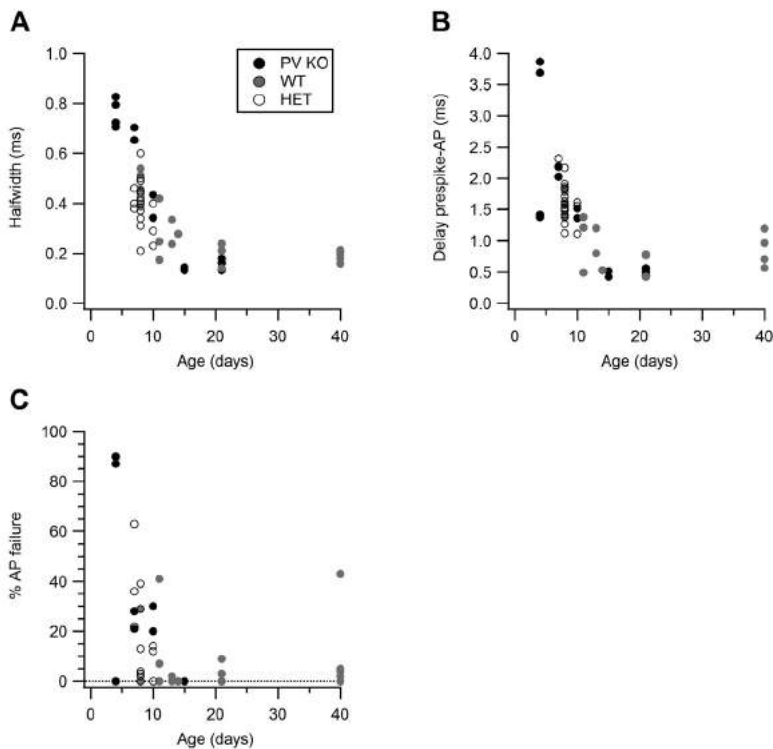


Figure 6. Developmental changes in timing and reliability of synaptic transmission in wild type, knock-out and heterozygote mice. **A**, developmental changes in eAP half-width. Black dots: parvalbumin knock-out (PV KO); Gray dots: wild type (WT); Open dots: heterozygote (HET). **B**, the same as **A** for changes in latency between prespike and AP. **C**, developmental changes in percentage AP failure.

Before hearing onset, different forms of short term plasticity (STP) could typically be observed. The mean amplitude of eEPSPs clearly depended on interval. On average, amplitudes were larger at interspike intervals of approximately 10 ms. Here consecutive eEPSPs were larger and were followed by an AP (Figure 7A). We interpret the increase at short intervals as evidence for synaptic facilitation and the increase at very long intervals as evidence for the presence of recovery from synaptic depression (Crins et al. 2011). Short-term depression was seen mostly at interspike intervals of 100 ms; the consecutive eEPSP amplitudes decreased, and eventually the transmission failed and no AP was seen (Figure 7). Just prior to hearing onset the STP markedly decreased, as judged by the amount of variance in the eEPSP amplitudes that could be explained by the STP model (Figure 9). Changes in the fraction of explained variance were similar between recordings from WT, PV KO, and HET animals. To quantify STP, a simple model was fitted, as described in the Methods (Varela et al. 1997). The goodness of fit depended on whether facilitation, depression, or a combination of both described the distribution of the data points the best. The separate components of the model are shown in Figure 8. Especially in young animals, in many cases the STP was dominated by short-term depression.

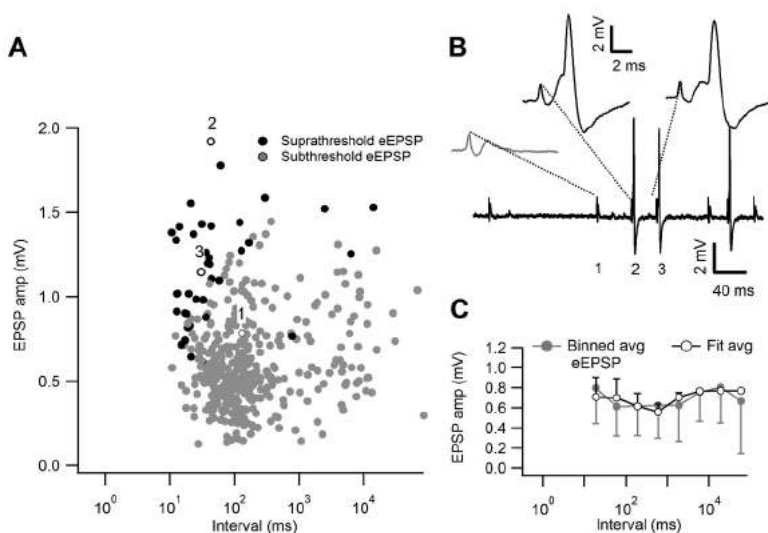


Figure 7. Characteristic complex waveforms. **A**, Relation between eEPSP and inter-event interval in a juxtacellular recording from a P4 mouse. The black symbols represent suprathreshold EPSPs, and the gray symbols subthreshold EPSPs. There is a clear dependence of eEPSP size on inter-event interval. Facilitation occurs mostly within inter-event intervals of <100 ms. Three consecutive events 1, 2 and 3 (open markers) are shown in **B**. **B**, trace with blow-up of 1 subthreshold event in gray followed by 2 suprathreshold EPSP's in black. **C**, Gray symbols show binned averages with SD, and black circles indicate the fit with an STP model with both facilitation and depression. Fit parameters were as follows: average amplitude of 0.77 mV, 203% facilitation per AP, decaying with a time constant of 135 ms and 35% depression per AP, recovering with a time constant of 877 ms. The fit could account for 25% of the variance in the amplitude of the eEPSPs.

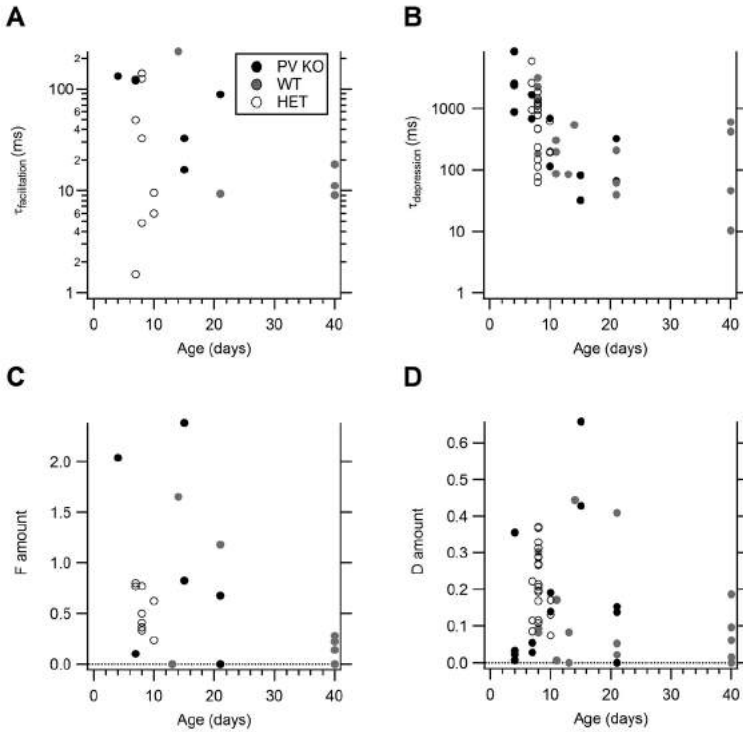


Figure 8. Developmental changes in STP in WT, PV KO and heterozygote (HET) mice. **A**, Developmental decrease in the time constant of facilitation, as obtained from the fit with an STP model. Black dots: parvalbumin knock-out (PV KO); Gray dots: wild type (WT); Open dots: heterozygote (HET). **B**, Age dependence of the time constant for recovery from depression. **C**, Developmental changes in the amount of facilitation. Cells without significant facilitation are included as 0%. **D**, as in **C**, showing the developmental decrease in the amount of depression. Cells without significant depression are included as 0%.

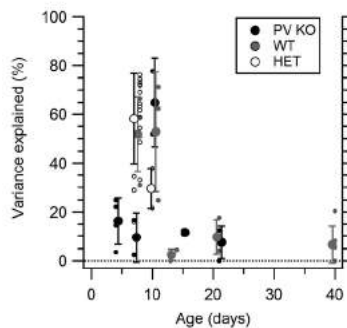


Figure 9. Variance in short-term plasticity. **D**, Developmental decrease in the percentage of variance that can be explained by the model fit (coefficient of determination). Cells without both significant facilitation and depression are included as 0%. Black dots: parvalbumin knock-out (PV KO); Gray dots: wild type (WT); open dots: heterozygote (HET). Larger markers represent the average explained variance. Error bars indicate SDs; a small horizontal offset is introduced for display purposes.

DISCUSSION

We have studied the developmental changes in the expression of parvalbumin (PV) in the calyx of Held synapse. We find that the immature calyx of Held contains a relatively high concentration of PV, but that a few days before hearing onset the PV concentration decreases dramatically both in mice and in rats. In young-adult rats the concentration of PV in the calyx of Held is much lower than in cerebellar basket cells. STP characteristics in PV KO and wild type mice were similar. Our results therefore indicate that it is unlikely that changes in the parvalbumin expression make a large contribution to the observed developmental changes in short-term plasticity at this synapse.

four

Developmental expression of parvalbumin at the calyx of Held synapse

We used immunocytochemistry to measure developmental changes in the concentration of PV in the MNTB. We kept conditions the same as much as possible, but even though the accessibility of the PV epitope is not expected to change during development since this is a soluble cytoplasmic protein, we cannot exclude that developmental changes in staining efficiency have affected some of our conclusions. By staining the presynaptic compartment with Vglut and the postsynaptic compartment, it was possible to measure the pre- and postsynaptic concentration separately. Our results on the developmental expression of PV at the calyx of Held synapse are in general agreement with earlier studies (Lohmann and Friauf 1996; Felmy and Schneggenburger 2004; Roebel 2006). We find a clear difference between rats and mice, as also observed by (Felmy and Schneggenburger 2004). In rats, the pre- and postsynaptic staining intensities were similar throughout development. The pre- and postsynaptic staining intensities peaked at P10, close to hearing onset, after which they declined again. To get an approximate estimate of the PV concentrations in the young-adult synapse, we compared the staining in principal neurons with the staining of rat cerebellar basket cells in the same slice, whose concentration has been carefully measured (Eggermann and Jonas 2012). Based on this comparison, we find that the PV concentration in the principal neurons was only about 0.1 mM. Even though this concentration is sufficient to have an effect on the decay of short-term synaptic facilitation, it was much lower than in the cerebellar basket cells, and similar to the estimated concentration in the calyx of Held of P8-10 mice (Müller et al. 2007). The similarity between the presynaptic concentrations before hearing onset and in young-adult rodents indicates that the shortening of the decay of the facilitation observed after hearing onset (Crins et al. 2011; Sonntag et al. 2011) was not caused by an increase in the presynaptic PV concentration. In the mouse, the PV concentration showed a different developmental pattern than in the rat. At P4, the youngest age studied, the staining intensity was much higher in the calyx of Held than in the principal neurons, in agreement with earlier results on pre-hearing animals (Felmy and Schneggenburger 2004; Roebel 2006). We found a gradual decrease afterwards, with the pre- and postsynaptic

concentrations eventually becoming similar. Also in the mouse, our immunofluorescence results do not provide an indication for a prominent role for PV in the changes in STP around hearing onset .

***In vivo* synaptic transmission of the calyx of Held synapse in PV KO mice**

four

To test the functional consequences of the absence of PV, we measured *in vivo* synaptic transmission in the PV KO mice by making juxtacellular recordings from principal neurons in the MNTB. We found no obvious changes in synaptic transmission in the PV KO mice. Even though firm conclusions cannot be drawn since the number of cells studied was generally not very high, both the shape of the complex extracellular waveform and the amount of STP did not show obvious differences between wild type and KO mice. We studied spontaneous activity *in vivo*. In animals younger than P13 (hearing onset) in many cases there were only a few inter event intervals short enough to reveal facilitation. Another explanation for little facilitation could be that depression dominates and counteracts facilitation. We cannot exclude that a more detailed study would reveal differences, but based on our results we conclude that PV is unlikely to play a substantial role in mediating the large differences in synaptic transmission that have been shown to occur around hearing onset (Futai et al. 2001; Nakamura and Takahashi 2007; Nakamura et al. 2008; Sonntag et al. 2009; Crins et al. 2011; Sonntag et al. 2011). It is possible that in the PV KO there is a compensatory increase in the levels of other Ca-binding proteins. Alternatively, and more likely, a faster clearance of presynaptic Ca^{2+} rather than an increased buffering may underlie the developmental speeding of the decay of synaptic facilitation at the calyx of Held. Indeed, recently a clear developmental increase in the $\text{Na}^+/\text{Ca}^{2+}$ exchanger NCKX was shown (Lee et al. 2013), providing a good alternative explanation for the developmental speedup of synaptic facilitation at the calyx of Held synapse.

ACKNOWLEDGMENTS

We want to thank Dr. Beat Schwaller for the parvalbumin knockout mice, Dr. Tiantian Wang for genotyping, prof. Ype Elgersma and dr. Steven Kushner for the use of their confocal microscope, Elize Haasdijk for excellent technical assistance with immunocytochemistry. This work was supported by the Heinsius Houbolt fund and by the Dutch Fund for Economic Structure Reinforcement (FES, 0908 'NeuroBasic PharmaPhenomics project').

REFERENCES

1. Ashida G and Carr CE (2011). Sound localization: Jeffress and beyond. *Current Opinion in Neurobiology* **21**: 745-751 <http://dx.doi.org/10.1016/j.conb.2011.05.008>.
2. Blatchley BJ, Cooper WA and Coleman JR (1987). Development of auditory brainstem response to tone pip stimuli in the rat. *Brain-Res* **429**: 75-84 [http://dx.doi.org/10.1016/0165-3806\(87\)90140-4](http://dx.doi.org/10.1016/0165-3806(87)90140-4).

3. Casseday JH and Neff WD (1975). Auditory localization: role of auditory pathways in brain stem of the cat. *Journal of Neurophysiology* **38**: 842-858.
4. Crins TTH, Rusu SI, Rodríguez-Contreras A and Borst JGG (2011). Developmental changes in short-term plasticity at the rat calyx of Held synapse. *J Neurosci* **31**: 11706-11717 <http://dx.doi.org/10.1523/JNEUROSCI.1995-11.2011>.
5. Eggermann E and Jonas P (2012). How the 'slow' Ca^{2+} buffer parvalbumin affects transmitter release in nanodomain-coupling regimes. *Nat Neurosci* **15**: 20-22 <http://dx.doi.org/10.1038/nn.3002>.
6. Ehret G (1976). Development of absolute auditory thresholds in the house mouse (*Mus musculus*). *J Am Audiol Soc* **1**: 179-184 <http://www.ncbi.nlm.nih.gov/pubmed/956003>.
7. Felmy F and Schneggenburger R (2004). Developmental expression of the Ca^{2+} -binding proteins calretinin and parvalbumin at the calyx of Held of rats and mice. *Eur J Neurosci* **20**: 1473-1482 <http://www3.interscience.wiley.com/cgi-bin/fulltext/118791538/HTMLSTART>.
8. Futai K, Okada M, Matsuyama K and Takahashi T (2001). High-fidelity transmission acquired via a developmental decrease in NMDA receptor expression at an auditory synapse. *J Neurosci* **21**: 3342-3349 <http://www.jneurosci.org/cgi/content/full/21/10/3342>.
9. Geal-Dor M, Freeman S, Li G and Sohmer H (1993). Development of hearing in neonatal rats: air and bone conducted ABR thresholds. *Hear Res* **69**: 236-242 [http://dx.doi.org/10.1016/0378-5955\(93\)90113-F](http://dx.doi.org/10.1016/0378-5955(93)90113-F).
10. Grothe B, Pecka M and McAlpine D (2010). Mechanisms of sound localization in mammals. *Physiol Rev* **90**: 983-1012 <http://dx.doi.org/10.1152/physrev.00026.2009>.
11. Guinan JJ, Jr. and Li RY-S (1990). Signal processing in brainstem auditory neurons which receive giant endings (calyces of Held) in the medial nucleus of the trapezoid body of the cat. *Hearing Research* **49**: 321-334 [http://dx.doi.org/10.1016/0378-5955\(90\)90111-2](http://dx.doi.org/10.1016/0378-5955(90)90111-2).
12. Held H (1893). Die centrale Gehörleitung. *Archiv für Anatomie und Physiologie, Anatomie Abtheil*: 201-248.
13. Horvitz DG and Thompson DJ (1952). A generalization of sampling without replacement from a finite universe. *Journal of the American Statistical Association* **47**: 663-685 <http://www.jstor.org/stable/2280784>
14. Jeffress LA (1948). A place theory of sound localization. *J Comp Physiol Psychol* **41**: 35-39 <http://dx.doi.org/10.1037/h0061495>.
15. Jewett DL and Romano MN (1972). Neonatal development of auditory system potentials averaged from the scalp of rat and cat. *Brain Res* **36**: 101-115 [http://dx.doi.org/10.1016/0006-8993\(72\)90769-X](http://dx.doi.org/10.1016/0006-8993(72)90769-X).
16. Lee JS, Kim MH, Ho WK and Lee SH (2013). Developmental upregulation of presynaptic NCKX underlies the decrease of mitochondria-dependent posttetanic potentiation at the rat calyx of Held synapse. *J Neurophysiol* **109**: 1724-1734 <http://dx.doi.org/10.1152/jn.00728.2012>.
17. Lohmann C and Friauf E (1996). Distribution of the calcium-binding proteins parvalbumin and calretinin in the auditory brainstem of adult and developing rats. *J Comp Neurol* **367**: 90-109 [http://dx.doi.org/10.1002/\(SICI\)1096-9861\(19960325\)367:1<90::AID-CNE7>3.0.CO;2-E](http://dx.doi.org/10.1002/(SICI)1096-9861(19960325)367:1<90::AID-CNE7>3.0.CO;2-E).
18. Lorteije JAM, Rusu SI, Kushmerick C and Borst JGG (2009). Reliability and precision of the mouse calyx of Held synapse. *J Neurosci* **29**: 13770-13784 <http://dx.doi.org/10.1523/JNEUROSCI.3285-09.2009>.
19. Masterton B, Jane JA and Diamond IT (1967). Role of brainstem auditory structures in sound localization. I. Trapezoid body, superior olive, and lateral lemniscus. *Journal of Neurophysiology* **30**: 341-359.
20. McLaughlin M, van der Heijden M and Joris PX (2008). How secure is *in vivo* synaptic transmission at the calyx of Held? *J Neurosci* **28**: 10206-10219 <http://dx.doi.org/10.1523/JNEUROSCI.2735-08.2008>.
21. Morest DK (1968). The growth of synaptic endings in the mammalian brain: a study of

- the calyces of the trapezoid body. *Zeitschrift für Anatomie und Entwicklungsgeschichte* **127**: 201-220 <http://www.springerlink.com/content/xm87n023050434t1/fulltext.pdf>.
22. Müller M, Felmy F, Schwaller B and Schneggenburger R (2007). Parvalbumin is a mobile presynaptic Ca^{2+} buffer in the calyx of Held that accelerates the decay of Ca^{2+} and short-term facilitation. *J Neurosci* **27**: 2261-2271 <http://dx.doi.org/10.1523/JNEUROSCI.5582-06.2007>.
 23. Nakamura T, Yamashita T, Saitoh N and Takahashi T (2008). Developmental changes in calcium/calmodulin-dependent inactivation of calcium currents at the rat calyx of Held. *J Physiol* **586**: 2253-2261 <http://jp.physoc.org/content/586/9/2253.long>.
 24. Nakamura Y and Takahashi T (2007). Developmental changes in potassium currents at the rat calyx of Held presynaptic terminal. *J Physiol* **581**: 1101-1112 <http://dx.doi.org/10.1113/jphysiol.2007.128702>.
 25. Rodriguez-Contreras A, van Hoeve JS, Habets RLP, Locher H and Borst JGG (2008). Dynamic development of the calyx of Held synapse. *Proc Natl Acad Sci U S A* **105**: 5603-5608 <http://dx.doi.org/10.1073/pnas.0801395105>.
 26. Roebel JL (2006). Developmental expression of calcium-binding proteins in the AVCN and MNTB of normal hearing and congenitally deaf mice. Anatomy, Wright State University. **MSc**: 114.
 27. Rusu SI and Borst JGG (2011). Developmental changes in intrinsic excitability of principal neurons in the rat medial nucleus of the trapezoid body. *Dev Neurobiol* **71**: 284-295 <http://dx.doi.org/10.1002/dneu.20856>.
 28. Rybak LP, Whitworth C and Scott V (1992). Development of endocochlear potential and compound action potential in the rat. *Hear Res* **59**: 189-194 [http://dx.doi.org/10.1016/0378-5955\(92\)90115-4](http://dx.doi.org/10.1016/0378-5955(92)90115-4).
 29. Schneider Gasser EM, Straub CJ, Panzanelli P, Weinmann O, Sassoè-Pognetto M and Fritschy J-M (2006). Immunofluorescence in brain sections: simultaneous detection of presynaptic and postsynaptic proteins in identified neurons. *Nat Protoc* **1**: 1887-1897 <http://dx.doi.org/10.1038/nprot.2006.265>.
 30. Schwaller B, Dick J, Dhoot G, Carrolls, Vrbova G, Nicotera P, Pette D, Wyss A, Bluethmann H, Hunziker W and Celio MR (1999). Prolonged contraction-relaxation cycle of fast-twitch muscles in parvalbumin knockout mice. *Am J Physiol* **276**: C395-403 <http://ajpcell.physiology.org/content/276/2/C395.long>.
 31. Sonntag M, Englitz B, Kopp-Scheinpflug C and Rübsamen R (2009). Early postnatal development of spontaneous and acoustically evoked discharge activity of principal cells of the medial nucleus of the trapezoid body: an *in vivo* study in mice. *J Neurosci* **29**: 9510-9520 <http://dx.doi.org/10.1523/JNEUROSCI.1377-09.2009>.
 32. Sonntag M, Englitz B, Typlt M and Rübsamen R (2011). The calyx of Held develops adult-like dynamics and reliability by hearing onset in the mouse *in vivo*. *J Neurosci* **31**: 6699-6709 <http://www.jneurosci.org/content/31/18/6699.full>.
 33. Tan ML and Borst JGG (2007). Comparison of responses of neurons in the mouse inferior colliculus to current injections, tones of different durations, and sinusoidal amplitude-modulated tones. *J Neurophysiol* **98**: 454-466 <http://dx.doi.org/10.1152/jn.00174.2007>.
 34. Taschenberger H and von Gersdorff H (2000). Fine-tuning an auditory synapse for speed and fidelity: developmental changes in presynaptic waveform, EPSC kinetics, and synaptic plasticity. *J Neurosci* **20**: 9162-9173 <http://www.jneurosci.org/cgi/content/full/20/24/9162>.
 35. Tollin DJ and Yin TCT (2005). Interaural phase and level difference sensitivity in low-frequency neurons in the lateral superior olive. *J Neurosci* **25**: 10648-10657 <http://dx.doi.org/10.1523/JNEUROSCI.1609-05.2005>.
 36. Uziel A, Romand R and Marot M (1981). Development of cochlear potentials in rats. *Audiology* **20**: 89-100 http://www.ncbi.nlm.nih.gov/entrez/query.fcgi?cmd=Retrieve&db=PubMed&dopt=Citation&list_uids=7224981.

37. Varela JA, Sen K, Gibson J, Fost J, Abbott LF and Nelson SB (1997). A quantitative description of short-term plasticity at excitatory synapses in layer 2/3 of rat primary visual cortex. *Journal of Neuroscience* **17**: 7926-7940 <http://www.jneurosci.org/content/17/20/7926.long>.



chapter **FIVE**

General discussion

In this thesis several aspects of the development of synaptic transmission in the medial nucleus of the trapezoid body (MNTB) of rodents were addressed. In Chapter 2 we studied the origin and pattern of the spontaneous activity in the MNTB from a few days after birth until after hearing onset. Before hearing onset this activity is instigated by the Kölliker's organ, a group of specialized supporting cells in the cochlea (Tritsch et al. 2007). At about postnatal day 10 (P10) this activity generator goes into regression, after which the characteristic spontaneous firing pattern we observed disappears and is replaced by a more random, 'principal-like' firing pattern. We showed that before hearing onset spontaneous activity in the MNTB depended on the cochlea, since spontaneous activity entirely disappeared following cochlear ablation. The characteristic firing pattern showed preferred frequencies, which we could trace back to distinct events in the cochlea: a prolonged depolarization of immature hair cells, leading to a burst of calcium action potentials, each leading to action potentials in the auditory nerve fibers. Chapter 3 describes developmental changes in short-term plasticity (STP) in the MNTB before and after hearing onset. We found clear *in vivo* evidence for the presence of STP in immature synapses, whereas right before hearing onset the impact of STP greatly decreased or even disappeared. Control experiments, both in slices and *in vivo*, suggested that these differences mostly resulted from presynaptic changes, including upstream changes in firing patterns, and changes in postsynaptic voltage dependent ion channels, with a possible additional role for a change in the composition of the extracellular environment. The observed dramatic changes in STP just before hearing onset are likely to play an essential role in the conversion of the calyx of Held synapse into an auditory relay synapse. To address the hypothesis whether a change in the presynaptic concentration of parvalbumin (PV), a slow-binding calcium buffer, plays an important role in this disappearance of STP, we measured in Chapter 4 the amount of parvalbumin in the presynaptic terminal and the postsynaptic principal cell with immunocytochemical methods. Instead of the hypothesized increase in parvalbumin, we observed a decrease around hearing onset in both rats and mice. Moreover, in parvalbumin knock-out mice the amount of STP during *in vivo* experiments was not significantly different from wild type littermates, providing further support for the lack of a role for parvalbumin in the decreased STP impact.

One of the main questions of this thesis has not been fully answered; we still do not precisely understand the exact mechanisms that allow the calyx of Held synapse to become a reliable relay synapse. From the results in Chapter 4 it has become clear that parvalbumin does not play a major role in the decrease of STP around hearing onset. Several functional changes have already been described to occur in slice studies, but they were insufficient to explain the observed dramatic change in STP impact.

THE ROLE OF ELECTRICAL ACTIVITY AND SHORT TERM PLASTICITY DURING DEVELOPMENT

five

Development of neuronal networks, including the auditory system, is regulated by both activity-dependent and activity-independent processes (Friauf and Lohmann 1999). Two types of neuronal activity can be distinguished: spontaneous activity and sensory-evoked activity. The crude topography of the network is largely activity-independent, and depends on genetic and molecular markers (Friauf and Lohmann 1999). Both molecular markers and spontaneous activity influence target selection, cell survival, neurotransmitter specification and cell size (Blankenship and Feller 2010; Spitzer 2012). These processes occur before the onset of sensory-evoked activity. In the auditory system, sensory-evoked activity after hearing onset induces further refinement of synaptic connectivity and strength (Friauf and Lohmann 1999; Walmsley et al. 2006). A comparable dependency on spontaneous and sensory-evoked activity is seen in the visual system (Katz and Shatz 1996; Rochefort et al. 2009; Colonnese et al. 2010; Feller 2012; Winnubst et al. 2015).

During the first ten postnatal days we saw a characteristic firing pattern of spontaneous activity consisting of high frequency bursts interspersed with long silent intervals (Chapter 2; Tritsch et al. 2010). In this period, the synapses are still immature, and they are not yet specialized for high-frequency signalling. The release probability (P_r) of vesicles in the readily releasable pool is relatively high, and, as a result, the readily releasable pool easily gets depleted. The resulting synaptic depression may lead to transmission failures. The long silent intervals in the bursting pattern, however, give the synapse time to recover from the synaptic depression. Moreover, presynaptic calcium clearance is still relatively slow (Chuhma and Ohmori 2001; Lee et al. 2013b) most likely leading to considerable build-up of presynaptic 'residual' calcium within the bursting period. This results in synaptic facilitation, which can counteract the synaptic depression during the bursts. We observed that the decay of synaptic facilitation shortened about tenfold during development. Whereas the recovery time constant for synaptic depression did not change significantly after hearing onset, the amount of synaptic depression decreased dramatically. At about P10 the spontaneous pattern changes into a 'primary-like' firing pattern and the calyx synapse becomes a fast and reliable synapse with transmission largely independent of recent history (Lorteije et al. 2009). We cannot exclude that a more precise control of the stimulation pattern would uncover that a larger portion of the variance in EPSP amplitudes can be ascribed to short-term plasticity than is estimated from the random, Poisson-like spontaneous firing patterns we observed *in vivo* after hearing onset (Yang and Xu-Friedman 2015). The observation that the recovery from STD remained slow after hearing onset has interesting implications. In combination with the high spontaneous firing frequency, it implies that most calyx of Held synapses are tonically depressed (Hermann et al. 2007; Hermann et al. 2009; Lorteije et al. 2009; Wang et al. 2013). This tonic depression is a bit of a puzzling phenomenon. In

the absence of any spontaneous activity, as happens in slice recordings, the terminal has a population of 'superprimed' vesicles with a very high P_r , presumably located right next to calcium channels at the active zone, and equipped with a full set of SNARE proteins (Lee et al. 2013a). However, since it takes several seconds for them to become superprimed, and since they have a very high P_r in the *in vivo* situation, they will not be given the time to fully mature. A limitation of the experiments in Chapter 3 is that STP was not studied during sound-evoked activity. More recent experiments in which the relation between spontaneous activity and sound-evoked activity was investigated showed that there is an inverse relation between the spontaneous firing frequency and the amount of STD that is evoked during sound exposure (Wang et al. 2013). This is not entirely predicted by our data, since the STD recovery was projected to be in the seconds range, but in the more recent experiments a recovery time constant in the hundreds of milliseconds was observed (Wang et al. 2013). In addition, some evidence for synaptic facilitation at the sound onset was found. It is remarkable that after two decades of detailed studies on the STP mechanisms, it is still largely unclear what the rate-limiting steps are in the formation of vesicles with a high P_r , and to what extent they contribute to sound-evoked activity. Because of its high spontaneous activity, the calyx synapse is a low P_r synapse which is able to sustain high frequency activity at the cost of a somewhat decreased precision (Borst and Soria van Hoeve 2012). In contrast, synapses between hippocampal inhibitory interneurons and pyramidal neurons exhibit high release probability, allowing them to respond more optimally to single spikes, but less to sustained presynaptic activity (Klyachko and Stevens 2006; Klug et al. 2012). We conclude that in the young-adult calyx synapse, STP has an important function in propagating the instructive firing pattern from the cochlea to ascending auditory nuclei such as the MNTB, but that its function in the adult relay calyx of Held synapse is quite limited.

Patterned activity is important for development and refinement of neural circuits (Friauf and Lohmann 1999; Rochefort et al. 2009; Blankenship and Feller 2010; Hoffpauir et al. 2010; Kirkby et al. 2013; Ko et al. 2014; Winnubst et al. 2015). Multiple molecular mechanisms, e.g. transcription factors or micro-RNAs, also have a role in development and in homeostatic adaptation to sensory-evoked activity (Friauf 1992; Saint Marie et al. 1999; Verhage et al. 2000; Borodinsky et al. 2004; Spiegel et al. 2014; Blosa et al. 2015; Dehorter et al. 2015). How activity regulates the development at the molecular level is still only partially understood. Neuronal activity is coupled to transcriptional programs to regulate the development of neural circuits (Flavell and Greenberg 2008). Transcription factors like Npas 4 (Spiegel et al. 2014), or Er81 (Dehorter et al. 2015) are found in excitatory and inhibitory neurons, respectively, and are expressed in reaction to activity. These factors regulate synaptic input in a homeostatic manner, promoting inhibition onto excitatory neurons and excitation onto inhibitory neurons (Spiegel et al. 2014). The expression of Er81 seems to be activity-dependent and the characteristics of the interneurons can be reversibly tuned to adapt to the changing levels of activity during development (Dehorter et al. 2015). The immediate

early gene *c-fos* is expressed in response to high-frequency stimulation and is involved in the refinement of tonotopical topography throughout the auditory nuclei (Friauf 1992). Its products, the *c-fos* mRNA and Fos protein, are upregulated in response to auditory stimulation (Saint Marie et al. 1999). When in an experimental setup the cochlea of adult rat was ablated, the expression of *c-fos* mRNA was decreased and did not recover (Luo et al. 1999). Unfortunately, no recordings were performed before hearing onset and the role of *c-fos* or other immediate-early genes during development of the calyx synapse remains unclear.

Similar to parvalbumin-positive neurons in the forebrain, the principal neurons in the MNTB are surrounded by a perineuronal net (Blosa et al. 2013), which may be important for synaptic maturation. The proteoglycan brevican is a major component of these perineuronal nets (PNs). Synaptic transmission at the calyx synapse was reduced in young adult brevican-deficient mice and the duration of the prespike and postsynaptic AP was increased, suggesting a role for brevican in the refinement of high-speed synaptic transmission (Blosa et al. 2015). Again, the developmental role remains unclear because of the lack of recordings before hearing onset.

Thus, although the importance of molecular markers for development of neural circuits has been demonstrated at other model synapses, the exact developmental function of molecular markers in the formation of a fully functional calyx synapse still remains unclear. Furthermore, it is still somewhat unclear to what extent molecular mechanisms are hardwired and activity independent (Friauf and Lohmann 1999; Kirkby et al. 2013; Ko et al. 2014).

DEVELOPMENTAL ROLE OF PARVALBUMIN

Parvalbumin is present in the MNTB but also in other inhibitory synapses, e.g. in the cerebellum and visual cortex. It has been postulated that parvalbumin-containing cells could have a role in controlling the plasticity of the onset and closure of a critical period (Anomal et al. 2013; Gu et al. 2013; Spatazza et al. 2013)(for review: (Takesian and Hensch 2013)). A similar role for parvalbumin in the MNTB does not seem very likely since the synaptic physiology was similar in the PV KO as in wild-type littermates. Although the number of recorded cells was relatively low, we have seen both in wild type and PV KO a strong decrease in STP at about P10-12.

Parvalbumin speeds up the decay of short-term facilitation at the calyx of Held synapse (Müller et al. 2007), but the hypothesized developmental increase and contribution of the developmental changes in facilitation was not seen in our study (Chapter 4). Apparently, calcium clearance mechanisms contribute more to the decrease in facilitation and faster decay of facilitation. Presynaptic Ca^{2+} -exchanger pumps like the K^{+} -dependent $\text{Na}^{+}/\text{Ca}^{2+}$ exchangers (NCKX), $\text{Na}^{+}/\text{Ca}^{2+}$ exchangers (NCX), plasma membrane Ca^{2+} -ATPase

and mitochondria all contribute to calcium clearance (Kim et al. 2005). Recently, a clear developmental increase in the K^+ -dependent Na^+/Ca^{2+} exchanger (NCKX) was shown (Lee et al. 2013b). Around hearing onset, the calyx starts to assume its mature, floral-like structure (Kandler and Friauf 1993; Kil et al. 1995; Ford et al. 2009). These morphological changes may also contribute to faster Ca^{2+} clearance. By increasing the surface-to-volume ratio, the more fenestrated, open structure may speed up presynaptic calcium clearance. A faster clearance of presynaptic Ca^{2+} rather than an increased buffering by calcium-binding proteins such as parvalbumin may therefore underlie the developmental speeding of the decay of synaptic facilitation at the calyx of Held.

five

LIMITATIONS

Anaesthesia

We studied the developmental changes in STP at the rodent calyx of Held synapse during *in vivo* recordings performed in the presence of anaesthetics. Anaesthetics can affect excitability, firing rates and synaptic release probabilities. We used isoflurane, a inhalation anaesthetic which is known to act on neurotransmitter release, most likely by inhibition of presynaptic Ca^{2+} influx via an effect on the presynaptic action potential (Wu et al. 2004; Baumgart et al. 2015). These studies were performed in brain slices at isoflurane concentrations between 0.35 – 1.05 mM. The exact isoflurane concentration during our *in vivo* experiments was unknown, but, to be able to compare results between animals and several cells within one animal, all the *in vivo* experiments have been conducted under the same conditions as much as possible. In addition, control experiments were performed in slices, showing comparable results as *in vivo*, suggesting that the effect of isoflurane on the presynaptic action potential was not large during our *in vivo* experiments.

To immobilize the animal during the auditory brainstem responses (ABR) measurements ketamine and xylazine were used. The combination of the two drugs is applied intraperitoneally and often used in laboratory animals. It is known that ketamine and xylazine have a limited effect on the hearing thresholds measured with ABR, compared to isoflurane (Ruebhausen et al. 2012).

Numbers

We cannot rule out that with a higher number of cells and animals, different results would have been obtained. Especially in Chapter 4, statistical power is limited due to logistic reasons.

Location of recordings

Especially in the *in vivo* experiments, we cannot clearly tell where exactly in the MNTB the recording was made. The presence of a characteristic waveform signifies that the recording cell is located within the MNTB, but a more precise localization was not possible. In Chapter 2

the recording location was verified using a dye, which was injected at the location of the last recording. After removal of the brain and fixation of the tissue the MNTB was identified in slices using a light microscope. Occasionally, after injection of the dye, the brainstem was acutely sliced to verify the recording location. During development there is a developmental gradient within the MNTB, with medial ahead of lateral (Rodriguez-Contreras et al. 2008), which could add to the observed variability at a certain age. However, other qualitative differences have not yet been described, suggesting that the lack of a more precise estimate of the recording site is not a major limitation of the experiments described in this thesis.

OUTLOOK

The bursting firing pattern is not only seen in the auditory system, but also among others in the visual system (Katz and Shatz 1996; Winnubst et al. 2015) and in the hippocampus (Kleindienst et al. 2011). The role of electrical activity in the development of the calyx is still inconclusive. One way to study this is to alter the firing patterns by cochlear ablation, with ototoxic medication, or by study mutants with altered activity patterns. A deaf mutant (*dn/dn*) has been studied and surprisingly no changes in synaptic transmission at the calyx synapse were found in slices of P11-16 mice (Oleskevich et al. 2004); the calyx morphology also was similar to normal hearing mice (Youssoufian et al. 2008). The deafness locus (*dn*) causes hair cell degeneration soon after birth (Keats et al. 1995). A potential weakness of the studies on calyx development in these mutant mice was that *in vivo* spontaneous activity was not studied in detail. Because of the possibly relatively late onset of the impact of this mutation, it would be interesting to study their *in vivo* electrical activity during early development in more detail. Until these control experiments are done, it is too early to draw firm conclusions about the lack of impact of electrical activity on the development of the calyx of Held synapse. Calcium channel subunit KO mice ($\text{Ca}_v1.3^{-/-}$) do not release glutamate in the inner hair cells (IHCs) and are deaf, because there is a complete lack of cochlea-driven activity (Erazo-Fischer et al. 2007). Compared to wild type mice, at P14-17 $\text{Ca}_v1.3^{-/-}$ mice showed broader presynaptic action potentials, resulting in a higher release probability and more depression during repetitive stimulation. *In vivo* recordings were not done in this study, as well as recordings at P5-12. It would be interesting to know whether these mice have spontaneous activity in the first 10 postnatal days. In addition, the calyx morphology was not studied yet. Somewhat mixed results were obtained in slice studies following cochlear ablation (Grande et al. 2014). In conclusion, the role of activity in calyx development has at present still been insufficiently investigated to draw firm conclusions about it, and it would thus be interesting to investigate this in more detail in future experiments.

Perhaps there are other factors playing a role in development. (Adise et al. 2014) found evidence that manipulations of maternal care could accelerate hearing onset in rats. Cross-fostering pups (whose adoptive mothers tend to have increased contact time with the pups),

or handled pups (whose mothers tend to perform more licking and grooming) had a half day earlier hearing onset compared to naïve pups. Further research could involve studying STP in cross-fostering pups and handled pups compared to naïve pups. Will STP also decrease earlier when the critical period is shortened?

Another question which could be addressed in future experiments is to what extent transmitter release is necessary for calyx development. A way to study this could be to use light chain tetanus toxin (L-TeTX). L-TeTX can be microinjected into presynaptic terminals (Llinás et al. 1994) or can be expressed by presynaptic neurons (Sweeney et al. 1995) and block neurotransmitter release by interfering with the docking and fusion of the synaptic vesicles at the active zone in the neuron, leaving nearby neurons unperturbed. The technique has been shown to work in giant squid motor neurons (Llinás et al. 1994) and was also used amongst other toxins to block neurotransmitter release in studying vesicle pools in the calyx synapse (Sakaba et al. 2005). What would be the effect of blocking neurotransmitter release on synaptic development? Will it delay the closure of the critical period of the calyx synapse and will hearing onset still occur at P12? It would also be interesting to study the impact of neurotransmitter release on the developmental mechanisms that ensure the characteristic one-to-one relation of the calyx terminal with its principal cell. Will blocking transmitter release of one calyx lead to pruning of that calyx?

In Chapter 4 we presented evidence that parvalbumin does not have an important role in the change in STP around hearing onset. We did not observe an evidently different type of STP in PV KO mice, and the characteristic decrease of STP at about P10 was seen as well. Since parvalbumin is not the only calcium buffer, could it be that in these KO mice other calcium binding proteins were upregulated, which compensated for the lack of parvalbumin? Although Müller et al suggest that the speeding up of the decay of facilitation is mainly due to slow binding calcium buffer, like parvalbumin (Müller et al. 2007), no studies have been done to quantify the amount of calretinin and calmodulin in the calyx synapse of prehearing PV KO mice. Only Roebel et al studied the expression of parvalbumin, calretinin and calmodulin in normal hearing and congenital deaf (*dn/dn*) mice, but the quantification of the data was troublesome, because when parvalbumin was highly expressed, the presynaptic terminal and the postsynaptic cell could not be distinguished from each other in the measurements (Roebel 2006). Their main finding was that in the deaf mouse, which lacks sensory-evoked input, the expression of the calcium binding proteins did not change after hearing onset, whereas in the normal hearing mouse the expression did change.

In line with studying the KO, studying synaptic function in a model with parvalbumin overexpression would be equally interesting. Will overexpression lead to less facilitation? If so, we could study the role of facilitation in the developing MNTB. In the parvalbumin KO we did not see an effect on for example hearing onset. Overexpression of parvalbumin might allow us to study the consequences of a change in STP during early development.

I expect the calyx synapse to remain a key model synapse to study synaptic activity and plasticity because of its accessibility for electrophysiological research. The experiments shown in this thesis demonstrate its virtue in allowing quantitative measurements on synaptic transmission and plasticity under physiological conditions. Moreover, the ability to unambiguously identify this synapse throughout development and the ability to control its input makes it a very valuable model synapse for developmental studies. As such, it may serve to elucidate the molecular mechanisms of the formation of central synapses, analogous to what has been achieved for the neuromuscular junction.

REFERENCES

1. Adise S, Saliu A, Maldonado N, Khatri V, Cardoso L and Rodriguez-Contreras A (2014). Effect of maternal care on hearing onset induced by developmental changes in the auditory periphery. *J Neurosci* **34**: 4528-4533 <http://dx.doi.org/10.1523/jneurosci.4188-13.2014>.
2. Anomal R, de Villers-Sidani E, Merzenich MM and Panizzutti R (2013). Manipulation of BDNF signaling modifies the experience-dependent plasticity induced by pure tone exposure during the critical period in the primary auditory cortex. *PLoS One* **8**: e64208 <http://dx.doi.org/10.1371/journal.pone.0064208>.
3. Baumgart JP, Zhou ZY, Hara M, Cook DC, Hoppa MB, Ryan TA and Hemmings HC, Jr. (2015). Isoflurane inhibits synaptic vesicle exocytosis through reduced Ca^{2+} influx, not Ca^{2+} -exocytosis coupling. *Proc Natl Acad Sci USA* **112**: 11959-11964 <http://dx.doi.org/10.1073/pnas.1500525112>.
4. Blankenship AG and Feller MB (2010). Mechanisms underlying spontaneous patterned activity in developing neural circuits. *Nat Rev Neurosci* **11**: 18-29 <http://dx.doi.org/10.1038/nrn2759>.
5. Blosa M, Sonntag M, Brückner G, Jäger C, Seeger G, Matthews RT, Rübsamen R, Arendt T and Morawski M (2013). Unique features of extracellular matrix in the mouse medial nucleus of trapezoid body--implications for physiological functions. *Neuroscience* **228**: 215-234 <http://dx.doi.org/10.1016/j.neuroscience.2012.10.003>.
6. Blosa M, Sonntag M, Jäger C, Weigel S, Seeger J, Frischknecht R, Seidenbecher CI, Matthews RT, Arendt T, Rübsamen R and Morawski M (2015). The extracellular matrix molecule brevican is an integral component of the machinery mediating fast synaptic transmission at the calyx of Held. *J Physiol* **593**: 4341-4360 <http://dx.doi.org/10.1113/JP270849>.
7. Borodinsky LN, Root CM, Cronin JA, Sann SB, Gu X and Spitzer NC (2004). Activity-dependent homeostatic specification of transmitter expression in embryonic neurons. *Nature* **429**: 523-530 <http://dx.doi.org/10.1038/nature02518>.
8. Borst JGG and Soria van Hoeve J (2012). The calyx of Held synapse: from model synapse to auditory relay. *Annual Review of Physiology* **74**: 199-224 <http://dx.doi.org/10.1146/annurev-physiol-020911-153236>.
9. Chuhma N and Ohmori H (2001). Differential development of Ca^{2+} dynamics in presynaptic terminal and postsynaptic neuron of the rat auditory synapse. *Brain Res* **904**: 341-344 [http://dx.doi.org/10.1016/S0006-8993\(01\)02506-9](http://dx.doi.org/10.1016/S0006-8993(01)02506-9).
10. Colonnese MT, Kaminska A, Minlebaev M, Milh M, Bloem B, Lescure S, Moriette G, Chiron C, Ben-Ari Y and Khazipov R (2010). A conserved switch in sensory processing prepares developing neocortex for vision. *Neuron* **67**: 480-498 <http://dx.doi.org/10.1016/j.neuron.2010.07.015>.
11. Dehorter N, Ciceri G, Bartolini G, Lim L, del Pino I and Marin O (2015). Tuning of

- fast-spiking interneuron properties by an activity-dependent transcriptional switch. *Science* **349**: 1216-1220 <http://dx.doi.org/10.1126/science.aab3415>.
12. Erazo-Fischer E, Striessnig J and Taschenberger H (2007). The role of physiological afferent nerve activity during *in vivo* maturation of the calyx of Held synapse. *J Neurosci* **27**: 1725-1737 <http://www.jneurosci.org/cgi/content/full/27/7/1725>.
 13. Feller M (2012). Cortical development: the sources of spontaneous patterned activity. *Curr Biol* **22**: R89-91 <http://dx.doi.org/10.1016/j.cub.2011.12.036>.
 14. Flavell SW and Greenberg ME (2008). Signaling mechanisms linking neuronal activity to gene expression and plasticity of the nervous system. *Annu Rev Neurosci* **31**: 563-590 <http://dx.doi.org/10.1146/annurev.neuro.31.060407.125631>.
 15. Ford MC, Grothe B and Klug A (2009). Fenestration of the calyx of Held occurs sequentially along the tonotopic axis, is influenced by afferent activity, and facilitates glutamate clearance. *J Comp Neurol* **514**: 92-106 <http://dx.doi.org/10.1002/cne.21998>.
 16. Friauf E (1992). Tonotopic Order in the Adult and Developing Auditory System of the Rat as Shown by c-fos Immunocytochemistry. *Eur J Neurosci* **4**: 798-812 http://www.ncbi.nlm.nih.gov/entrez/query.fcgi?cmd=Retrieve&db=PubMed&dopt=Citation&list_uids=12106303
 17. Friauf E and Lohmann C (1999). Development of auditory brainstem circuitry. Activity-dependent and activity-independent processes. *Cell Tissue Res* **297**: 187-195.
 18. Grande G, Negandhi J, Harrison RV and Wang LY (2014). Remodelling at the calyx of Held-MNTB synapse in mice developing with unilateral conductive hearing loss. *J Physiol* **592**: 1581-1600 <http://dx.doi.org/10.1113/jphysiol.2013.268839>.
 19. Gu Y, Huang S, Chang MC, Worley P, Kirkwood A and Quinlan EM (2013). Obligatory role for the immediate early gene NARP in critical period plasticity. *Neuron* **79**: 335-346 <http://dx.doi.org/10.1016/j.neuron.2013.05.016>.
 20. Hermann J, Grothe B and Klug A (2009). Modeling short-term synaptic plasticity at the calyx of Held using *in vivo*-like stimulation patterns. *J Neurophysiol* **101**: 20-30 <http://dx.doi.org/10.1152/jn.90243.2008>.
 21. Hermann J, Pecka M, von Gersdorff H, Grothe B and Klug A (2007). Synaptic transmission at the calyx of Held under *in vivo*-like activity levels. *J Neurophysiol* **98**: 807-820 <http://jn.physiology.org/content/98/2/807.long>.
 22. Hoffpauir BK, Kolson DR, Mathers PH and Spirou GA (2010). Maturation of synaptic partners: functional phenotype and synaptic organization tuned in synchrony. *J Physiol* **588**: 4365-4385 <http://onlinelibrary.wiley.com/doi/10.1113/jphysiol.2010.198564/full>
 23. also see: <http://onlinelibrary.wiley.com/doi/10.1113/jphysiol.2010.200089/full>.
 24. Kandler K and Friauf E (1993). Pre- and postnatal development of efferent connections of the cochlear nucleus in the rat. *Journal of Comparative Neurology* **328**: 161-184 <http://www3.interscience.wiley.com/cgi-bin/fulltext/109692752/PDFSTART>.
 25. Katz LC and Shatz CJ (1996). Synaptic activity and the construction of cortical circuits. *Science* **274**: 1133-1138 http://www.ncbi.nlm.nih.gov/entrez/query.fcgi?cmd=Retrieve&db=PubMed&dopt=Citation&list_uids=8895456
 26. Keats BJ, Nouri N, Huang JM, Money M, Webster DB and Berlin CI (1995). The deafness locus (dn) maps to mouse chromosome 19. *Mamm Genome* **6**: 8-10.
 27. Kil J, Kageyama GH, Semple MN and Kitzes LM (1995). Development of ventral cochlear nucleus projections to the superior olivary complex in gerbil. *J Comp Neurol* **353**: 317-340 <http://www3.interscience.wiley.com/cgi-bin/fulltext/109693965/PDFSTART>.
 28. Kim M-H, Korogod N, Schneggenburger R, Ho W-K and Lee S-H (2005). Interplay between Na⁺/Ca²⁺ exchangers and mitochondria in Ca²⁺ clearance at the calyx of Held. *J Neurosci* **25**: 6057-6065 <http://www.jneurosci.org/cgi/content/full/25/26/6057>.

29. Kirkby LA, Sack GS, Firl A and Feller MB (2013). A role for correlated spontaneous activity in the assembly of neural circuits. *Neuron* **80**: 1129-1144 <http://dx.doi.org/10.1016/j.neuron.2013.10.030>.
30. Kleindienst T, Winnubst J, Roth-Alpermann C, Bonhoeffer T and Lohmann C (2011). Activity-dependent clustering of functional synaptic inputs on developing hippocampal dendrites. *Neuron* **72**: 1012-1024 <http://dx.doi.org/10.1016/j.neuron.2011.10.015>.
31. Klug A, Borst JGG, Carlson BA, Kopp-Scheinflug C, Klyachko VA and Xu-Friedman MA (2012). How do short-term changes at synapses fine-tune information processing? *J Neurosci* **32**: 14058-14063 <http://www.jneurosci.org/content/32/41/14058.long>.
32. Klyachko VA and Stevens CF (2006). Excitatory and feed-forward inhibitory hippocampal synapses work synergistically as an adaptive filter of natural spike trains. *PLoS Biol* **4**: e207 <http://dx.doi.org/10.1371/journal.pbio.0040207>.
33. Ko H, Mrcic-Flogel TD and Hofer SB (2014). Emergence of feature-specific connectivity in cortical microcircuits in the absence of visual experience. *J Neurosci* **34**: 9812-9816 <http://dx.doi.org/10.1523/JNEUROSCI.0875-14.2014>.
34. Lee JS, Ho W-K, Neher E and Lee S-H (2013a). Superpriming of synaptic vesicles after their recruitment to the readily releasable pool. *Proc Natl Acad Sci U S A* **110**: 15079-15084 <http://dx.doi.org/10.1073/pnas.1314427110>.
35. Lee JS, Kim MH, Ho WK and Lee SH (2013b). Developmental upregulation of presynaptic NCKX underlies the decrease of mitochondria-dependent posttetanic potentiation at the rat calyx of Held synapse. *J Neurophysiol* **109**: 1724-1734 <http://dx.doi.org/10.1152/jn.00728.2012>.
36. Llinás R, Sugimori M, Chu D, Morita M, Blasi J, Herreros J, Jahn R and Marsal J (1994). Transmission at the squid giant synapse was blocked by tetanus toxin by affecting synaptobrevin, a vesicle-bound protein. *J Physiol* **477** (Pt 1): 129-133.
37. Llinás R, Sugimori M, Chu D, Morita M, Blasi J, Herreros J, Jahn R and Marsal J (1994). Transmission at the squid giant synapse was blocked by tetanus toxin by affecting synaptobrevin, a vesicle-bound protein. *Journal of Physiology* **477**: 129-133.
38. Lorteije JAM, Rusu SI, Kushmerick C and Borst JGG (2009). Reliability and precision of the mouse calyx of Held synapse. *J Neurosci* **29**: 13770-13784 <http://dx.doi.org/10.1523/JNEUROSCI.3285-09.2009>.
39. Luo L, Ryan AF and Saint Marie RL (1999). Cochlear ablation alters acoustically induced c-fos mRNA expression in the adult rat auditory brainstem. *J Comp Neurol* **404**: 271-283.
40. Müller M, Felmy F, Schwaller B and Schneggenburger R (2007). Parvalbumin is a mobile presynaptic Ca²⁺ buffer in the calyx of Held that accelerates the decay of Ca²⁺ and short-term facilitation. *J Neurosci* **27**: 2261-2271 <http://dx.doi.org/10.1523/JNEUROSCI.5582-06.2007>.
41. Oleskevich S, Youssoufian M and Walmsley B (2004). Presynaptic plasticity at two giant auditory synapses in normal and deaf mice. *J Physiol* **560**: 709-719 <http://jp.physoc.org/content/560/3/709.long>.
42. Rochefort NL, Garaschuk O, Milos RI, Narushima M, Marandi N, Pichler B, Kovalchuk Y and Konnerth A (2009). Sparsification of neuronal activity in the visual cortex at eye-opening. *Proc Natl Acad Sci U S A* **106**: 15049-15054 <http://dx.doi.org/10.1073/pnas.0907660106>.
43. Rodriguez-Contreras A, van Hoeve JS, Habets RLP, Locher H and Borst JGG (2008). Dynamic development of the calyx of Held synapse. *Proc Natl Acad Sci U S A* **105**: 5603-5608 <http://dx.doi.org/10.1073/pnas.0801395105>.
44. Roebel JL (2006). Developmental expression of calcium-binding proteins in the AVCN and MNTB of normal hearing and congenitally deaf mice. Anatomy, Wright State University. **MSc**: 114.
45. Ruebhausen MR, Brozoski TJ and Bauer CA (2012). A comparison of the effects of isoflurane and ketamine anesthesia on auditory brainstem response (ABR) thresholds in rats. *Hear Res* **287**: 25-29 <http://dx.doi.org/10.1016/j.heares.2012.04.005>.

46. Saint Marie RL, Luo L and Ryan AF (1999). Effects of stimulus frequency and intensity on c-fos mRNA expression in the adult rat auditory brainstem. *J Comp Neurol* **404**: 258-270 http://www.ncbi.nlm.nih.gov/entrez/query.fcgi?cmd=Retrieve&db=PubMed&dopt=Citation&list_uids=9934998
47. Sakaba T, Stein A, Jahn R and Neher E (2005). Distinct kinetic changes in neurotransmitter release after SNARE protein cleavage. *Science* **309**: 491-494 <http://www.sciencemag.org/cgi/content/full/309/5733/491>.
48. Spatazza J, Lee HH, Di Nardo AA, Tibaldi L, Joliot A, Hensch TK and Prochiantz A (2013). Choroid-plexus-derived Otx2 homeoprotein constrains adult cortical plasticity. *Cell Rep* **3**: 1815-1823 <http://dx.doi.org/10.1016/j.celrep.2013.05.014>.
49. Spiegel I, Mardinly AR, Gabel HW, Bazinet JE, Couch CH, Tzeng CP, Harmin DA and Greenberg ME (2014). Npas4 regulates excitatory-inhibitory balance within neural circuits through cell-type-specific gene programs. *Cell* **157**: 1216-1229 <http://dx.doi.org/10.1016/j.cell.2014.03.058>.
50. Spitzer NC (2012). Activity-dependent neurotransmitter respecification. *Nat Rev Neurosci* **13**: 94-106 <http://dx.doi.org/10.1038/nrn3154>.
51. Sweeney ST, Broadie K, Keane J, Niemann H and O'Kane CJ (1995). Targeted expression of tetanus toxin light chain in *Drosophila* specifically eliminates synaptic transmission and causes behavioral defects. *Neuron* **14**: 341-351.
52. Takesian AE and Hensch TK (2013). Balancing plasticity/stability across brain development. *Prog Brain Res* **207**: 3-34 <http://dx.doi.org/10.1016/B978-0-444-63327-9.00001-1>.
53. Tritsch NX, Rodríguez-Contreras A, Crins TTH, Wang HC, Borst JGG and Bergles DE (2010). Calcium action potentials in hair cells pattern auditory neuron activity before hearing onset. *Nat Neurosci* **13**: 1050-1052 <http://dx.doi.org/10.1038/nn.2604>.
54. Tritsch NX, Yi E, Gale JE, Glowatzki E and Bergles DE (2007). The origin of spontaneous activity in the developing auditory system. *Nature* **450**: 50-55 <http://www.nature.com/nature/journal/v450/n7166/full/nature06233.html>.
55. Verhage M, Maia AS, Plomp JJ, Brussaard AB, Heeroma JH, Vermeer H, Toonen RF, Hammer RE, van den Berg TK, Missler M, Geuze HJ and Sudhof TC (2000). Synaptic assembly of the brain in the absence of neurotransmitter secretion. *Science* **287**: 864-869 <http://www.ncbi.nlm.nih.gov/htbin-post/Entrez/query?db=m&form=6&dopt=r&uid=10657302>.
56. Walmsley B, Berntson A, Leao RN and Fyffe REW (2006). Activity-dependent regulation of synaptic strength and neuronal excitability in central auditory pathways. *J Physiol* **572**: 313-321 <http://jp.physoc.org/content/572/2/313.full>.
57. Wang T, Rusu SI, Hruskova B, Turecek R and Borst JGG (2013). Modulation of synaptic depression of the calyx of Held synapse by GABA_B receptors and spontaneous activity. *J Physiol* **591**: 4877-4894 <http://dx.doi.org/10.1113/jphysiol.2013.256875>.
58. Winnubst J, Cheyne JE, Niculescu D and Lohmann C (2015). Spontaneous activity drives local synaptic plasticity in vivo. *Neuron* **87**: 399-410 <http://dx.doi.org/10.1016/j.neuron.2015.06.029>.
59. Wu X-S, Sun J-Y, Evers AS, Crowder M and Wu L-G (2004). Isoflurane inhibits transmitter release and the presynaptic action potential. *Anesthesiology* **100**: 663-670 http://www.ncbi.nlm.nih.gov/entrez/query.fcgi?cmd=Retrieve&db=PubMed&dopt=Citation&list_uids=15108983
60. Yang H and Xu-Friedman MA (2015). Skipped-stimulus approach reveals that short-term plasticity dominates synaptic strength during ongoing activity. *J Neurosci* **35**: 8297-8307 <http://dx.doi.org/10.1523/JNEUROSCI.4299-14.2015>.
61. Youssoufian M, Couchman K, Shivdasani MN, Paolini AG and Walmsley B (2008). Maturation of auditory brainstem projections and calyces in the congenitally deaf (*dn/dn*) mouse. *J Comp Neurol* **506**: 442-451 <http://dx.doi.org/10.1002/cne.21566>.



chapter **SIX**

Summary / Samenvatting

SUMMARY

The calyx of Held synapse is a giant synapse in the medial nucleus of the trapezoid body (Medial Nucleus of the Trapezoid Body; MNTB) located in the brain stem. This synapse plays an important role in sound localization. The function of this synapse is to convert electrical signals from the contra-lateral cochlear nucleus into an inhibiting signal for the ipsilateral superior olivary complex (SOC) and other auditory nuclei in the brain stem. The adult calyx synapse functions as a relay synapse and exhibits little plasticity and action potentials are generally transmitted in a reliable manner. Mice and rats start to airborne sounds at about 13 days after birth. The calyx synapses in rats and mice begin to emerge a few days after birth and then function still suboptimal. Because the calyx synapse is so large, it is a popular synapse for electrophysiological studies. When a recording electrode is placed close to the synapse, both the presynaptic and the postsynaptic action potential can be measured. In Chapter 2 we have done recordings in anesthetized young rats, who could not yet hear. It was found that although no auditory signals can be received yet, the calyx synapse was already spontaneously active. This activity was found to be generated by the inner ear (cochlea). A group of cells in the cochlea (Kölliker's organ) causes a characteristic firing pattern in the calyx synapse with periodic increases in activity, wherein the action potentials often occur at intervals of around 10 or around 100 milliseconds, followed by long silent intervals of 1 or more seconds. We carried out the measurements before and after ablation cochlea and it was found that the characteristic fire pattern was not seen after ablation, while the synapses in the MNTB could still be stimulated. The spontaneous activity and the effects on synaptic transmission were further investigated in Chapter 3. The changes in the synapse were quantified by analysing the shape of the waveform. The excitatory postsynaptic potential (EPSP) has been used as a measure of short-term synaptic plasticity (STP): the EPSP is higher (facilitation) or lower (depression) than the preceding EPSP. For Chapter 3 *in vivo* recordings in rats were done. In the first two postnatal weeks obvious STP was seen. Facilitation was mostly seen during high frequency bursts of activity. The synapse gets little time to recover from previous activity and to 'reset', therefore, calcium can accumulate in the presynaptic nerve terminal. As a result, more neurotransmitter vesicles will be able to fuse with the synaptic cleft during one action potential and the synaptic strength is increased. In depression, the synaptic strength is decreased. The main cause of depression is probably depletion of the available pool of neurotransmitter vesicles. In an immature synapse depression occurs relatively easily, but we found that only during the fast bursts with short intervals between the consecutive EPSP's also facilitation occurs. Thus, facilitation counteracts depression. The bursting spontaneous activity facilitates synaptic transmission despite an immature and unripe system. We found that both facilitation and depression often occurred during the first 10 days after birth, after which it decreased sharply and almost could no longer be measured after the hearing onset. The firing pattern itself also changed after about 10 days when the Kölliker's organ

went into regression. In Chapter 4, the role of the calcium-binding protein parvalbumin was examined. We hypothesized that the calcium buffer parvalbumin would play a star role in the developmental changes of STP. In experiments where the amount of parvalbumin pre- and postsynaptic is quantified by antibody staining, however, it was found that the amount of parvalbumin also decreased sharply around the time of the hearing onset. The marked decrease of facilitation can therefore not be explained by an increase in the buffer capacity for calcium due to an increase in the parvalbumin concentration at the calyx of Held synapse. In addition, electrophysiological measurements in parvalbumin knock-out mice exhibited comparable developmental plasticity changes as wild type controls. Thus, parvalbumin does not play a major role in the disappearance of short-term plasticity during the maturation of the calyx of Held synapse.

SAMENVATTING

De calyx van Held synaps is een zeer grote synaps, die zich in de mediale kern van het corpus trapezoïdeum (Medial Nucleus of the Trapezoid Body; MNTB) in de hersenstam bevindt. Deze synaps speelt een belangrijke rol bij geluidslokalisatie. Door deze synaps worden elektrische signalen vanuit de contralaterale nucleus cochlearis geconverteerd in een remmend signaal voor de ipsilaterale olijkernen en andere auditieve kernen in de hersenstam. De calyxsynaps functioneert op volwassen leeftijd als een relay synaps. Deze synaps vertoont weinig plasticiteit en signalen worden in het algemeen op betrouwbare wijze doorgegeven. Muizen en ratten gaan pas ongeveer 13 dagen na de geboorte via luchtgeleiding horen. De calyxsynapsen worden bij ratten en muizen enkele dagen na hun geboorte gevormd en functioneren dan nog suboptimaal. Omdat de calyx synaps zo enorm groot is, leent het zich goed voor electrofysiologisch onderzoek. Door een meetelektrode heel dicht bij de synaps te brengen, is zowel het presynaptische signaal als de postsynaptische potentiaal meetbaar. In Hoofdstuk 2 hebben we metingen onder volledige anesthesie gedaan in ratten, die nog niet konden horen. Het bleek dat hoewel er nog geen geluidssignalen opgevangen kunnen worden, de calyxsynaps wel al spontaan actief is. Deze activiteit bleek gegenereerd te worden door het binnenoor (cochlea). Een groepje cellen in de cochlea (Kölliker's orgaan) zorgt voor een karakteristiek vuurpatroon in de calyxsynaps met periodieke toenames van activiteit, waarbij de actiepotentialen vaak met intervallen van rond de 10 of rond de 100 ms voorkomen, gevolgd door langdurige pauzes van 1 of meerdere seconden. We deden deze metingen vóór en na cochlea-ablatie, waarbij bleek dat het karakteristieke vuurpatroon niet meer gezien werd na ablatie, terwijl de synapsen in de MNTB nog steeds gestimuleerd konden worden.

De spontane activiteit en de invloed op de synaptische transmissie werd verder onderzocht in Hoofdstuk 3. De veranderingen in de synaps werden gekwantificeerd door de vorm te analyseren. De excitatoire postsynaptische potentiaal (EPSP) heeft als maat voor STP gefungeerd: bij facilitatie is de EPSP hoger dan de voorafgaande EPSP en bij depressie lager. Ook voor dit hoofdstuk zijn *in vivo* metingen bij ratten gedaan. In de eerste twee weken vertoont de synaps duidelijke korte termijn plasticiteit (Short Term Plasticity, STP). Tijdens spontane activiteit konden wij twee verschillende vormen van STP, synaptische facilitatie en synaptische depressie, meten. Bij facilitatie neemt de synaptische transmissie toe. Dit komt doordat door snelle opeenvolging van signalen de synaps weinig tijd krijgt om te herstellen en te 'resetten', waardoor calcium kan ophopen in de presynaptische zenuweindiging. Hierdoor kunnen meer neurotransmitterblaasjes afgegeven worden aan de synaptische spleet. Bij depressie neemt de sterkte van de transmissie juist af. De belangrijkste oorzaak is waarschijnlijk uitputting van de beschikbare voorraad aan neurotransmitterblaasjes. In een onrijpe synaps treedt depressie relatief makkelijk op, maar we vonden dat door de karakteristieke spontane activiteit tijdens de hele snelle en kort op elkaar komende actiepotentialen, facilitatie optrad. De aanwezigheid van facilitatie gaat dus de effecten

van depressie tegen. Onze metingen geven dus zo een mogelijke verklaring voor het zeer algemene voorkomen van zgn. burst firing in zich ontwikkelende sensorische systemen. We vonden dat facilitatie en depressie beide veelvuldig optraden in de eerste 10 dagen na geboorte, waarna het sterk afnam en vrijwel niet meer was te meten op jongvolwassen leeftijd. Tevens veranderde na ongeveer 10 dagen het spontane vuurpatroon doordat het Kölliker's orgaan in regressie ging.

In Hoofdstuk 4 werd de rol van het calciumbindende eiwit parvalbumine onderzocht. In de zoektocht naar een bepalende factor in de evidente vermindering van STP tijdens de ontwikkeling leek op grond van literatuuronderzoek een glansrol voor de calciumbuffer weggelegd. Bij experimenten waarbij de hoeveelheid parvalbumine pre- en postsynaptisch gekwantificeerd is met antilichaamkleuringen, bleek echter dat de hoeveelheid parvalbumine ook sterk daalde rond het tijdstip dat de knaagdieren gingen horen. Het verdwijnen van de facilitatie kan daarom niet verklaard worden door een toename van de buffercapaciteit voor calcium door een toename van de parvalbumineconcentratie in de calyx van Held. Daarnaast toonden elektrofysiologische metingen in parvalbumine knock-out muizen aan dat het patroon van verminderende plasticiteit tijdens de ontwikkeling vergelijkbaar was met wild type nestgenoten. Parvalbumine speelt dus geen grote rol in het verdwijnen van korte termijn plasticiteit tijdens de rijping van de calyx van Held synaps.



addendum

CURRICULUM VITAE



De promovendus werd geboren op 27 februari 1980 te Tegelen en groeide op in het Limburgse dorp Swalmen. In 1998 behaalde hij aan het Bisschoppelijk College Broekhin te Roermond het gymnasium diploma en besloot om de opleiding operatieassistent te gaan volgen aan de Hoge School Zuyd te Heerlen. Het praktijkdeel van deze opleiding werd in het Laurentius Ziekenhuis te Roermond gevolgd. Na drie jaar werd deze opleiding in 2001 succesvol afgerond en werd na uitloting voor de studie Geneeskunde begonnen aan de propedeuse Biologie aan de bèta-faculteit van de Katholieke Universiteit Nijmegen (later

Radboud Universiteit Nijmegen geheten). Na behaalde propedeuse kon in 2002 begonnen worden aan de studie Geneeskunde aan de faculteit Medische Wetenschappen van dezelfde universiteit. In 2008 werd het doctoraal en basisarts examen gehaald, waarna in oktober 2008 gestart kon worden als arts-onderzoeker KNO aan het Erasmus MC te Rotterdam op de afdeling Neurowetenschappen onder begeleiding van professor Borst. Vanaf juni 2012 is de promovendus arts-assistent KNO (AIOS) bij de afdeling KNO onder professor Baatenburg de Jong en dr. Metselaar en hoopt in juni 2017 de opleiding tot Keel- Neus- Oorarts af te ronden.

Sinds 01 mei 2010 is de promovendus gehuwd met mw. drs. Marjolein Crins-Mattheij en wonen zij in Breda.

&

PHD PORTFOLIO

Courses

- Article 9 animal course, 2009
 - Residency program ENT:
 - Endoscopy, laryngology. Groningen 2013
 - Functional Endoscopic Sinus Surgery. Leiden, 2013
 - Nasal surgery. Utrecht, 2013
 - Radiology. Zaanse Schans, 2014
 - Ear surgery. Nijmegen, 2015
- Desiderius courses: ethics, EBM, communication. Rotterdam, 2013-2014
- 2nd Skills Lab Course. Antwerpen, 2015

&

Teaching activities

During Medical School:

- Several assistantships: “Beweging en sturing” and “onderwijskundige aspecten van anatomieonderwijs”.
- Several preparations of anatomical models

During PhD and ENT training:

- VO: echografie
- VO: epilepsie
- VKO: KNO
- “Traumatische KNO”. For residents emergency medicine.
- “KNO voor operatie-assistenten”.

Oral presentations and poster presentations

| | |
|------|--|
| 2015 | Crins TTH. <i>Korte termijn plasticiteit in de calyx van Held synaps.</i> Presentatie 226 ^e KNO-vergadering, Nieuwegein. |
| 2013 | Crins TTH en Borst JGG. <i>Centraal auditieve verwerking: van plastisch naar robuust.</i> Poster 223 ^e KNO-vergadering, Maastricht. |
| 2012 | Crins TTH, Borst JGG. <i>Developmental changes in short term plasticity at the calyx of Held synapse.</i> Presentatie ENP, Lunteren. |
| 2011 | Crins TTH, Rusu SI, Rodríguez-Contreras A, Borst JGG, <i>Developmental changes in short term plasticity at the calyx of Held synapse.</i> Poster ARO, Baltimore, USA. |
| 2010 | Crins TTH, Rusu SI, Rodríguez-Contreras A, Borst JGG. <i>Developmental changes in short-term plasticity at the rat calyx of Held.</i> Poster FENS, Amsterdam. |
| 2010 | Crins TTH. <i>Korte termijn plasticiteit in de calyx van Held synaps.</i> Presentatie KNO-vergadering, Nieuwegein. |

- 2008 **Crins TTH**, Vorstenbosch M, Marres H. *Toepassing van 3D techniek in anatomie onderwijs*. Poster KNO-vergadering, Maastricht.
- 2008 – 2015 multiple labtalks and ‘Monday Morning Meetings’
- 2008 – 2016 multiple ENTER presentations.

Articles

- 2012 Nagtegaal, AP, Spijker S, **Crins TT**, Neuro-Bsik Mouse Phenomics Consortium, Borst JG. *A novel QTL underlying early-onset, low-frequency hearing loss in BXD recombinant inbred strains*. Genes Brain Behav. Nov 2012. 11(8):911-20.
- 2011 **Crins TTH**, Rusu SI, Rodríguez-Contreras A, Borst JGG. *Developmental Changes in Short-Term Plasticity at the Rat Calyx of Held Synaps*. J. Neurosci., Aug 2011. 31(32):11706 –11717
- 2010 Tritsch NX, Rodríguez-Contreras A, **Crins TTH**, Wang HC, Borst JGG, Bergles DE. *Calcium action potentials in hair cells pattern auditory neuron activity before hearing onset*. Nat Neurosci, Sept 2010. 13(9):1050-1052
- 2009 **Crins TTH**, Iserle, M.; Roebroek, R.M.J.A.; Graamans, K. *Blind na otitis media*. Nederlands Tijdschrift voor Keel- Neus- en Oorheelkunde, 2009. 15:73-76
- 2008 Thomeer HG, **Crins TT**, Kamsteeg EJ, Buijsman W, Cruysberg JR, Knoers NV, Cremers CW. *Clinical presentation and the presence of hearing impairment in branchio-oculo-facial syndrome : a new mutation in the TFAP2A gene*. , Dec 2010. 119(12):806-14.
- 2008 **Crins TTH**, Kunst D. M. *Ménière: diagnose, etiologie en therapeutische mogelijkheden bij invaliderende Ménière*. Nederlands Tijdschrift voor KNO, Apr 2008.

DANKWOORD

Gerard. Niet gehinderd door enige vorm van kennis kwam ik in jouw groep. Je hebt altijd heel goed begrepen dat ik meer dokter dan (fundamenteel) onderzoeker ben. Ik ken niemand die zo intelligent, tijdsefficiënt, eerlijk en toegankelijk is. Altijd kon ik bij je binnenlopen om weer even wat overzicht te krijgen; dat soms het tegenovergestelde bereikt werd, ligt meer aan mij dan aan jou. Heel veel respect en dank.

Rob. Fundamenteel neurowetenschappelijk onderzoek en KNO is best een lastige combinatie en een erfenis uit het verleden. Kwaliteit van zorg en van leven; hoe dat te meten en te beïnvloeden, daar ligt jouw hart. Desondanks heb jij waar mogelijk, wanneer een kritische blik gewenst was, je bijdrage geleverd. Ik ben je zeer dankbaar dat je mij 7 1/2 jaar geleden hebt aangenomen. Hopelijk blijf je nog lange tijd het hoofd van mijn en onze afdeling.

&

Mijn paranymfen: John en Paul, Paul en John. Vrienden voor het leven. Ik hoop nog vaak met jullie naar concerten te gaan en naar weer een onverslaanbare superheld te gaan kijken in de bios; liefst in IMAX en 3D natuurlijk. John (spreek uit als 'Sjon'). Een mooie tijd hadden we op de twaalfde; jij hebt me vooral in het begin wegwijs gemaakt op die afdeling en ik heb veel van je geleerd, ook een hoop onzin trouwens. Paul. Goede vrind, gelukkig zijn in het Erasmus MC genoeg koffiebars aanwezig om een goed gesprek te faciliteren. Ik koester onze gezamenlijke aversie jegens de 'Starbucks'.

Rudiger. Rü. Altijd behulpzaam en zeer kundig. Ik heb graag van je hulp gebruik gemaakt en daarvoor ben je zeer erkentelijk. En ik weet dat je dit in het nederlands kunt lezen hoewel we toch meestal engels met elkaar spraken, ondanks je duitse achtergrond.

Silviu. For chapter three your work has been vital. I am proud that we pulled that of. We had a nice time in the Borstlab. Thanks.

Jeannette. In vivo electrofysiologie, daar was jij als postdoc mee bezig toen ik begon eind 2008. Ik leerde dat proeven fout konden gaan, maar dat met genoeg geduld en doorzetting vaak mooie data verzameld kunnen worden. Bedankt.

TianTian. You came to the Borstlab and immediately created your own place within the group. Working straight towards your goals paid off and in a relatively short period you got your PhD. We had fun days at the lab. Thanks for maintaining the parvalbumin mouse strain.

Kees. Hoe vaak ik jou wel niet gevraagd heb om even mee te kijken of te denken ten aanzien van een technisch probleem, of omdat ik het weer eens niet begreep. En doorgaans kwam het vervolgens netjes in orde! Dankjewel.

Elize. Je hebt kleuringen en je hebt kleuringen. En je hebt schaterlach en je hebt schaterlach. Zeker voor hoofdstuk vier heb jij veel kleuringen voor mij gedaan en dat heeft mooie beelden en data opgeleverd. Duizendmaal dank. En dank voor je kenmerkende schaterlach. Samen met die van Erika natuurlijk!

&

Marcel, Corstiaen, Thomas en Andrius: Van der Heyden lab. Iedere maandag bijeenkomst waar lopend onderzoek werd besproken. Altijd een kritische blik en aanvullende vragen in een meestal zeer ontspannen sfeer. Marcel, dank je voor de fijne samenwerking, ik mocht je vrijwel altijd storen voor vragen en natuurlijk dank dat je zitting hebt willen nemen in de grote commissie. Corstiaen. Mooie humor, veel gelachen, je deed prachtig onderzoek en doet dat waarschijnlijk ook nog in New York. Thomas. Onder de indruk van je kennis was ik de eerste keer dat ik je meemaakte tijdens een labbijeenkomst. En dat ben ik gebleven. Andrius. I enjoyed the conversations we had during lunch. Keep up the great work.

Hans. Eigenlijk vanaf het begin dat ik op de twaalfde kwam hebben we geregeld met elkaar gesproken. Je deed en doet interessant evenwichtsonderzoek en kon mooi vertellen over je reizen naar Azië om daar banden met universiteiten aan te halen. Veel dank dat je als secretaris van de leescommissie hebt willen optreden.

Steven en Ype. Vooral voor het vierde hoofdstuk had ik iets nodig dat van jullie was: de confocal microscoop op de veertiende. Veel dank dat ik daar gebruik van heb mogen maken. En een extra dank voor jou, Ype, dat je zitting hebt willen nemen in de grote commissie.

AIOS, ANIOS en onderzoekers. Ik ben trots op ons. Het is best lastig om een groep te hebben waarbij continu de samenstelling verandert en toch een bepaalde verwachting heerst dat we kwalitatief goed werk leveren en daar ondertussen ook nog eens iets van leren. Onze groep is fantÁstisch!! Ik hoop nog vele assistentenuitjes te beleven.

Pa en ma. Ondanks dat jullie het waarschijnlijk lastig vonden te begrijpen wat ik allemaal heb gedaan tijdens mijn promotie, zijn jullie altijd blijven vragen hoe het ging. Van jullie heb ik geleerd om dingen waaraan je begint ook af te maken. Veel dank.

Marjolein. Geduldig heb je afgewacht tot het af was. Je hebt je zelfs door taaie teksten heen geworsteld om zoek naar foutjes. Jij bent voor mij de allerliefste en ik hou van jou.